Sede Amministrativa: Università degli Studi di Padova
Dipartimento di Scienze del Farmaco

SCUOLA DI DOTTORATO DI RICERCA IN
BIOLOGIA E MEDICINA DELLA RIGENERAZIONE
INDIRIZZO UNICO
CICLO XXVII

A SPATIO-TEMPORAL DISSECTION OF THE TRANSCRIPTIONAL ACTIVITY OF GLUCOCORTICOIDS IN ZEBRAFISH: A NEW TRANSGENIC LINE AS A LIVING BIOSENSOR MODEL.

Direttore della Scuola: Ch.ma Prof.ssa Maria Teresa Conconi
Supervisore: Ch.ma Prof.ssa Luisa Dalla Valle

Dottorando: Elisa Colletti

INDEX

SUMMARY

Glucocorticoids (GCs) are steroid hormones exerting several essential functions during embryo development and physiological processes in adult life. They bind to their specific receptor, which upon ligand binding migrates to the nucleus, dimerizes and binds to specific glucocorticoid responsive elements (GREs) on DNA, which regulate in a positive or negative (nGREs) way the transcription of target genes. Besides, glucocorticoid receptor can indirectly regulate gene transcription, by means of protein-protein interactions with other transcription factors.

This thesis is focused on the transcriptional analysis of GCs activity in the zebrafish model organism. In the first part of my PhD, we set and validated a glucocorticoid responsive zebrafish transgenic line (ia20), in which the green fluorescent protein EGFP (Enhanced-GFP) is located downstream of nine tandem GRE repeats. Thus, this line enables us to follow *in vivo* GCs transcriptional activity, by means of fluorescence observation. Endogenous fluorescence is first ubiquitously detectable during somitogenesis, becoming then more localized in discrete sites during the first days of development, where it persists until adulthood.

EGFP signal increases in a dose-dependent way in response to different DEX concentrations, while *gr* inactivation through antisense morpholino causes a strong fluorescence decrease and the loss of DEX responsiveness.

To validate the ia20 line specificity, we exposed embryos to different steroids at the same concentration: we observed a signal increase only in response to GCs treatments, while fluorescence was not modified by mineralocorticoids, androgens and estrogens treatments. Besides, we collected larvae every 2 hours for 28 hours and demonstrated that the ia20 line is sensitive to the daily endogenous GCs concentration fluctuations due to the circadian rhythm. For all

these features, we can consider the ia20 line a potent biosensor to analyze GCs activity from a spatio-temporal point of view.

In the last part of this thesis, we put the ia20 line in *gr*^{s357} mutant background. In these mutants, the transcriptional activity of the glucocorticoid receptor mediated by a direct DNA binding is missing because of a single amino acid substitution in the DNA binding domain. The receptor function not requiring a direct DNA binding is maintained in mutants. Indeed, the mutation is not lethal in homozygosis. This line was generated in order to characterize the possible cross-reactivity among different steroid hormones, since glucocorticoid, mineralocorticoid, androgen and progestin receptors share the ability to bind GREs (that for this reason are also called "Hormone Responsive Elements", HREs). In the ia20 line in gr^{s357} background we observed a clear fluorescence decrease and a complete loss of GCs responsiveness at 3 dpf (days post fertilization), even at high GCs concentrations, suggesting that, at least during early development, the ia20 line is able to respond only to GCs. We also observed a decrease of endogenous fluorescence intensity at later stages, at 21 dpf and in some tissues in adults (but the latter result derives from a preliminary experiment).

Besides, preliminary experiments on adult fish suggest that liver and gut only respond to glucocorticoid receptor in the ia20 line, because these tissues do not show endogenous fluorescence and do not respond to DEX in mutant background. In gonads, instead, and although to lesser extent in muscle, we hypothesize that androgens and progestins receptors may contribute to GREs-mediated transcriptional activity.

RIASSUNTO

I glucocorticoidi sono ormoni steroidei con un ruolo di fondamentale importanza durante lo sviluppo embrionale e in molti processi fisiologici durante tutta la vita. Svolgono la loro funzione legandosi al loro recettore che in risposta al legame migra nel nucleo, dimerizza e si lega a specifiche sequenze di DNA responsive ai glucocorticoidi (glucocorticoid responsive elements, GREs). In questo modo regolano positivamente o negativamente (nGREs) la trascrizione di geni bersaglio. Il recettore per i glucocorticoidi può inoltre regolare la trascrizione genica in modo indiretto, mediante interazioni proteina-proteina con altri fattori di trascrizione.

Questo lavoro di tesi si è focalizzato sull'analisi trascrizionale dell'attività dei glucocorticoidi nell'organismo modello zebrafish. Durante la prima parte del percorso di dottorato è stata messa a punto e validata una linea transgenica di Zebrafish (ia20) responsiva ai glucocorticoidi, nella quale la proteina fluorescente EGFP (Enhanced-GFP) si trova a valle di nove ripetizioni in tandem della sequenza GRE. Mediante l'osservazione della fluorescenza è quindi possibile monitorare *in vivo* l'attività trascrizionale dei glucocorticoidi. La fluorescenza endogena inizia ad essere apprezzabile a partire dalla somitogenesi ed è inizialmente ubiquitaria, per poi localizzarsi in siti discreti nei primi giorni di sviluppo dove rimane rilevabile anche in età adulta. In risposta al trattamento con diverse concentrazioni del glucocorticoide sintetico desametasone (DEX), il segnale della EGFP aumenta in modo dose-dipendente, mentre l'inattivazione del trascritto per il *gr,* ottenuta mediante l'iniezione di un morpholino antisenso, provoca una considerevole diminuzione del segnale e la mancata risposta al DEX. La specificità della linea è stata validata trattando gli embrioni con diversi steroidi alla stessa concentrazione: il segnale aumenta solo in risposta ai glucocorticoidi mentre rimane invariato nei trattamenti con mineralocorticoidi, androgeni ed

estrogeni. Inoltre, un campionamento ogni 2 ore nell'arco di un periodo di tempo di 28 ore ha dimostrato che la linea transgenica ia20 è sensibile alle variazioni di concentrazione dei glucocorticoidi endogeni dovute al ritmo circadiano. Queste caratteristiche rendono la linea ia20 un efficace biosensore per analizzare l'attività dei glucocorticoidi *in vivo* dal punto di vista spaziale e temporale.

Durante l'ultimo periodo di dottorato, la linea ia20 è stata messa in background mutante gr^{s357}. In questi mutanti, l'attività trascrizionale del recettore dei glucocorticoidi legata ad un'interazione diretta con il DNA viene persa a causa di una singola sostituzione amminoacidica a livello del dominio di legame al DNA. Vengono invece mantenute le altre funzioni di controllo della trascrizione del recettore. La linea è stata generata con lo scopo di caratterizzare l'eventuale presenza di cross-reattività da parte dei diversi ormoni steroidei, in quanto i recettori per i glucocorticoidi, mineralocorticoidi, androgeni e progestinici condividono la capacità di legarsi ai siti GRE (definiti per questo motivo anche "Hormone Responsive Elements", HREs). Nella linea ia20 in background mutante abbiamo osservato una notevole riduzione nella fluorescenza endogena ed una totale perdita di responsività ai glucocorticoidi anche a concentrazioni elevate su embrioni di tre giorni. Questo risultato suggerisce la mancanza di cross-reattività fra i diversi ormoni steroidei nei primi giorni di sviluppo, e questo a causa della mancata espressione di alti livelli dei recettori degli altri ormoni steroidei. Per quanto riguarda gli stadi più avanzati, la diminuzione nella fluorescenza endogena nei mutanti è stata osservata anche a tre settimane e in alcuni tessuti dell'adulto, in un esperimento preliminare che dovrà essere in seguito approfondito. Esperimenti preliminari su pesci adulti suggeriscono inoltre che la fluorescenza osservata nella linea ia20 su fegato ed intestino derivi solo dall'attivazione del recettore dei glucocorticoidi, in quanto nel mutante questi tessuti non presentano alcun segnale di fluorescenza e non rispondono al trattamento con il DEX. Per quanto

riguarda le gonadi, e in misura minore il tessuto muscolare, il segnale fluorescente presente negli esemplari mutanti e la mancata risposta al DEX, possono essere spiegati dall'attività trascrizionale determinata dai recettori per gli androgeni e i progestinici.

1. GLUCOCORTICOIDS

1.1 Glucocorticoids physiological effects

Glucocorticoids (GCs) are steroid hormones involved in several physiological processes and essential for a proper embryo development. They exert a fundamental role in homeostasis maintenance and stress response. Endogenous GCs control metabolism through carbohydrates and protein breakdown, lipid deposition and breakdown regulation. Moreover, they can raise blood pressure and inhibit cell growth (Buckingham, 2006). GCs promote immune cell apoptosis and regulate inflammatory cytokines expression: they suppress the expression of pro-inflammatory cytokines like Il-1β, Il-6, Il-8, TNF-α and enhance the expression of anti-inflammatory cytokines, such as Il-10; they also impair leukocyte migration to the site of inflammation, and disrupt endothelium, leukocytes and fibroblasts functions during inflammation (De Bosscher *et al*., 2003). Due to these potent anti-inflammatory effects, they have been used in the last decades for the symptomatic treatment of acute and chronic inflammation, autoimmune diseases such as asthma, allergy, sepsis, rheumatoid arthritis, ulcerative colitis and multiple sclerosis (Sorrels and Sapolsky, 2006; Oakley *et al.*, 2013). Besides, GCs play a cardinal role in stress response. Stress occurs when the homeostasis is threatened, or perceived to be threatened, by physical or emotional factors (stressors), and the stress system acts on several tissues in order to cope with the stressful situation (Charmandari *et al.*, 2005; Buckingham, 2006; Chrousos, 2009). Physical changes include an increase of blood pressure, heart and respiratory rate, gluconeogenesis and lipolysis and the inhibition of growth, reproduction and immune response. Moreover, the stress response brings about some behavioral adaptations, like an increase of

cognition and attention and the suppression of appetite (Charmandari *et al.*, 2005).

1.2 Circulating GCs synthesis and regulation

Cortisol is the predominant endogenous GC in humans and teleosts, whereas corticosterone is the main GC in rodents, reptiles, amphibians and birds; sheep, pig and dog produce an equal amount of cortisol and corticosterone (Buckingham, 2006). GCs are synthetized from cholesterol in the *zona fasciculata* of the adrenal cortex in mammals and in the homologous structure, the interrenal tissue of the head kidney, in teleosts (Buckingham, 2006; Bury and Sturm, 2007). Circulating GCs levels are not constant during day time, but their biosynthesis varies according to the circadian rhythm. In diurnal species, GCs reach their maximum concentration peak just before waking. Then the GCs levels remain high during the day, i.e. during activity period, while they reach nadir at the beginning of the sleep phase, remaining low during the night (Buckingham *et al.*, 2006; Chung *et al.*, 2010).

GCs production is finely regulated by the hypothalamus-pituitary-adrenal axis (HPA) in mammals, and the hypothalamus-pituitary-interrenal axis (HPI) in fish, consisting in stimulatory signals regulated by a feed-back mechanism. The hypothalamus receives and integrates neural and humoral *stimuli* deriving from the presence of stressors or circadian factors, and releases a neuropeptide, the corticotropin-releasing-hormone (CRH), also known as corticotropin-releasing-factor (CRF). In most vertebrates, CRH reaches the adenohypophysis through the hypophyseal–portal blood vessels. This portal system is lacking in fish, where CRH reaches the adenohypophysis carried by nerve fibers of the preoptic region (Levavi-Sivan *et al.*, 2009). In both cases, the result is the release induction of the adrenocorticotrophic hormone (corticotrophin, ACTH)

from the adenohypophysis to the systemic circulation. The target tissue of ACTH is the adrenal/interrenal tissue, where it activates proteins and induces the expression of genes involved in GCs biosynthesis, thus stimulating GCs synthesis and secretion (Buckingham, 2006; Nesan and Vijayan, 2013; Nicolaides *et al.*,

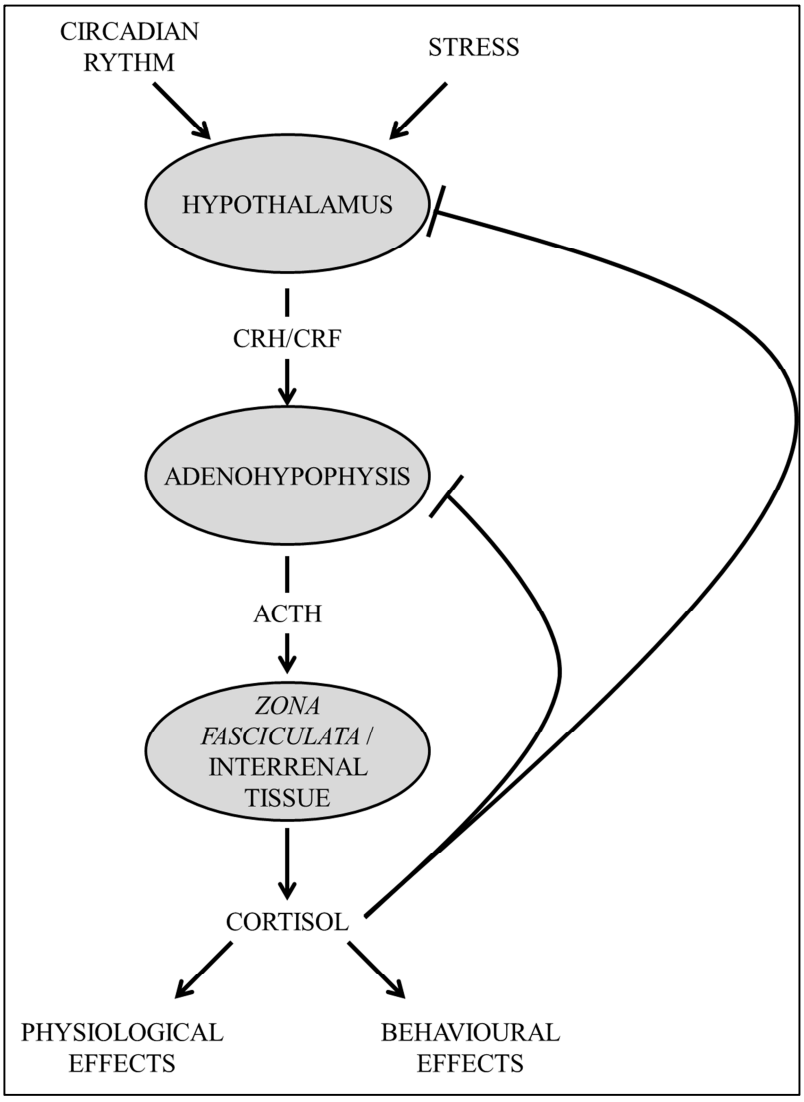

2014). HPA and HPI axis regulation is summarized in Figure 1.

Fig. 1. Summary of HPA and HPI axis.

An unbalance of circulating GCs is pathological in humans: an excess of GCs causes Cushing's syndrome, which main features are centripetal obesity, muscle weakness, hyperglycemia, diabetes mellitus, immunodeficiency, an impairment in wound healing and a delay in growth and development. Addison's syndrome, instead, is characterized by an increase in stress vulnerability and is caused by an insufficient GCs amount (Buckingham, 2006).

2. GLUCOCORTICOID RECEPTOR

2.1. The nuclear receptor superfamily

Nuclear receptors are a superfamily of DNA-binding transcription factors exerting a plethora of physiological functions through genomic or non-genomic, ligand dependent or non-dependent actions. They can act as transcription factors by contributing to gene activation, repression or release of gene expression (Germain et al., 2006).

According to DNA binding and dimerization properties, the members of the nuclear receptors superfamily can be divided into four classes: steroid receptors, RXR heterodimers, homodimeric orphan receptors and monomeric orphan receptors (orphan receptors are so called because no specific ligand has been identified yet) (Mangelsdorf *et al.*, 1995). They can also be split into two subtypes: type 1 nuclear receptors, acting as homodimers upon ligand binding, and type 2 nuclear receptors, acting as heterodimers. Type 1 receptors include the "steroid hormone receptors family" composed by the receptors for estrogens (ERα and ß), glucocorticoids (GR), mineralocorticoids (MR), progestins (PR) and androgens (AR). Type 2 receptors include non-steroid hormone receptors like vitamin D receptor (VDR), thyroid hormone receptor (TR), retinoic acid receptor (RARα, ß and γ) and peroxisome proliferator-activated receptor (PPAR), that act mainly as heterodimers with the retinoic X receptor (RXR) (Mangelsdorf *et al.*, 1995).

The human glucocorticoid receptor (GR) was the first nuclear receptor protein cloned by Evans and colleagues in 1985 (Hollenberg et al., 1985; Germain et al., 2006; Heitzer et al., 2007).

Nuclear receptors share a common modular structure, in which three major domains are highly conserved among vertebrates: a N-terminal domain (NTD), a DNA binding domain (DBD) and a C-

terminal ligand binding domain (LBD) (Kumar and Thompson, 2005; Germain et al., 2006).

The N-terminal domain is poorly conserved, except for a ligand-independent region, AF-1 (activate function-1), which is able to autonomously activate transcription by a direct interaction with the transcription machinery (Germain et al., 2006; Heitzer et al., 2007).

The most conserved domain is DBD (DNA binding domain), especially a sixty-six residue core containing eight cysteines that tethraedrally clusterize two zinc atoms (zinc finger DNA binding motifs), two α-helices and a COOH extension. The DBDs of glucocorticoid receptor, mineralocorticoid receptor, progesterone receptor and androgen receptor recognize the same consensus motif on DNA (hormone responsive element, HRE), an imperfect palindromic sequence made of two inverted repeats of an hexanucleotide, separated by a 3-bp spacer (GGTACAnnnTGTTCT) (Germain et al., 2006; Heitzer et al., 2007; Merkulov and Merkulova, 2009). HREs are normally located upstream of nuclear receptors target genes, and are involved in the correct positioning of the receptors and the transcriptional complexes (Oakley et al., 2013). When referring to the glucocorticoid receptor, HREs are also called glucocorticoid responsive elements (GREs).

Tissue specificity is determined in different ways:

- expression of the receptors in specific cell types (McKenna and O'Malley, 2002);
- post-translational modification of the receptors by means of cell specific kinases that can modulate the receptors activity through the phosphorylation of the NTD, the hinge region or the LBD (Weigel and Moore, 2007; Oakley and Cidlowski, 2011);
- different chromatin accessibility and recruitment of different transcriptional co-activators or co-repressors (Heitzer *et al.*, 2007; Oakley *et al*., 2013).

The LBD (ligand-binding-domain) is located at the C-terminus and contains the ligand binding pocket. The ligand is bound by means of hydrophobic residues, and the hormone-specificity is determined by the shape of the ligand binding pocket. Besides, in the glucocorticoid receptor, in the absence of ligand, LBD interacts with HSP90 (heat shock protein 90), that prevents the receptor from binding DNA. Upon ligand binding, HSP90 is released, thus allowing receptor dimerization and translocation to the nucleus. LBD also contains the hormone-dependent AF-2 (activation function-2) domain, which interacts with transcriptional co-activators or co-repressors (Germain *et al*., 2006; Heitzer *et al.*, 2007; Oakley *et al.*, 2013). The general steroid nuclear receptor structure is summarized in Figure 2.

Fig. 2. Schematic representation of steroid hormone receptor domains. NTD: N-terminal domain, containing AF-1 region; DBD: DNA binding domain; H: poorly conserved hinge region; LBD: ligand binding domain, also containing AF-2 region. Figure from Heitzer *et al.*, 2007.

2.2. Glucocorticoid receptor gene in zebrafish

Despite the whole genome duplication that occurred in teleosts 300-450 million years ago (Volff, 2005), in the zebrafish genome only one glucocorticoid receptor gene (*gr*, *nr3c1*) is present (Schaaf *et al.*, 2009). *gr* is highly conserved between humans and zebrafish. Both human and zebrafish glucocorticoid receptor genes are made of nine exons: noncoding exon 1, exon 2 encoding for NTD, exons 3 and 4 encoding for DBD and exons 5-9 encoding for the hinge region and LBD. Exon 9 undergoes alternative splicing, thus generating two Gr

isoforms, named Gr-α and Gr-β, that differ in the C-terminal residues. This alternative splicing has not been found in rodents (Otto *et al.*, 1997). The structure of the human and zebrafish genes and the splicing variants are shown in Figure 3 (Schaaf *et al.*, 2009). Gr-α is responsible for the canonical glucocorticoid signaling, while Gr-β, located in the nucleus, is unable to bind glucocorticoids or their agonists and acts as a Gr-α dominant-negative inhibitor. The Gr-β isoform may be the cause of glucocorticoids resistance (Schaaf *et al.*, 2009; Oakley *et al.*, 2013). In this thesis, when referring to glucocorticoid receptor, only the Gr-α isoform will be considered.

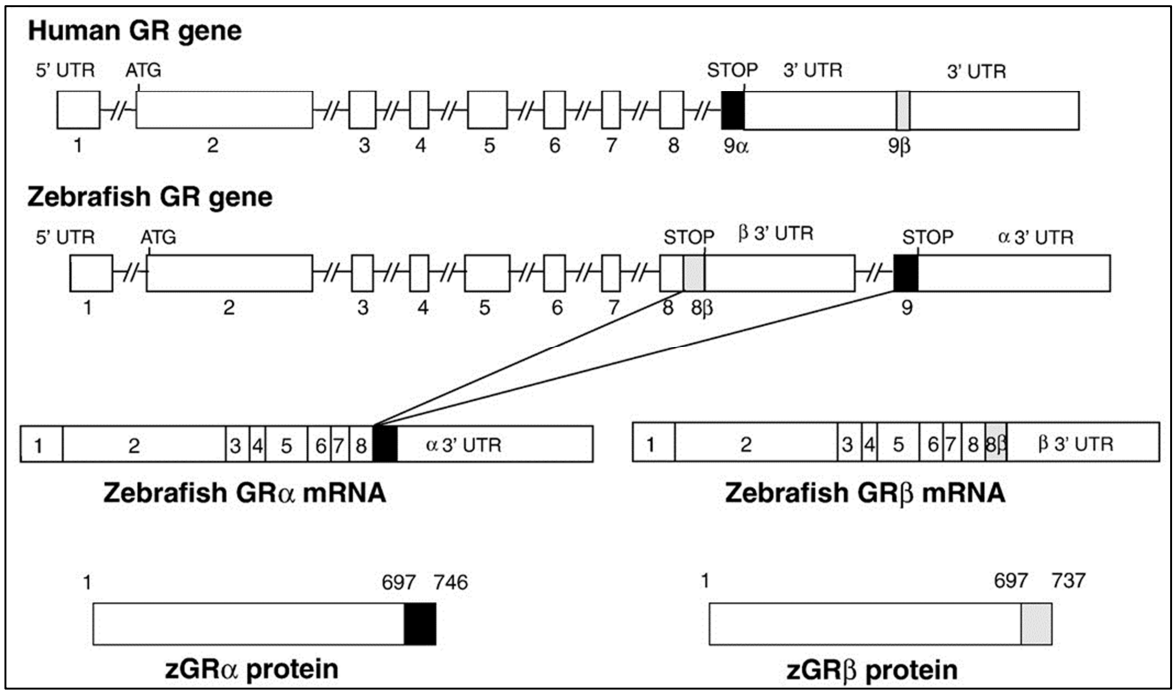

Fig. 3. Comparison between the structures of human and zebrafish glucocorticoid receptor genes and splicing variants. Two isoforms (Gr-α and Gr-β), which differ for 40 amino acids at the C-terminus, are present in both species. In humans, the two forms derive from the alternative splicing of exon 9. In zebrafish, Gr-α contains a shorter exon 8 plus exon 9 whereas the specific sequence encoding for Gr-β isoform is constituted by a longer exon 8. Figure modified from Schaaf *et al.*, 2009.

Alternative splicing also produces several less characterized isoforms in the human *GR* (*hGR*) (summarized in Figure 4) with different

effects on GCs signaling (Oakley and Cidlowski, 2011). *GR-*γ derives from the use of an alternative splice donor site between exons 3 and 4, causing the insertion of an arginine residue in the DBD, between the two zinc finger domains. This single amino acid modification causes the activation of different target genes with respect to the α isoform, while the binding of the ligand is not compromised (Oakley and Cidlowski, 2011). *GR-A* is lacking of the N-terminal part of the LBD, due to alternative splicing linking exon 4 to exon 8. In *GR-P*, exons 8 and 9 are missing, so this isoform lacks of the C-terminal region of the LBD. These two isoforms are not able to bind hormones (Oakley and Cidlowski, 2011). Moreover, *GR-*α also undergoes alternative translation initiation in exon 2, thus generating eight additional isoform. Similarly, also *GR-*β is predicted to generate eight alternative isoforms (Kadmiel and Cidlowski, 2013).

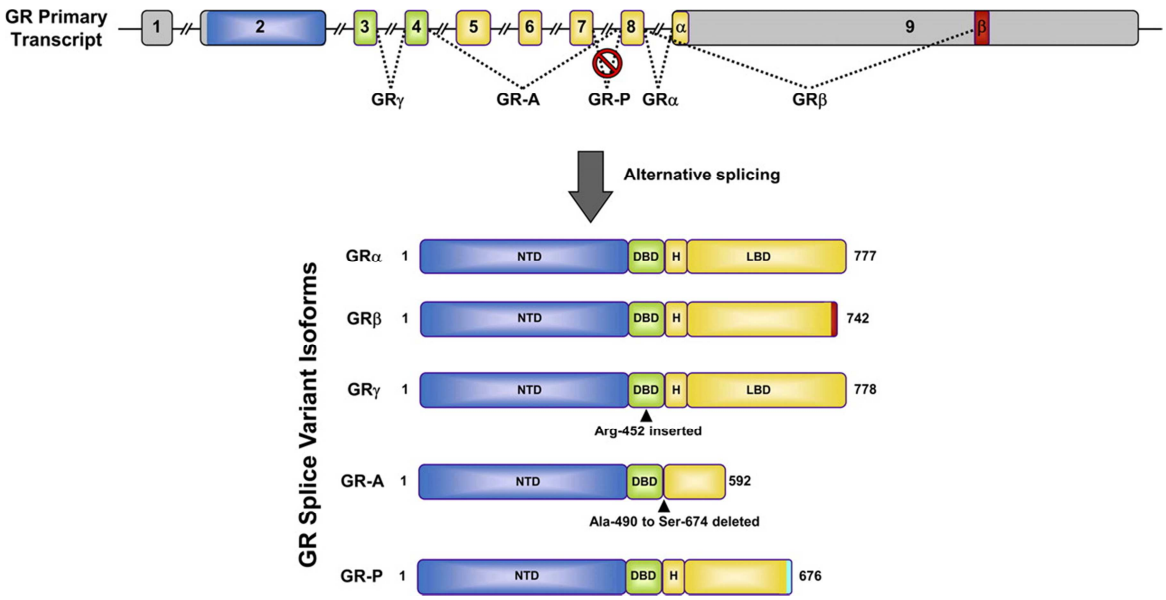

Fig. 4. *hGR* isoforms, deriving from alternative splicing. Figure from Oakley and Cidlowski, 2011.

2.3 Glucocorticoid receptor physiology

2.3.1 Direct gene expression regulation

In the absence of ligand, glucocorticoid receptor is located in the cell cytoplasm as part of a multimeric complex, including Hsp40, Hsp70, Hsp90, P23, Fkbp51 and Fkbp52. In this conformation Gr is transcriptionally inactive and Hsp90 keeps the hydrophobic ligand domain pocket open, in order to allow high-affinity ligand bond (Morishima *et al.*, 2001). Cortisol can pass through the plasma membrane by simple diffusion, but its bioavailability inside the cell is finely regulated by the equilibrium between two enzymes: 11β-Hydroxysteroid dehydrogenase type 1 that converts inactive cortisone to its active form, cortisol, and 11β-Hydroxysteroid dehydrogenase type 2 that oxidizes cortisol to inactive cortisone (Oakley *et al.*, 2013).

Upon ligand binding, Gr undergoes a conformational change and the multiprotein complex dissociates, thus exposing the Gr nuclear localization signals that trigger Gr translocation to the nucleus through nuclear pores. After migrating to the nucleus, Gr directly binds to DNA on GRE sequences, in the promoter region of target genes, where a new conformational change triggers Gr homodimerization, for which the 3 basis pair spacer is critical, and the recruitment of transcriptional co-activators (Smoak and Cidlowski, 2004; Oakley *et al.*, 2013).

Besides canonical GREs-mediated signaling, Gr can also act as a transcriptional repressor when it directly binds to negative GREs (nGREs), thus preventing other transcription factors recruitment. As GREs, nGREs are imperfect palindromic sequences ($CTCC(n)_{0-2}GGAGA$) but, differently from GRE sequences, the variable length of the spacer does not trigger receptor dimerization (Schoneveld et al, 2004; Smoak and Cidlowski, 2004; Oakley *et al.*, 2013). Pro-opiomelanocortin (POMC), corticotropin-releasing hormone (CRH) and

neuronal serotonin receptor are among the genes that are nGREs-repressed (Revollo and Cidlowski, 2009).

2.3.2 Crosstalk with other transcription factors

Gr can indirectly regulate gene expression through protein-protein interactions with Nuclear Factor κB (NFκB), Activator Protein-1 (AP-1), Signal Transduction and Activator of Transcription (STAT) family and Sma-MAD (Smad) family transcription factors.

NFκB is activated by infection products and pro-inflammatory cytokines and induces the transcription of genes encoding for other pro-inflammatory cytokines and their receptors, such as tumor necrosis factor α (TNFα), Il-1β, granulocyte monocyte colony stimulating factor (GMCSF) and inflammatory mediators, like cyclooxygenase-2 (COX-2) and inducible nitric oxide synthase (iNOS). Interestingly, it also represses Gr GREs-mediated transcriptional activation. Gr inhibits NFκB by binding to its p65 subunity, thus impairing transcriptional activation. Several mechanisms have been suggested for this Gr-mediated antagonism: a physical impairment for NFκB to reach the nucleus, a competition for transcriptional co-activators recruitment, or the interference with RNA polymerase activation (De Bosscher *et al.*, 2003; Smoak and Cidlowski, 2004; Revollo and Cidlowski, 2009).

Ap-1 is activated by TNF- α and Il-1β and, similarly to NFκB, activates the transcription of pro-inflammatory cytokines and tissue-destructive enzymes, like collagenase. Gr inhibits Ap-1-mediated transcriptional activation with mechanisms that are similar to NFκB inhibition, after binding to c-Jun subunity on Ap-1 (De Bosscher *et al.*, 2003; Smoak and Cidlowski, 2004; Revollo and Cidlowski, 2009).

The members of the STAT family are indirectly activated by pro-inflammatory cytokines, by induction of the Janus Kinase (JAK) pathway, and regulate genes involved in growth, survival, apoptosis, host defense, stress, and differentiation. Gr interacts with several

members of the STAT family (STAT-1, STAT-3, STAT-5 and STAT-6). Transcriptional regulation can either be positive or negative, according to the specific STAT involved, the promoter context and external *stimuli* (Smoak and Cidlowski, 2004; Revollo and Cidlowski, 2009). Upon Il-6 activation, STAT3 is a potent co-activator of glucocorticoid receptor (Zhang *et al.*, 1997).

Smad family transcription factors are activated by the TGF-β pathway that triggers Smad3 phosphorylation, after which Smad3 binds Smad4 and they activate the transcription of target genes, involved in cell differentiation, extracellular matrix production and immune and inflammatory responses. With a still unclear mechanism, Gr physically binds the Smad3-4 complex and inhibits its transcriptional activation of genes encoding for extracellular matrix proteins and protease inhibitors. When phosphorylated, Smad3 can also activate Gr-mediated gene transcription (Song *et al.*, 1999; Smoak and Cidlowski, 2004; Necela and Cidlowski, 2004; Revollo and Cidlowski, 2009).

Figure 5 summarizes the Gr direct and indirect mechanisms of gene regulation.

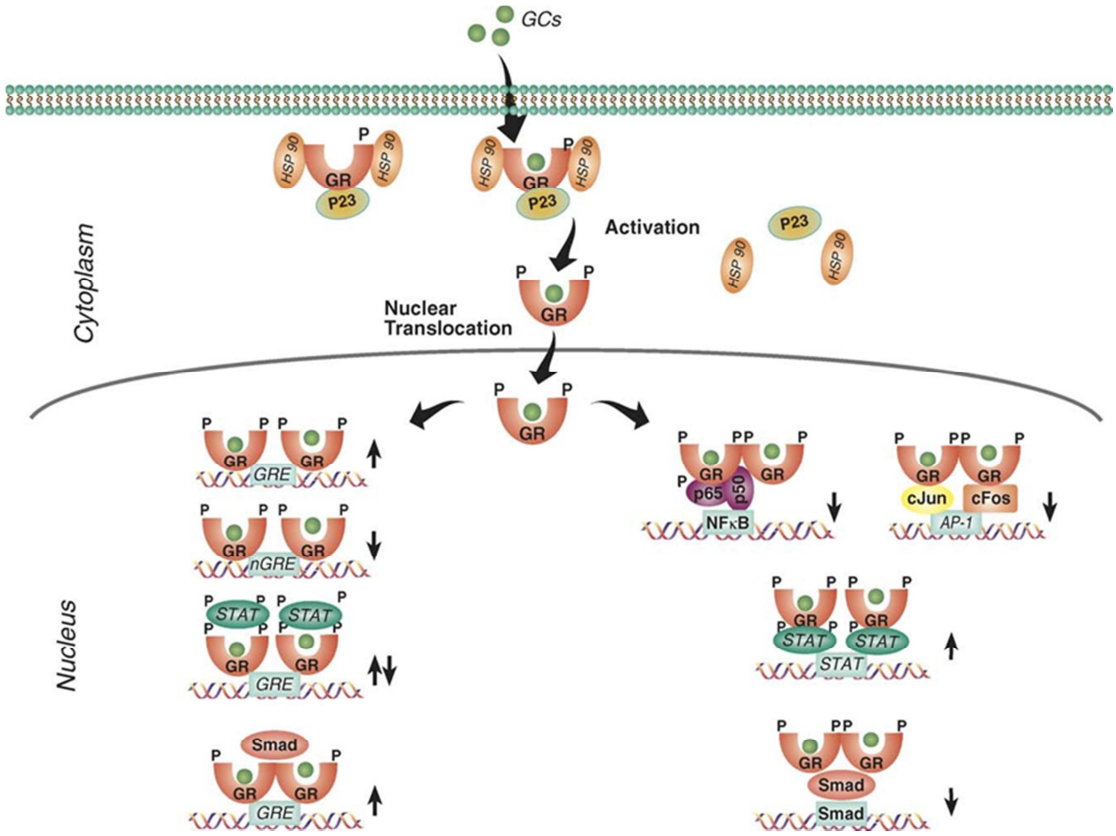

Fig. 5. Mechanisms of action of the glucocorticoid receptor. Figure from Smoak and Cidlowski, 2004.

3. THE GLUCOCORTICOID RECEPTOR IN ZEBRAFISH DEVELOPMENT

3.1. Glucocorticoids in early development

Many studies in mammals have demonstrated that glucocorticoid signaling plays a key role in the development of heart, lungs, gut, pancreas, kidneys, bone and brain. Due to external fertilization, zebrafish overcomes *in utero* studies and can be considered more suitable than mammals model organisms for the characterization of glucocorticoids effects in early development (Nesan and Vijayan, 2013). Moreover, differently from other teleosts, only one *gr* gene is present in the genome of zebrafish, thus improving gene manipulation amenability (Schaaf et al, 2009; Alsop and Vijayan, 2009).

The HPI axis is specified within the first day of development and its formation is completed by 48 hpf, but no stress response is detectable before 72 hpf (Nesan and Vijayan, 2013). Before the beginning of *de novo* cortisol synthesis, only maternal cortisol is present in zebrafish eggs. Maternal cortisol shows a 70% decrease at 25 hpf, and its concentration remains low until the beginning of larval cortisol synthesis (Alsop and Vijayan, 2008). The delay in the arising of stress response has probably a protective function, to avoid an alteration of GCs sensitive pathways in early development (Nesan and Vijayan, 2013). Also the glucocorticoid receptor is maternally provided in the ovulated egg and its messenger shows a decline during the first hours of development, reaching nadir at 8 hpf. Maternal transcripts are then replaced by the corresponding embryonic RNAs (Pikulkaew *et al.*, 2010; Pikulkaew *et al*., 2011). The spatio-temporal *gr* expression is shown in Figure 6.

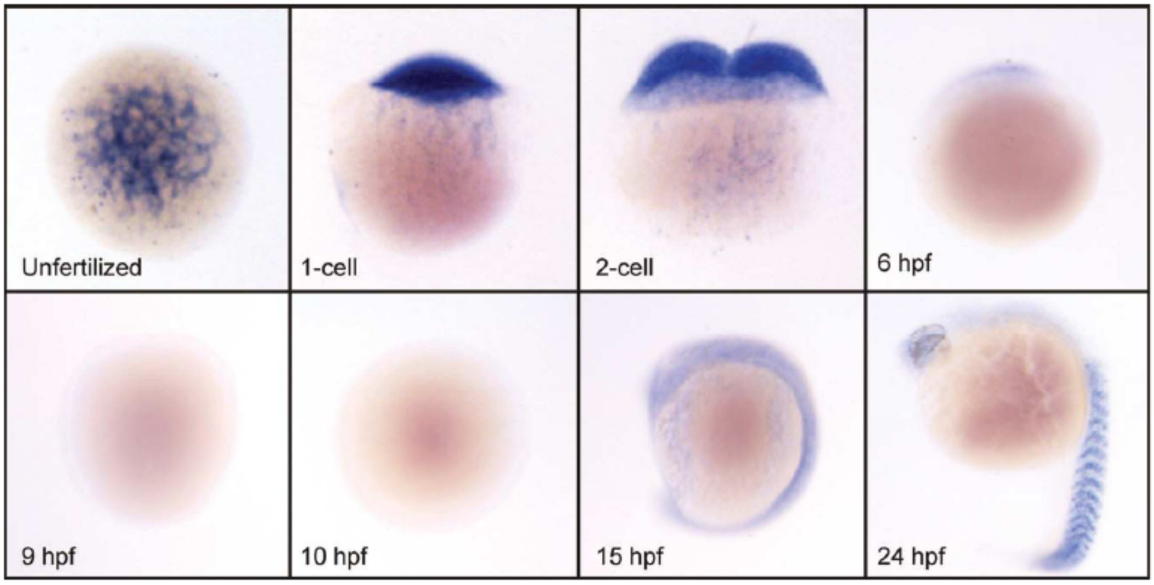

Fig. 6. Whole mount *in situ* hybridization with *gr* probe on wild type embryos. *gr* mRNA is present in the ovulated egg and its concentration declines until MBT, being then replaced by zygotic *gr* transcripts in later stages. Figure from Pikulkaew *et al.*, 2011.

3.2. The role of the glucocorticoid receptor in development: effects of gr knock-down

Most of nowadays knowledge about the essential role that maternal glucocorticoids play in early development was provided by *gr* knock-down experiments performed with the use of morpholino (see chapter 4.3.2). A previous work in our laboratory (Pikulkaew *et al*., 2011) demonstrated that the absence of the glucocorticoid receptor during the first developmental stages causes severe phenotypes in embryos and a mortality increase in the early days of life. Morphant embryos displayed a delay in growth and development, a small head, reduced eyes and otic vesicles. Besides, they showed pericardial oedema, a delay in fin and trunk development and a reduced yolk absorption, probably caused by reduced or absent sub-intestinal veins. Moreover, in morphants swim bladder inflation did not occur and head cartilage formation was compromised. They were not able

to swim, and poorly responded to touch *stimuli*. These embryos also displayed a dramatic increase of apoptosis rate, corresponding to an increase of *caspase8* expression, which is involved in apoptosis promotion (Pikulkaew *et al*., 2011). These results were also confirmed by the knockdown experiments performed by Nesan and coworkers that suggested a role for glucocorticoids in mesoderm and muscle formation. In morphants, they observed an expression decrease of genes involved in mesoderm specification, that could explain the trunk and somite altered phenotypes (Nesan *et al*., 2012). The *gr* trascriptomics analysis revealed a linkage between *gr* and the BMP family. Particularly, *bmp2a*, *bmp2b* and *bmp4* expression is reduced in *gr* morphants. BMPs are deeply involved in development, being implicated in dorso-ventral and mesodermal patterning, somitogenesis, myogenesis, organogenesis and craniofacial morphogenesis (Nesan *et al*., 2012; Nesan and Vijayan, 2013b). Moreover, the expression of genes involved in heart development, angiogenesis, connective tissue development, retinal development and endocrine signaling components was altered in these morphants. These data, put together, might provide an explanation to the phenotypes observed in morphants (Nesan and Vijayan, 2013b).

3.3. In gr^{s357} mutants, Gr transcriptional activity is disrupted

During a large-scale screening after ENU mutagenesis (see chapter 4.2.1), Muto and colleagues identified the gr^{s357} mutants. The screening was carried out in order to detect new mutations causing alteration of visual behavior (Muto *et al.*, 2005).
In gr^{s357} mutants, a missense point mutation in *gr* coding region (Fig. 7) causes the substitution of an arginine with a cysteine in one of the zinc finger motifs in the DNA binding domain. The positive charge of

that arginine is essential for DNA binding, hence this mutation impairs Gr transcriptional activity, when this is mediated to a direct binding to DNA. The hormone binding and the translocation to the nucleus are not compromised by the mutation (Ziv *et al.*, 2013).

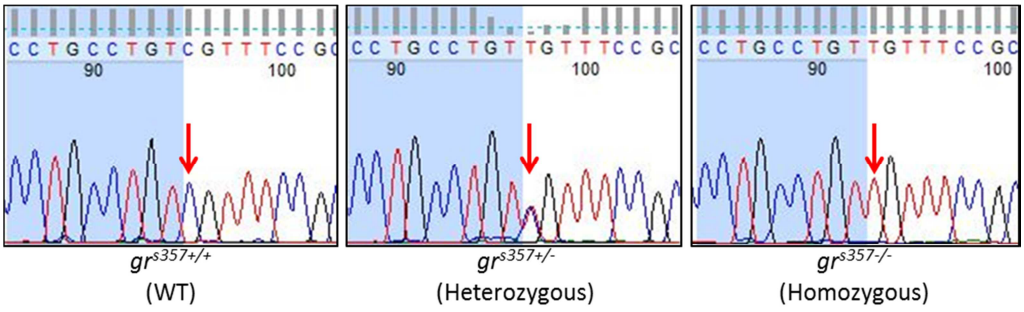

Fig. 7. Genotyping of gr^{s357} mutants: a missense single nucleotide substitution (a C substituted with a T) causes a single amino acid substitution in zebrafish Gr, that impairs DNA binding.

In mouse, the constitutive knock-out of GR is lethal at embryonic stages (Kellendonk *et al.*, 1999), similarly to *gr* knock-down in zebrafish (Pikulkaew *et al.*, 2011). gr^{s357} homozygous mutants, instead, do not display morphological phenotypes and are viable until adulthood. However, they show a delay in light/dark adaptation during larval stage (Muto *et al.*, 2013). Muto and colleagues observed that the optokinetic response (OKR) recovery after dark to light transition was delayed in homozygous mutants with respect of wild type (WT) larvae (30 minutes in $gr^{s357-/-}$ larvae vs 5 minutes in WT) (Muto *et al.*, 2013). Moreover, gr^{s357} homozygous mutant larvae showed an altered visual background adaptation (VBA): the melanine granules in the skin are contracted when the larva is exposed to the light, while melanine is dispersed in a dark environment. In $gr^{s357-/-}$ mutants, the VBA adaptation after dark to light transition was delayed (Fig. 8) (Muto *et al.*, 2013). *gr* is widely expressed in the retina and Muto and colleagues showed that the expression of several

retinal genes, controlled by the glucocorticoid receptor, were altered in homozygous *gr*^{s357} mutants, thus demonstrating that the observed phenotype was caused by the disruption of Gr transcriptional activity (Muto *et al.*, 2013).

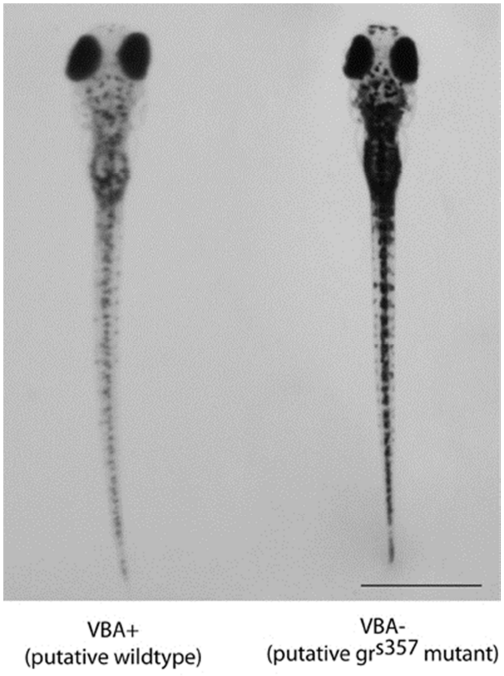

Fig. 8. VBA delay in *gr*$^{s357-/-}$ 5 dpf larvae (scale bar = 1 mm). Figure from Griffiths *et al.*, 2012.

Ziv and colleagues demonstrated that in homozygous mutants the HPA axis is hyper-activated: the concentration of circulating cortisol is chronically elevated, but it is not raised by the exposition to stressors or the treatment with synthetic glucocorticoids. Moreover, they did not display any HPA axis feed-back inhibition in response to high concentrations of glucocorticoids (Ziv *et al.*, 2013). Adult *gr*^{s357} homozygous mutants, due to HPA hyper-activation, displayed exaggerated reactions to anxiogenic environments, resembling chronic stress syndrome (Ziv *et al.*, 2013).

Moreover, the expression of stress markers (*crh*, *pomc*) was increased in homozygous mutants (Ziv *et al.*, 2013). Interestingly, *crh* and *pomc* are negatively regulated by Gr through nGRE sequences (Revollo and Cidlowski, 2009), thus suggesting that their increased expression is caused by Gr transcriptional disruption (Griffiths *et al.*, 2012; Muto *et al.*, 2013).

The loss of *gr* transcriptional activity in gr^{s357} mutants was *in vitro* confirmed by Ziv and colleagues in 2013, by means of cell lines that do not express the glucocorticoid receptor. These cell lines were co-transfected with the WT or mutated Gr and a construct containing Gr-dependent transcriptional activatory or repressive sequences upstream of target genes. They observed that, in the mutated Gr, the transcriptional activity mediated by GREs, nGREs or the tethering of other transcription factors upon Gr DNA binding was largely eliminated, even after GCs treatment (Ziv *et al*., 2013).

4. ZEBRAFISH

4.1. A brief *excursus* on zebrafish: breeding and development

Zebrafish, *Danio rerio*, is a small tropical fishwater teleost. It belongs to the Cyprinidae family and its natural habitat is South-East Asia. Due to its several advantages, it has been widely used in research in the last decades to characterize vertebrate development, genetics, physiology and for biomedical, toxicological, behavioral and *in vivo* cell biology studies.

Zebrafish can be bred in laboratory, under reproducible and not too expensive conditions. The mechanisms of sex determination are not known to date (Nasiadka and Clark, 2012), but males and females usually display a clear sex dimorphism (Fig. 9.) that enables researchers to set focused husbandries. Males are streamline-shaped and their abdomen region is gold-reddish, while in females the abdomen is larger than in males and light-silver colored (Nasiadka and Clark, 2012).

Fig. 9. Adult male (top) and female (bottom) Zebrafish. Figure from http://carnivoraforum.com/topic/9774568/1/.

Fertilization and development are external and every female can produce about 200 eggs per spawn. Embryos transparency in the early days of development and their small size (about 1 mm diameter/length) make them suitable for microinjection, drug treatments and *in vivo* imaging. Development is very fast when compared to other vertebrate model species (e.g. mouse), and it can be easily followed in the transparent embryos. In zebrafish, gastrulation occurs within 10 hours post fertilization (hpf) and by 24 hpf the body axes have already been established and neurogenesis and primary organogenesis are ongoing. By 5 days post fertilization (dpf), organogenesis is complete and embryos have already developed into swimming and feeding larvae. Figure 10 shows some exemplificative embryos and larvae stages from fertilization (0 hpf) to 5 dpf. At 3-4 months they reach sexual maturity, so generation time is very short and 3-4 generations can be obtained in one year (Kimmel *et al*., 1995; Dahm and Geisler, 2006; Vacaru *et al*., 2014).

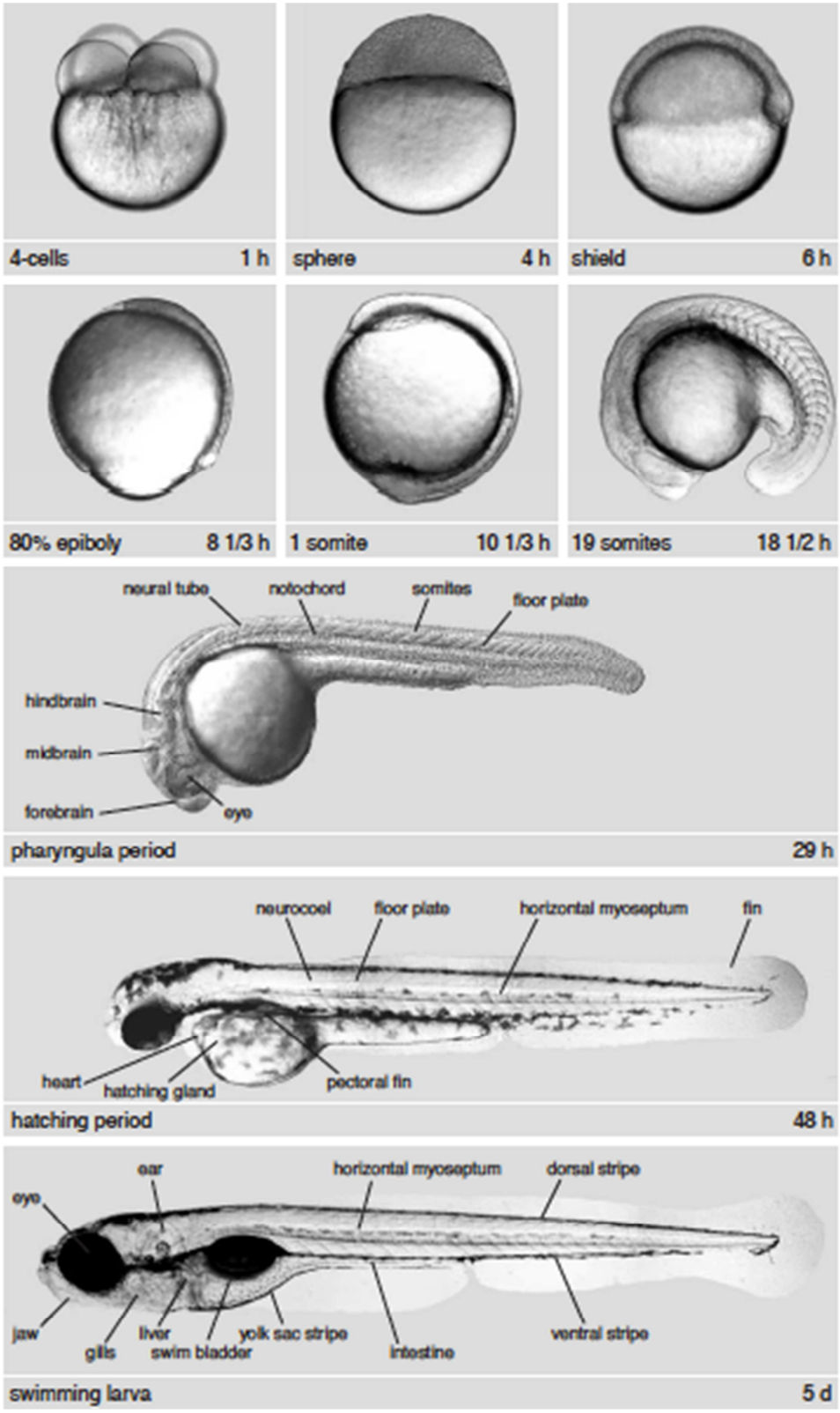

Fig. 10. Living wild type embryos and larvae of relevant stages from 0 hpf to 5 dpf. Figure from Haffter et al., 1996.

4.2. Zebrafish genetics tools: a model organism for human disease

Zebrafish is currently used in research as an animal model for several disorders, including muscular dystrophies, neurodegenerative disease, cancer, diabetes and cardiovascular disease (Ingham, 2009; Tavares and Santos Lopes, 2013).

4.2.1. Forward genetics

Forward genetics studies are mainly based on the screening of mutants, randomly generated with chemical compounds (N-ethyl-N-nitrosourea ENU), retroviruses or transposons. These approaches were widely used in past years, but they are time-consuming and display a great disadvantage: since most of the zebrafish genome was duplicated, many genes are redundant and it might not be possible to identify the phenotype of each of them (Huang *et al*., 2012; Varshney and Burgess, 2013).

4.2.2. Reverse genetics

After the sequencing of human genome, with the arising of reverse genetics approaches, the zebrafish importance as a model for human genetic disorders has been quickly growing. The zebrafish genome sequencing has been completed and annotated by the Wellcome Trust Sanger Institute. It contains about 26000 protein-coding genes, 70% of which were identified as human orthologs (Howe *et al*., 2013). As reverse genetics approaches in zebrafish, both gene knock-down and gene knock-out are now possible. In these cases, the issue of redundancy can be solved by targeting both paralogs.

Gene knock-down is based on the microinjection, in one cells embryos, of morpholinos (MOs), 18-25 basis long artificial single strand oligonucleotides in which the nucleotides backbone is chemically modified in order to prevent nuclease-mediated

degradation, without disrupting the Watson-Crick base pairing between morpholinos and nucleic acids (Eisen and Smith, 2008). Antisense morpholinos are used to target specific mRNAs and prevent the transcript maturation and translation. The resulting phenotypes will be phenocopies of those caused by genomic mutations (Huang *et al.*, 2012).

They can bind to the ATG site, thus blocking maternal and zygotic transcripts translation, or to a splice site, thus affecting only zygotic transcripts. In this thesis, *gr* will be silenced both with ATG-morpholino and splicing-morpholino, previously validated in the laboratory (Pikulkaew et al, 2011).

Morpholino effects do not need to be confirmed by genotyping and the knock-down can be performed on many embryos simultaneously. However, MO knock-down displays some limits: it undergoes dilution at every cell division, thus losing efficiency after 4-5 days, and its effects are not heritable (Dahm and Geisler, 2006; Huang *et al.*, 2012).

Moreover, several additional controls are necessary in order to confirm that the observed phenotype is specific and not caused by toxicity:

- One critical step is the determination of MO effectiveness. If a specific antibody is available, the knock-down efficiency can by validated by western blot. For MOs targeting splicing sites, the effectiveness can be tested simply by PCR (Eisen and Smith, 2008).
- To detect the possible effects caused by injection toxicity, a mismatch MO, differing from the working MO for five bases, should be co-injected in parallel with the active MO. If MO effects are specific, the embryos injected with this control MO should display no altered phenotypes (Eisen and Smith, 2008).
- If the phenotype is specific, it should be rescued by co-injection of MO with the target gene mRNA (Eisen and Smith, 2008).

- 15-20% of MOs, for still unknown mechanisms, activate the p53 pathway, causing apoptosis induction and non-specific phenotypes. This limit can be overcome by co-injection of a MO targeting *p53* (Eisen and Smith, 2008; Huang *et al.*, 2012).

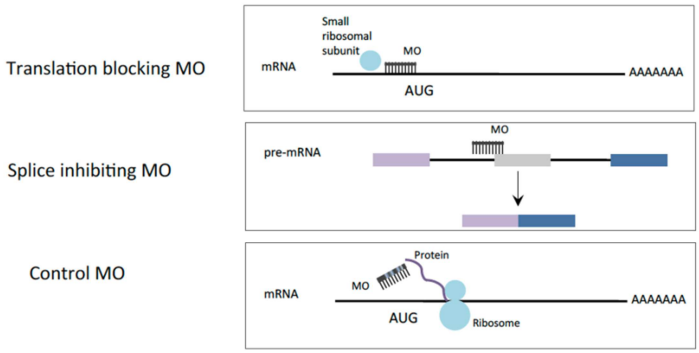

Fig. 11. Schematic representation of different types of MO oligos. Figure from PhD thesis of Tatjana Skobo, 2014.

In recent years, new promising knock-out techniques based on engineered DNA-binding proteins were developed, with the great advantage of enabling the generation of targeted mutations. TALENs mediated gene targeting exploits the transcription activator-like effectors (TALEs), DNA-binding proteins naturally produced by a plant pathogen bacterium, fused with the catalytic site of an endonuclease, FokI (Varshney and Burgess, 2013). CRISPR and Cas system is based on the engineering of a host defense system of bacteria and archaea. In this technique, a DNA site-specific cleavage is mediated by a CRISPR RNA that, when annealed to a *trans*-activating RNA, guides the nuclease *cas9* to the target site on DNA, producing a site-specific cleavage (Varshney and Burgess, 2013).

4.2.3. Transgenesis: the Tol2kit strategy

Transgenesis has been developing in the last decades as a potent tool to characterize *in vivo* cellular, biochemical and molecular processes such as gene expression, signaling pathways and transcriptional regulation during development, adult life and disease (Kwan *et al*., 2007; Moro *et al*., 2013).

Kwan and coworkers elaborated a new strategy (the Tol2kit), based on the Gateway system that overcame most of the disadvantages of previous transgenesis techniques, which were time-consuming and displayed low efficiency (Kwan *et al.*, 2007). In the Gateway cloning system, three entry vectors (5' entry vector, middle entry vector and 3' entry vector) are directionally combined in a final destination vector by means of the recombination between two specific recombination sites (*att*) located at their extremities, deriving from lambda phage. The 5' entry vector contains the enhancer-promoter elements. They can be constitutive promoters (e.g. *β-actin2*) for whole organism expression, conditionally activated promoters (e.g. *hp70* for heat-shock activation or UAS for Gal4-induced activation) or minimal promoters (e.g. *thymidine kinase*) located downstream of transcriptional regulatory elements. The middle entry vector supplies the reporter gene, which is usually a fluorophore such as the enhanced green fluorescent protein (EGFP) or the monomeric red fluorescent protein (mCherry). The 3' entry vector contains the transcription termination signal (PolyA) from SV40. If necessary, it can also carry a subcellular localization tag. After joining the three entry vectors, they are cloned in a Tol2-based destination vector. The destination vector is flanked by Tol2 transposon sequences, which are essential for transposition (Kwan et al, 2007; Moro et al, 2013). The building of the expression donor construct is represented in Figure 12.

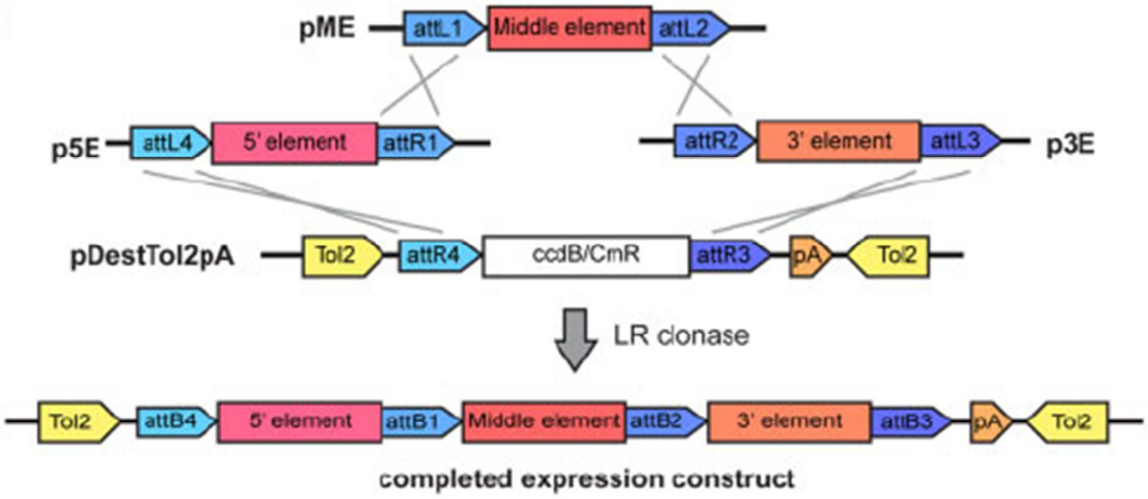

Fig. 12. The building of a transgenic expression donor construct: the 5' entry vector (p5E), the middle entry vector (pME) and the 3' entry vector (p3E) are combined together and cloned to a destination vector (pDestTol2pA), flanked by Tol2 transposon sequences. Figure modified from Kwan *et al.*, 2007.

The donor construct is then microinjected in one cell embryos, together with the mRNA encoding for a transposase, which is translated into protein in the receiving cells. The transposase recognizes the Tol2 sequences and catalyzes the excision of the donor construct and its integration in the genome. The integration becomes stable after transposase degradation. F_1 offspring of the injected F_0 embryos (outcrossed with wild type fish) is then screened for reporter detection, to identify the founders in which the construct has stably integrated in the germ line (Kawakami, 2007) (Fig. 13).

This thesis mainly deals with the generation and validation of a transgenic line by means of the Tol2kit, in which nine tandem repeats of the glucocorticoid responsive elements (GREs), located upstream of the *thymidine kinase* minimal promoter, drive the expression of the reporter gene EGFP in order to *in vivo* detect the GRE-mediated transcriptional activity of the glucocorticoid receptor. Results related to this transgenic line have been recently published (Benato *et al.*, 2014).

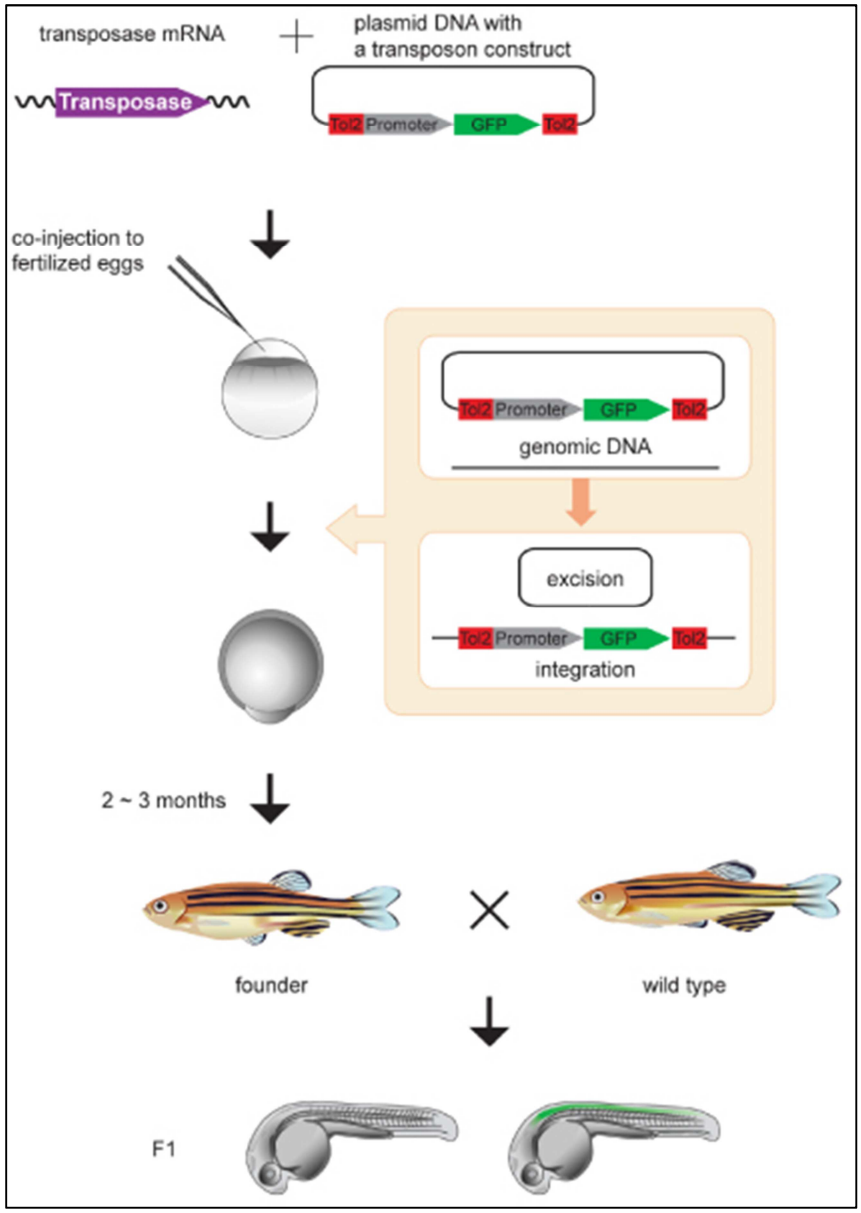

Fig. 13. Schematic representation of the transgenesis in Zebrafish. Figure from Kawakami, 2007.

5. MATERIALS AND METHODS

5.1. Animals maintenance and handling

Zebrafish (*Danio rerio*) were raised, staged and maintained according to standard protocols (Kimmel *et al.*, 1995; Westerfield, 1995; Lawrence, 2007). Eggs are obtained by natural mating and raised up to 6 dpf in Petri capsules. Feeding larvae and juvenile fish (from 6 dpf to one month post fertilization) are bred in one-liter tanks, while adults are transferred to 5-liters tanks with continuous UV-sterilized water circulation.

Larvae are fed starting from 6 dpf with the commercial diet Novotom, Premium Baby (JBL, Neuhofen, Germany) twice a day, while juveniles and adults are fed twice a day with dry food (AZ300, Tetra) and once a day with *Artemiae salinae*, which are purchased as cysts and incubated into saline water for 48 h. Zebrafish are grown and bred at their *optimum* temperature, which is 28.5°C, with a pH range of 7.0-7.4 and conducibility between 200 and 400 μS, in fish water (50X: 75 g Instant Ocean; 25 mM Na_2HPO_4; 25 mM NaH_2PO_4 in deionized water). Fish are kept in a 14 h light/10 h dark light cycle with light turning on at 8.00 am and off at 10.00 pm, which is critical for experiments concerning glucocorticoids, since their regulation depends on the light/dark rhythm. Natural matings are set in the late afternoon in suitable tanks where fish are kept separated during all night; mating occur in early morning, upon light onset. Eggs are collected with a tea net and immediately transferred in Petri dishes filled with fish water. All live animals procedures were approved by the institutional ethics committee for animal testing (C.E.A.S.A.).

5.2. Imaging

5.2.1. Microscopy

For confocal and fluorescence microscopy transgenic embryos, larvae and adult tissues were embedded in 0.8% low-melting agarose (Sigma-Aldrich) and placed on a Petri capsule filled with fish water or on a depression microscope glass. Confocal images were recorded with the Nikon C2 confocal system. Fluorescent images were acquired with a Leica DFC300 FX digital camera on a Leica MZ16F stereomicroscope.
WMISH-stained embryos were mounted in 87% glycerol in PBT or cleared and mounted in 2:1 benzyl benzoate/benzyl alcohol, observed under a Leica DMR microscope, and photographed with a Leica DC500 digital camera.

5.2.2. *In vivo* imaging

For screening after 48 hpf and *in vivo* imaging, embryos and larvae were anesthetized with 0.04% tricaine (ethyl 3-aminobenzoate methanesulfonate salt) (Westerfield, 1995). Screening and *in vivo* imaging were performed with the Leica MZ16F stereomicroscope and a Leica DFC300 FX camera. For *in vivo* imaging, anesthetized larvae were embedded in 2% methylcellulose (Sigma-Aldrich) on a depression microscope glass. The transgenic line Tg(12xGli-HSV.Ul23:nlsmCherry)ia10 was used to localize the floor plate cells (Corallo *et al*., 2013).

5.3. Nucleic acids extraction

5.3.1. Genomic DNA extraction

Genomic DNA was extracted by clipped fins or whole embryos with DNeasy Blood and Tissue Kit (Qiagen), according to the manufacturer's instructions. Final elution was performed with 100 μl

nuclease free water and samples were stored at -20°C until use. For tail fin clipping, adult zebrafish were anesthetized with 0.04% tricaine and laid on a sterile Petri dish; one third of the fin was clipped with surgical scissors an collected in a 1.5 ml microcentrifuge tube, then fish were transferred in a labelled tank and kept isolated to enable identification.

5.3.2. Total RNA extraction

10-30 embryos or larvae (according to their size) were fixed in 1 ml TRIzol Reagent (Invitrogen) in 2 ml microcentrifuge tubes and homogenized with glass beads in a Mini-Beadbeater (Biospec Products). After homogenization, samples were incubated for 5 minutes at room temperature (RT) for nucleoprotein dissociation. After that, 200 µl chloroform were added and the tubes were centrifuged at 13000 *g* for 15 minutes at +4°C. All the RNA was contained in the aqueous supernatant, which was carefully transferred in a new 1,5 ml microcentrifuge tube. An equal volume of isopropanol was added, and samples were incubated at -20°C for at least 3 hours for RNA precipitation. After precipitation, the tubes were centrifuged at 13000 *g* for 15 minutes at +4°C and supernatant was eliminated. The resulting pellet was washed twice with 500 µl 70% ethanol, dried and re-suspended in 10-30 µl nuclease-free water. RNA samples were treated with DNAseI (DNA Free RNA kit, Zymo Research) to eliminate possible genomic DNA contaminations, and stored at -80°C until use.

5.4. Reverse transcription

For qPCR, 1 µg of total RNA derived from three different pools of embryos at each developmental stage was used for cDNA synthesis, with M-MLV Reverse Transcriptase, RNase H Minus, Point Mutant (Promega). cDNAs were stored at -20°C until use.

MIX 1

• RNA	1 mg	70° C	5 min
• Random primers	0.5 ml		
• Nuclease-free water	to 10 ml	Ice	5 min

MIX 2 (added to MIX 1 after chilling)

• M-MLV 5X BUFFER	5 ml	25° C	10 min
• 10 mM dNTPs	1.2 ml	50° C	50 min
• M-MLV RT	1 ml	70° C	15 min
• Nuclease-free water	7.8 ml		

5.5. Quantitative polymerase chain reaction (qPCR)

qPCRs were performed with SYBR green method using a 7500 Real-Time PCR System (Applied Biosystems, Foster City, CA) and the GoTaq®qPCR Master Mix (Promega) following the manufacturer's protocol. We set reaction conditions for each couple of primers (listed in Table 1) and selected 56°C as an annealing and elongation temperature suitable for all couples. Cycling parameters:

95° C (enzyme activation)	10 min	
95° C (denaturation)	30 sec	X 45
56° C (annealing + elongation)	60 sec	

Threshold cycles (Ct) and dissociation curves were generated automatically by Applied Biosystems software. Sample Ct values were normalized with Ct values from Zebrafish housekeeping gene *elongation factor-1a* (*ef1a*), which was invariant in treated and control embryos at the same developmental stage. All analyses were performed in triplicate. The Relative Expression Software Tool 2009

(REST 2009) (Pfaffl et al., 2002) was used to estimate relative fold changes in the genes of interest, using a ratio of the Ct values and the PCR amplification efficiencies of the genes of interest and the housekeeping gene. REST 2009 uses randomization and bootstrapping methods to test the statistical significance of the gene expression ratios and calculate 95% confidence intervals for relative fold changes (Pfaffl, 2009). Significance of up-regulation of *egfp* expression with respect to *fkpb5* expression in the ia20 line response to pharmacological treatment with DEX was analyzed with GraphPad Prism Software. Primer sequences are reported in Table 1.

Primer	Sequence
ef1a-F	5'-GACAAGAGAACCATCGAG-3'
ef1a-R	5'-CCTCAAACTCACCGACAC-3'
fkbp5-F	5'-GTGTTCGTCCACTACACC-3'
fkbp5-R	5'-TCTCCTCACGATCCCACC-3'
egfp-F	5'-CCGACCACATGAAGCAGCAC-3'
egfp-R	5'-CCAGGATGTTGCCGTCCTC-3'

Tab. 1. List and sequences of primers used for qPCR in this thesis

5.6. Generation of Tg(9xGCRE-HSV.Ul23:EGFP)ia20 reporter plasmid

To prepare the GRE reporter plasmid, we placed in tandem nine consensus GREs (TGTACAggaTGTTCT, with uppercase letters representing the GRE from the rat *tyrosine aminotransferase* promoter) (Grange et al., 1991). Briefly, we annealed and PCR amplified two phosphorylated oligonucleotides (5'-GTA GCT GAA CAT CCT GTA CAG GAT GTT CTA GC-3' and 5'-GTA GCT AGA ACA TCC TGT ACA GCT CGA CGT AGC TAG AAC ATC CTG TAC A-3'; consensus GRE sequence is underlined), under the following reaction conditions: enzyme activation (Iproof High Fidelity PCR kit, Biorad, Milan, Italy) at 95°C for 30 s followed by 40 cycles of denaturation (95°C for 30 seconds), annealing (40°C for 5 seconds) and extension (72°C for 20 seconds). PCR conditions are here summarized:

95° C	30 sec	
95° C	30 sec	X 40
40° C	5 sec	
72° C	20 sec	

Reaction products were gel purified (Wizard® SV Gel and PCR Clean-Up System, Promega, Milan, Italy), ligated to one another using T4 DNA ligase (Promega) and cloned into pGEM-T Easy plasmid (pGEM®-T Easy Vector System, Promega), according to the manufacturer's instructions. Nine GRE tandem repeats were PCR amplified (from a positive clone using two specific oligonucleotides (pGEM-GRE-F: 5'- *CCC***AAGCTT***GGG*TTCGATTGGATG-3' with *Hind*III restriction site in bold letters and pGEM-GRE-R: 5'-*CCG***CTCGAG***CGG*TAGTGATTTAGC-3' with *Xho*I restriction site in bold), purified (Wizard® SV Gel and PCR Clean-Up System, Promega), digested with *Hind*III and *Xho*I (Promega), gel purified, and ligated into the *Hind*III/*Bam*HI sites of the p5E-MCS, a 5'-entry vector from the Tol2 kit (Kwan et al., 2007) together with the *thymidine kinase* promoter (*tk*), retrieved by *Sal*I/*Bam*HI double digestion from PCR-blunt II-TOPO-*tk* (Moro et al., 2009).

Ligated 9xGRE-*tk* products were confirmed by sequencing. The resulting plasmid (p5E-9xGCRE-HSV.Ul23) was a 5'-entry clone suitable for the Gateway system. This clone, along with two Multisite Gateway-compatible entry vectors from the Tol2 kit (Kwan et al., 2007), a middle entry vector carrying the *egfp* open reading frame named pME-EGFP and a 3'-entry vector carrying a SV40 polyA tail from pCS2+ (p3E-polyA), were incubated in the presence of the LR Clonase II Plus Enzyme mix (Invitrogen) and the destination vector pDestTol2pA2 as previously described (Kwan et al., 2007). The resulting destination plasmid contained a GRE-dependent EGFP reporter construct flanked by the minimal Tol2 transposon elements and was named Tg(9xGCRE-HSV.Ul23:EGFP) reporter plasmid.

Reporter plasmid DNA (25–50 pg) was co-injected along with 25–50 pg of *in vitro* transcribed Tol2 *transposase* mRNA (Kawakami et al., 2004) into wild type (WT) 1-cell stage embryos.

5.7. Drug treatments and microinjection of morpholinos (MOs)

Zebrafish transgenic embryos were incubated with different chemicals, all purchased from Sigma- Aldrich (Milan, Italy):

- Dexamethasone
- Cortisol
- Corticosterone
- Prednisolone
- Progesterone
- 17-β Estradiol
- 11-Ketotestosterone
- Aldosterone
- 11β-deoxycorticosterone (DOC)
- Mifepristone (RU486)

All the chemicals were dissolved in 100% ethanol to prepare stock solutions. Drug stocks were directly diluted in 25 ml fish water to reach the desired final concentrations. Each treatment was performed in triplicate with 15 embryos per replica. Controls were incubated with an equal volume of 100% ethanol diluted in fish water.

Morpholino (MO) (Gene Tools, Philomath, OR) treatment was performed with *gr*^{ATG}MO (MO2-*nr3c1*), an antisense MO against the ATG translation initiation site of *gr* mRNA, *gr*^{splic}MO (MO4-*nr3c1*), a splice-site targeting MO as well as *gr*^{mism}MO (MO2-*nr3c1*-5m), as specific control MO, all previously described (Pikulkaew et al., 2011). For each MO, 8.2 ng were injected in the yolk of 1-cell stage embryos. Injections were performed under a dissecting microscope using a microinjector attached to a micromanipulator (Leica Microsystems, Milan, Italy). MO-injected embryos were then

incubated in 1X fish water at 28.5°C up to the desired stages of development.

5.8. Circadian rhythm dissection

Analysis of light-dependent modulation of transgene reporter expression was performed in 5 dpf ia20 larvae, which were collected at 2 h intervals. Collection started from 2 h before light onset (6 a.m.) and continued for 28 h, until 10 a.m. of the following day. In order to avoid exposing accidentally larvae to light during the dark period (from 10 p.m. to 6 a.m.) or to stressful *stimuli* while collecting their siblings, larvae were split into 28 single Petri dishes before starting collection. For a more detailed analysis close to light onset, from 3 hours before light onset (5 a.m.) to 5 hours after light onset (1 p.m.), larvae were collected every hour.

5.9. Whole mount in situ hybridization (WMISH)

5.9.1. Embryos preparation

Zebrafish embryos were fixed overnight at +4°C in 4% paraformaldehyde (PFA, Sigma Aldrich) in phosphate-buffered saline (PBS, Sigma Aldrich) at the required stages of development. When necessary, pigmentation was removed by hydrogen peroxide treatment according to Thisse and Thisse (2008). Briefly, embryos and larvae were incubated in 0,5% KOH and 3% H_2O_2 (diluted in milliQ water) and observed under stereomicroscope until pigments bleaching. To stop the reaction, embryos were incubated for 5 minutes with PBS. After fixation and pigmentation removal, embryos were stocked in 100% methanol.
WMISHs were performed as previously described by Thisse and Thisse (2008). Protocol will be described in detail in chapters 5.9.2, 5.9.3 and 5.9.4.

5.9.2. WMISH day 1

1) Rehydratation

Embryos stocked in 100% methanol were incubated with decreasing methanol concentrations:

- 75% methanol in PBS (5 min)
- 50% methanol in PBS (5 min)
- 25% methanol in PBS (5 min)
- 100% PBT (PBS + 0,01% Tween20, Sigma Aldrich) (4x5min)

2) *Permeabilization*

From 1 dpf onwards, embryos were digested with 10 μg/ml Proteinase K (Promega) in PBT to improve their permeability to probes and antibodies. Incubation time depends on the embryos stage (15 additional minutes every further day post fertilization).

To stop the reaction, embryos were incubated with 4% PFA in PBS for 20 minutes, followed by PBT washing (5x5min).

3) *Hybridization*

Embryos are incubated for at least 2 hours with hybridization mix, HM (60% Formamide; 5x SSC; 0.46% pH 6.0 Citric Acid; 50 μg/ml Heparin; μg/ml tRNA) at hybridization temperature, which varies according to the probe used for hybridization. For all the probes used in this thesis (listed in Table 2), hybridization temperature was 65°C.

Gene	Reference	Vector	Endonuclease, RNA polymerase
egfp	Benato *et al*., 2014	p3E-EGFPpA	*ApaI*, T7
fgf8	Reifers *et al*., 1998	pCRII	*Xho*I, T7
fkbp5	Benato *et al*., 2014	pGem	*ApaI*, Sp6
otx5	Gamse *et al*., 2002.	pBS-IISK+	*NotI,* T7
zgr	Pikulkaew *et al.*, 2011	pGem	*ApaI, Sp6*

Table 2. List of riboprobes used for WMISH in this thesis.

Hybridization mix is then removed and replaced with Hybridization mix containing 100 – 200 ng of the probe. Embyos were hybridized overnight at 65°C.

5.9.3. WMISH day 2

1) *Post-hybridization washes*:

- 100% HM, (very brief wash);
- 75% HM /25% 2X SSC for 15 min at 65° C
- 50% HM /50% 2X SSC for 15 min at 65° C
- 25% HM /75% 2X SSC for 15 min at 65° C
- 2XSSC for 15 min at 65° C
- 0.2X SSC for 2X15min at 65° C
- 75% 0.2X SSC/25% PBT at room temperature (RT)
- 50% 0.2X SSC/50% PBT at RT
- 25% 0.2 X SSC/75% PBT at RT
- 100% PBT at RT

2) *Antibody incubation*

Embryos were pre-incubated for at least 2 hours with PBT containing 2% sheep serum and 2 mg /ml of BSA. After that, they were incubated overnight at 4°C with the antibody, anti-DIG or anti-FLUO conjugated with alkaline phosphatase (Roche) diluted 1:3000 in PBT-2% sheep serum-2 mg /ml of BSA.

5.9.4. WMISH day3

1) *Post antibody incubation washes*

PBT, 6x15 min

2) *Staining*

Prior to staining, embryos were washed three times for 5 minutes with staining buffer for NBT-BCIP (100 mM pH 9.5 TrisHCl; 50 mM $MgCl_2$; 100 mM NaCl; 0.1% Tween20 [Sigma-Aldrich] diluted in milliQ water) or staining buffer for Fast Red (100 pH 8.2mM TrisHCl; 0.1%Tween20 in milliQ water) in order to reach an alkaline pH. After that, they were incubated in staining solution, made of NBT-BCIP (Roche) or Fast Red tablets (Roche) diluted in staining buffer. Staining was carried out in the dark in 24 well-plates, until proper signal intensity was reached. Reaction was stopped through an incubation in 4% PFA in PBS, overnight at 4°C.

3) *Embryos preparation for observation*:

- For whole mount imaging, hybridized embryos were incubated in 87% glycerol or cleared and mounted in 2:1 benzyl benzoate/benzyl alcohol. If necessary, yolk was removed.
- For vibratome sectioning (Leica VT1000S), embryos were embedded in gelatin-albumin (2.2 g gelatin, 135 g BSA, 90 g sucrose, 450 ml PBS for 450 ml) in 24 well-plates. 52.5 μl of 25% gluteraldehyde were added to 750 μl of gelatin-albumin and quickly poured in the well; embryos were placed and oriented, then another gelatin-albumin-gluteraldehyde layer was added for a complete embedding.

5.10. *gr*^{s357} mutants

5.10.1. Genotyping

For genotyping, 100 ng of genomic DNA derived from fin clipping or single embryos was used for PCR with Biotherm Taq polymerase (Società Italiana Chimici, SIC). Primers were designed in order to amplify a 205 bp region which includes the *gr*^{s357} point mutation:

Forward primer:	5'-GTC TCT TGA CAC ATC CTG-3'
Reverse primer:	5'-CTG ACA TTT AAG GAC ACA-3'

PCR was performed under strict reaction conditions, in order to obtain pure PCR products that did not need to be purified prior to sequencing:

MIX:

10X buffer	2.5 ml
$MgCl_2$	2 ml
2.5 mM dNTPs	1.2 ml
Primer For + Rev	0.1 + 0.1 ml
Taq	0.2 ml
DNA	100 ng
Nuclease-free water	to 25 ml

Reaction conditions:

95°C	2 min	
95°C	30 sec	X 45
60°C	30 sec	
72°C	15 sec	
72°C	10 min	

Sequencing was performed by BMR Genomics (Padova, Italy). For sample preparation, 20 ng of PCR product were dried at 65°C with 3.2 pmol of the forward primer (5'-GTC TCT TGA CAC ATC CTG-3').

5.10.2. ia20/*gr*$^{s357-/-}$ line generation

In order to obtain the ia20 line in *gr*^{s357} background (Muto *et al*., 2005), we crossed ia20 males with homozygous (*gr*$^{s357-/-}$) females. All the resulting progeny was heterozygous and was screened to identify fluorescent larvae, which were grown until adulthood. We crossed heterozygous (ia20/ *gr*$^{s357+/-}$) male fish with heterozygous *gr*$^{s357+/-}$ females and we grew their fluorescent progeny until adulthood. Adults were genotyped through fin clipping in order to identify homozygous (ia20/*gr*$^{s357-/-}$) mutants. Experiments were performed with the fluorescent progeny of male ia20/*gr*$^{s357-/-}$ mutants crossed with female *gr*$^{s357-/-}$ mutants, which carries the transgene in heterozygosity.

6. RESULTS

All the results contained in chapters from **6.1** to **6.7** were published in the following research paper:

Francesca Benato*, **Elisa Colletti***, Tatjana Skobo, Enrico Moro, Lorenzo Colombo, Francesco Argenton, Luisa Dalla Valle.

"A living biosensor model to dynamically trace glucocorticoid transcriptional activity during development and adult life in zebrafish."

Mol Cell Endocrinol. 2014 Jul 5; 392(1-2):60-72.

doi: 10.1016/j.mce.2014.04.015. Epub 2014 May 4.

*The first and second authors contributed equally to this work.

6.1. Generation of a GC-responsive transgenic zebrafish line

The first step to generate a zebrafish model to analyze *in vivo* the GR-mediated GC activity was the building of a transgenic construct suitable for microinjection, by means of the Tol2 kit (see chapter 4.2.3). Thus, we assembled a transgenic construct containing nine consensus GREs upstream of a *thymidine kinase* (*tk*) minimal promoter [Herpes Simplex Virus (HSV) *thymidine kinase* gene (Ul23)] and the *egfp* coding sequence (Figure 13). The cassette obtained was used to generate the destination vector in the Tol2 transposon backbone (Kawakami, 2007; see chapter 4.2.3). One-cell stage embryos were co-microinjected with the transgenic construct and *in vitro* transcribed Tol2 *transposase* mRNA.

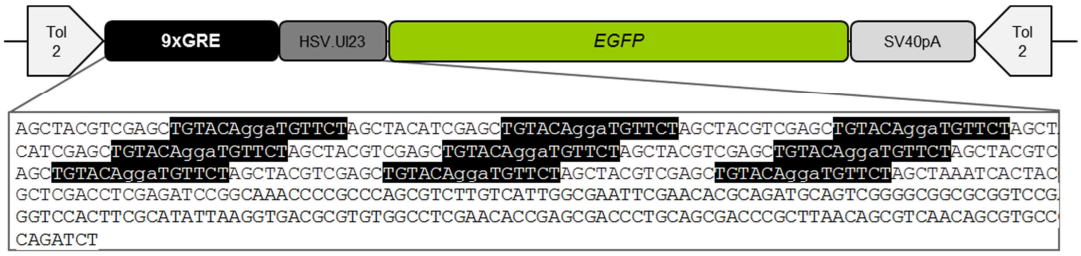

Fig. 13. Schematic representation of the 9xGCRE-HSV.Ul23:EGFP reporter construct designed in this study. The construct consists of a 0.45-kb fragment encoding nine repeating GREs (in black) from the rat *tyrosine aminotransferase* promoter (Grange *et al*., 1991) and a *thymidine kinase* (*tk*) promoter (HSV.Ul23, in dark grey) inserted upstream of the *egfp* ORF (in green). The SV40 polyA signal (SV40pA in grey), which contains a transcriptional termination element, is directly downstream of the EGFP ORF and the entire element is flanked by Tol2 transposable elements.

6.2. Transgene expression analysis

When we observed the injected embryos fluorescence, at the fluorescence microscope, we initially detected transient EGFP expression diffused throughout the embryo by 1 dpf. By 2-3 dpf the fluorescent protein became more spatially restricted and localized in many tissues such as liver, muscle and intestine. Injected embryos where grown until adulthood and outcrossed with wild type (WT) fish, in order to identify the transgenic founders, in which the injected construct had been integrated in the germ line cells. Six independent transgenic F_0 chimeric founders were identified and analyzed. We crossed them with WT fish, thus generating new stable transgenic lines and analyzed the *egfp* expression pattern in F_1 progeny. F_1 embryos from all the founders shared an almost identical EGFP expression pattern with differences only in the intensity of the fluorescent signal (data not shown), thus suggesting the independence of the degree of transgene expression from the genomic site of insertion. From these six lines, the one with the highest fluorescence intensity was selected and used to perform all the experiments described here. This transgenic line was named Tg(9xGCRE-HSV.Ul23:EGFP)ia20, (nicknamed ia20). From this point

onward, in all the described experiments we used the name ia20 to indicate this line.

Once the ia20 line was stabilized, we characterized in detail the transgene expression pattern during development in the F_2 generation, deriving by F_1 transgenic fish outcrossed with WT. EGFP fluorescence was detectable just after fertilization in the offspring of transgenic females mated with WT males (data not shown), while it was first visible from early somitogenesis (14 hpf) in the offspring of transgenic males crossed with WT females (Fig. 14 A-A').

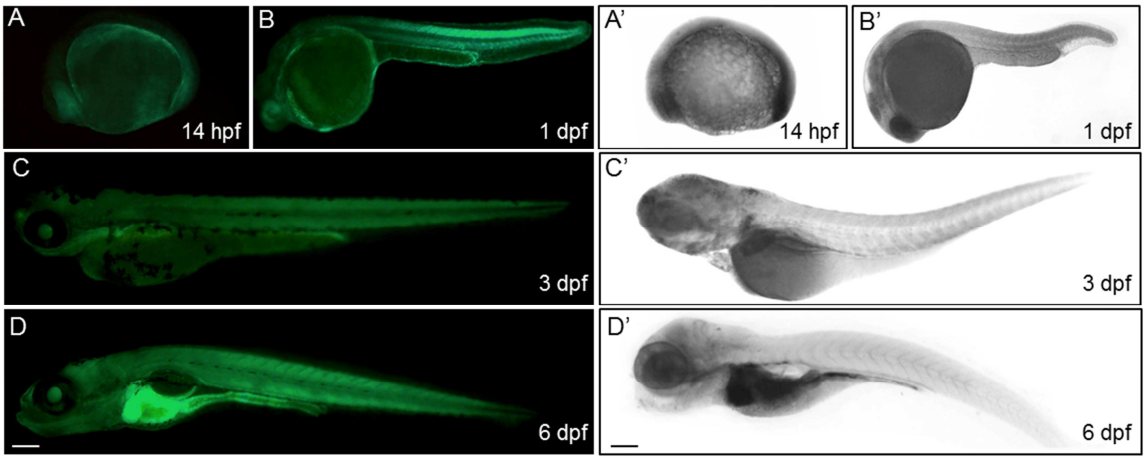

Fig. 14. Fluorescence microscopy (A-D) and light microscopy (A'-D') lateral views of zebrafish embryos and larvae at 14 hpf and 1, 3 and 6 dpf displaying the EGFP accumulation sites and the *egfp* mRNA localization during development. The protein and mRNA are first detectable at 14 hpf, when they both are ubiquitously distributed, with higher signals in the developing head and tail region (A-A'). The EGFP protein/mRNA localization remains the same by 1 dpf (B-B'), while it is visible in distinct domains, such as brain, liver and pronephros at 3 dpf (C-C'). By 6 dpf, the reporter expression is particularly intense in liver, intestine and pronephros (D-D'). Scale bar: 200 μM.

To validate and enhance the results we obtained through the observation of fluorescence, we performed RT-PCR essays, that has been repeated three times with embryos belonging to independent matings, to analyze *egfp* mRNA expression at 0, 1, 2, 3, 4, 5, 6, 7, 8, 16 and 24 hpf. Transgene transcripts were already detected at 0 hpf in the offspring of transgenic females (Fig. 15B), while they were

evidenced by 2 hpf in the offspring of transgenic males (Fig. 15 A). The results of fluorescence analysis and RT-PCR, put together, suggested that the *egfp* mRNA was maternally deposited in the ia20 line, as demonstrated by the presence of *egfp* mRNA and fluorescence (not shown) at 0 hpf, whereas zygotic transcription of the transgene, as highlighted in the offspring of transgenic males, started by approximately 2 hpf, although levels were very low until 4 hpf. From this point forward, we always used embryos and larvae deriving from the outcross of male ia20 fish with WT females for our experiments, in order to avoid every alteration of results caused by maternal effect in early development.

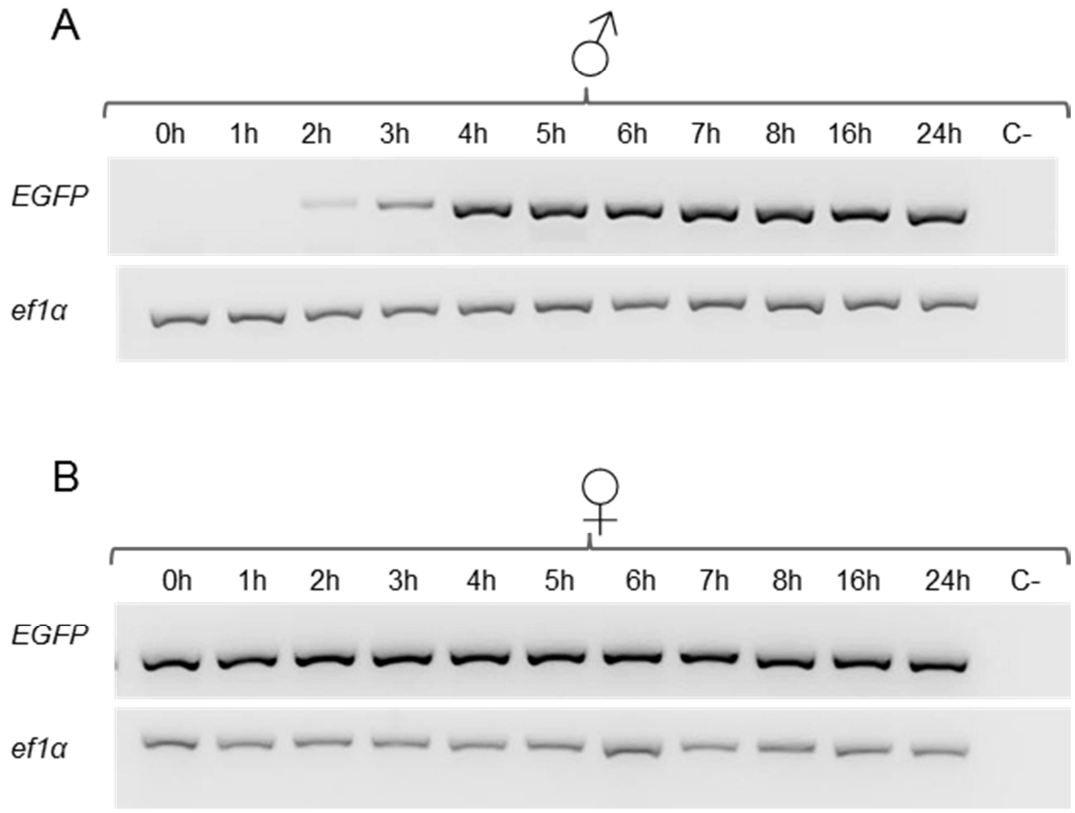

Fig. 15. RT-PCR analysis of egfp expression from the offspring of transgenic male (A) or female (B) and wild type mates at stages ranging from 0 up to 24 hpf. Expression of *ef1a* was used as a cDNA loading control.

The spatio-temporal endogenous expression of the reporter in the ia20 line was thoroughly analyzed during embryonic and early larval development by whole mount *in situ* hybridization (WMISH), fluorescence microscopy and confocal laser scanning microscopy.

Our analysis revealed that, in the absence of exogenous GC treatment, *egfp* mRNA and protein, first detected at 14 hpf, were more localized in the developing head, posterior trunk and tail bud (Fig. 14 A-A'). This *egfp* expression pattern is very similar to the *gr* pattern observed at 15 hpf by WMISH in a previous work of this laboratory (Pilkukaew *et al*., 2011; see figure 6 in chapter 3.1). The shift in temporal reporter expression detected by RT-PCR, WMISH analyses and *in vivo* fluorescence microscopy was clearly due to the different sensitivity of the three techniques and to the time required for messenger translation into protein.

At 1 dpf, fluorescence was still strong in the head and showed an ascending gradient along the caudal trunk, with some intensity around the yolk sac and its extension (Fig. 14 B). This expression pattern was confirmed by WMISH analysis of *egfp* mRNA (Fig. 14 B'). From 3 dpf on, fluorescence intensity in the head and tail regions started to decline, to become more localized in the internal organs at 6 dpf, especially in the abdominal region (Fig. 14 C-C'-D-D').

For comparison, we also analyzed the possible presence of non-specific auto fluorescence (Fig. 16, panel A'-D') and *egfp* expression (Fig. 16, panel A''-D'') in WT embryos at the same developmental stages. We did not detect any non-specific *egfp* mRNA or EGFP fluorescence signal, thus confirming that the results of fluorescence analysis and WMISH shown in figure 14 represent the actual expression of the transgene, i.e. the sites where the glucocorticoid receptor is active.

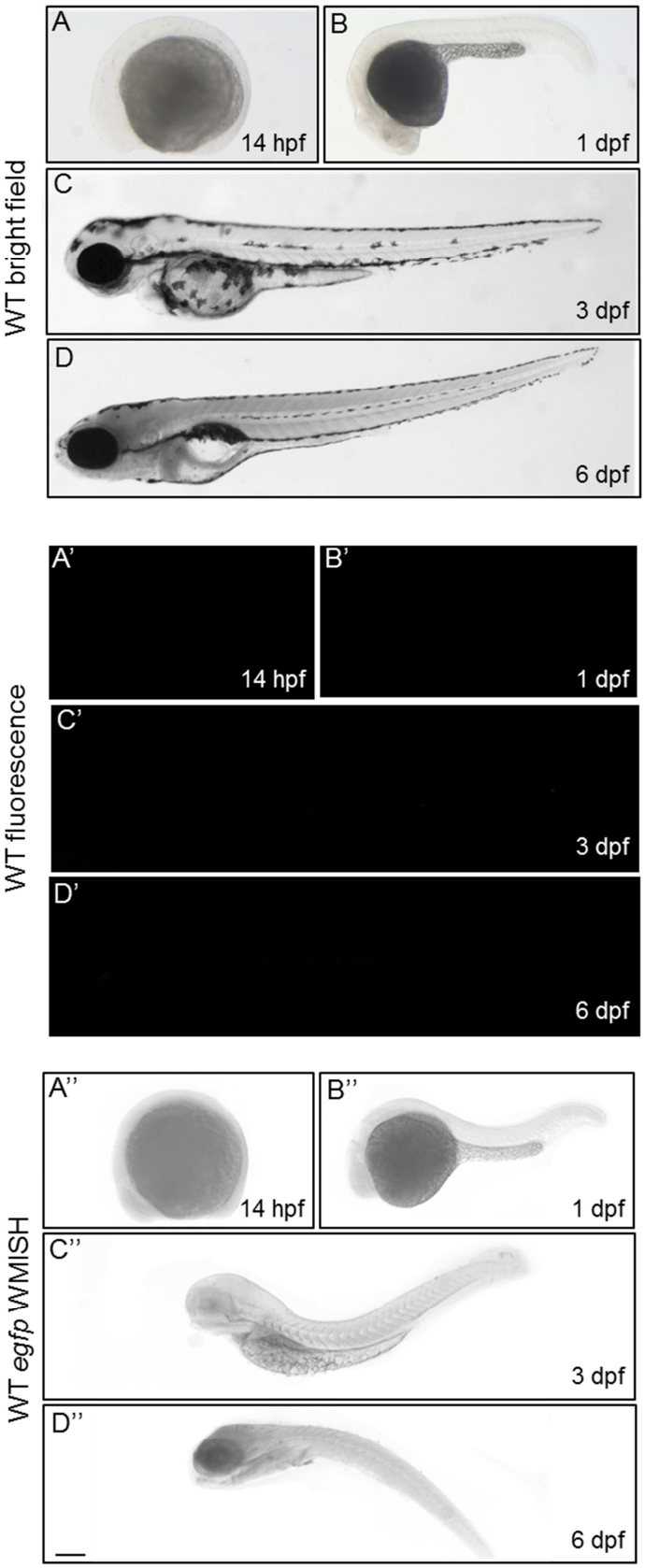

Fig. 16. Bright field (A-D), fluorescence microscopy (A'-D') and *egfp* WMISH (A''-D'') of wild type zebrafish embryos and larvae at 14 hpf and 1, 3 and 6 dpf displaying no transgene signal. Scale bar: 200 μM.

For a more exhaustive analysis of the EGFP fluorescence pattern in ia20 fish, we performed a thorough confocal analysis on larvae at 2 and 5 dpf. This additional analysis, shown in Figure 17, enabled us to obtain a detailed localization of cells and tissues responding to endogenous GCs. At 2 dpf, EGFP signal was detected in known GC-target organs, such as olfactory bulbs and tracts (Figure 17A), pituitary (Figure 17B), liver (Figure 17E), pronephros (Figure 17F) and eye lens (not shown). Moreover, fluorescence was also detected in novel tissue domains, such as in the anterior and posterior cristae and, more feebly, in the lateral canals of the otic vesicles (Figure 17C), in mesenchymal-like cells of the skin (Figure 17H) and, in the trunk, in two rows of cells located above the notochord (Figure 17G). At 2 dpf, EGFP was also detected in the pectoral fin bud epidermis (Figure 17D), where it co-localized with *fgf8a* mRNA (double WMISH shown in Figure 18B). By 5 dpf, the reporter was still expressed in the above mentioned structures as well as in the heart (Figure 17J), pancreas (Figure 17K) and intestine (Figure 17L).

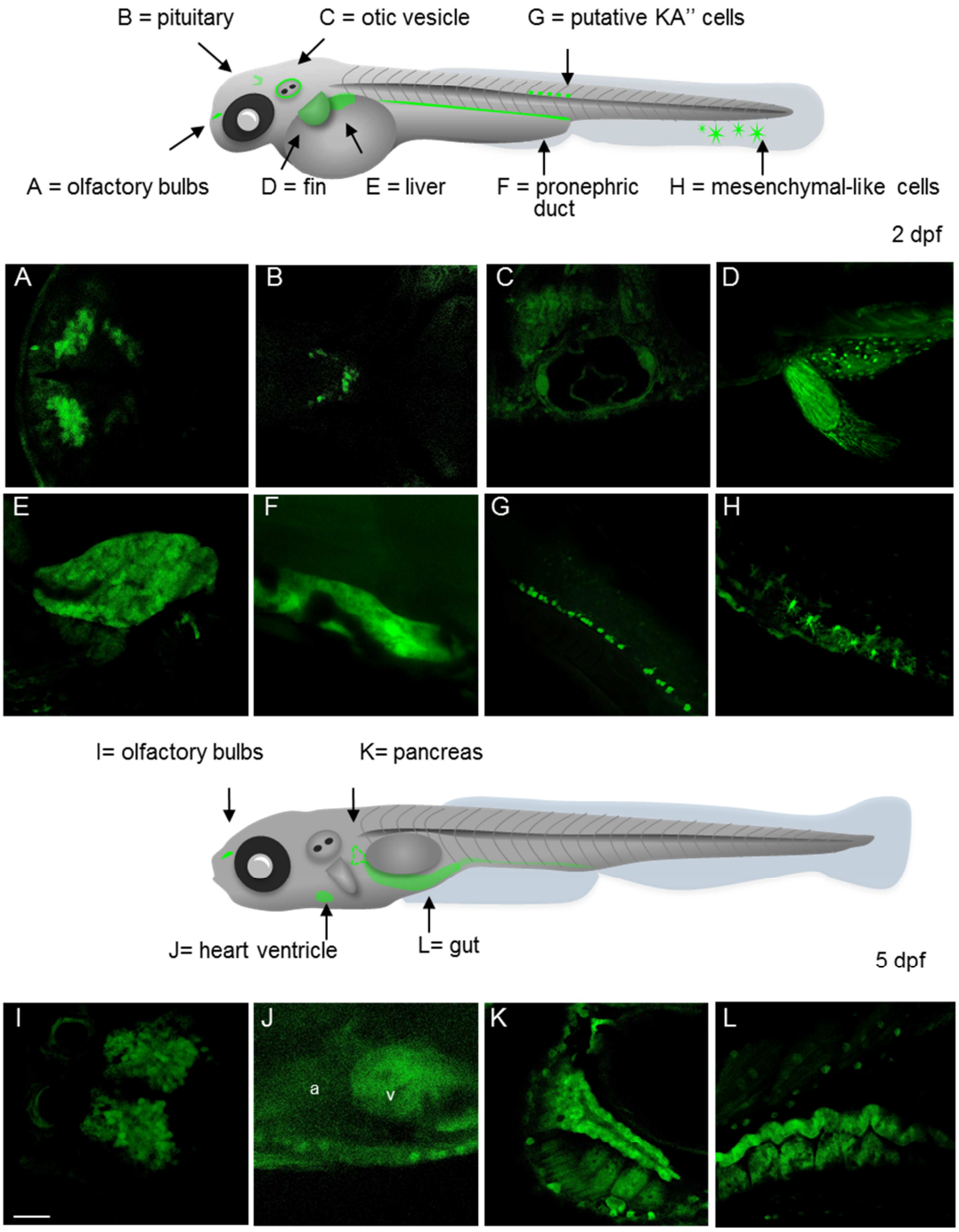

Fig. 17. Reporter expression in untreated 2 dpf and 5 dpf transgenic zebrafish (transgenic males crossed with WT females). Top panel: schematic representation of a 2 dpf embryo indicating the EGFP positive cells and tissues. Below: 20x confocal microscopy pictures showing EGFP in olfactory bulbs and tracts (A, dorsal view), pituitary (B, dorsal view), otic vesicle (C, lateral view), pectoral fin (D, dorsal view), liver (E, lateral view), pronephros (F, lateral view), putative KA'' cells (G, lateral view) and dermal mesenchymal-like cells (H, lateral view). Bottom panel: schematic representation of a 5-dpf larva indicating the newly detectable EGFP-positive districts in addition to those already revealed at 2 dpf. Below: 20x confocal images showing fluorescence in the olfactory bulbs (I, dorsal view), heart (J, lateral view), pancreas (K, lateral view) and gut (L, lateral view). Scale bar: 200 μM.

A detailed analysis of the two rows of cells located above the notochord revealed that their density was not uniform along the antero-posterior axis, but decreased going towards the posterior (Figure 17G). To identify their localization with respect to the floor plate cells, we crossed ia20 fish with the Tg(12xGli-HSVTK:nlsmCherry)ia10 line (Corallo *et al.,* 2013), a stable transgenic line which display mCherry fluorescent protein expression in the floor plate cells, thus generating double transgenic embryos. At 2 dpf, their localization is mostly lateral with respect to the floor plate cells of the ia10 line (Figure 18D). For their expression domain, we speculated that these cells might possibly be Kolmer-Agduhr" (KA'') interneurons (Huang *et al*., 2012).

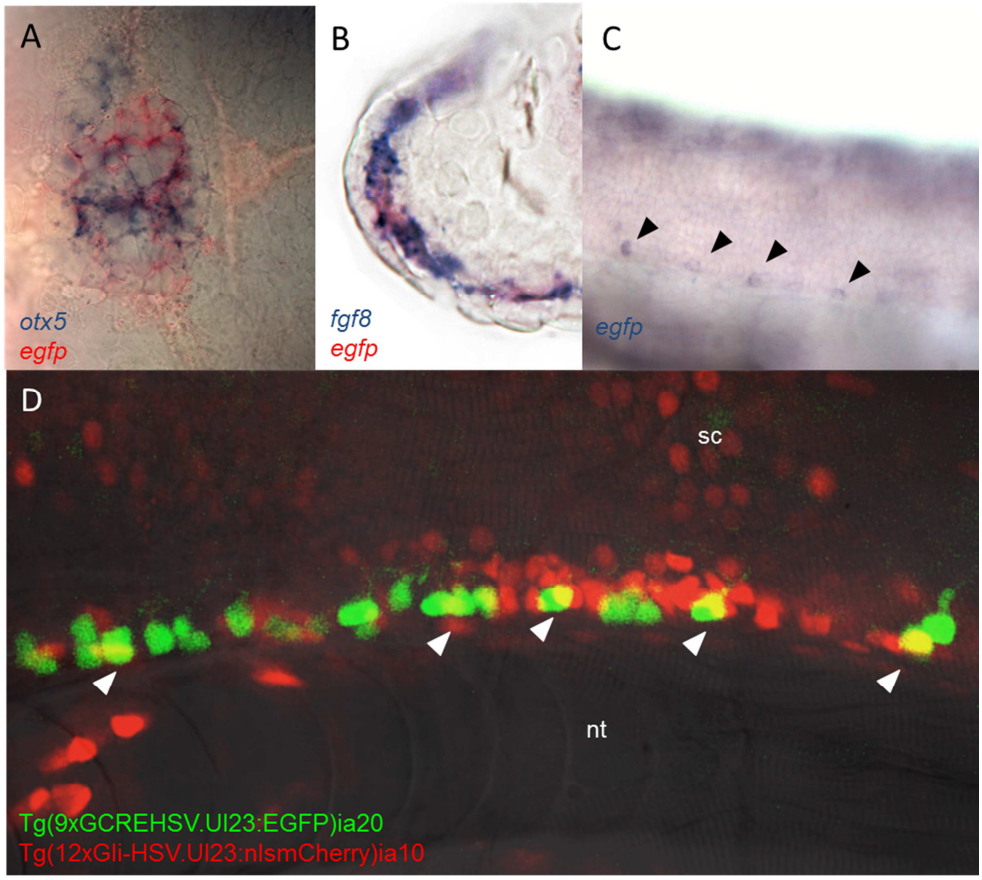

Fig. 18. A) Transgene expression (red) colocalizes, at 3 dpf, with *otx5* transcripts (blu) in the pineal gland as shown by double WMISH (see chapter 6.3). B) Transgene expression (red) colocalizes, at 2 dpf, with *fgf8* transcripts (blue) in the fin as shown by WMISH. C) Lateral section of *egfp* WMISH at 2 dpf showing

putative KA'' interneurons. D) Transgene expression (green) colocalizes at 2 dpf with *shh-reporter* (red) expression in few KA'' cells close to the floor plate as shown by confocal analysis of double transgenic embryos [Tg(9xGCRE-HSV.Ul23:EGFP)ia20 X Tg(12xGli-HSV.Ul23:nlsmCherry)ia10].

We then performed a WMISH to compare *gr* spatio-temporal expression and transgene activity at the same stages reported in Figures 15 and 17. Notably, we here show that the *gr* messenger is expressed in the same area showing transgene activity (Fig. 18).

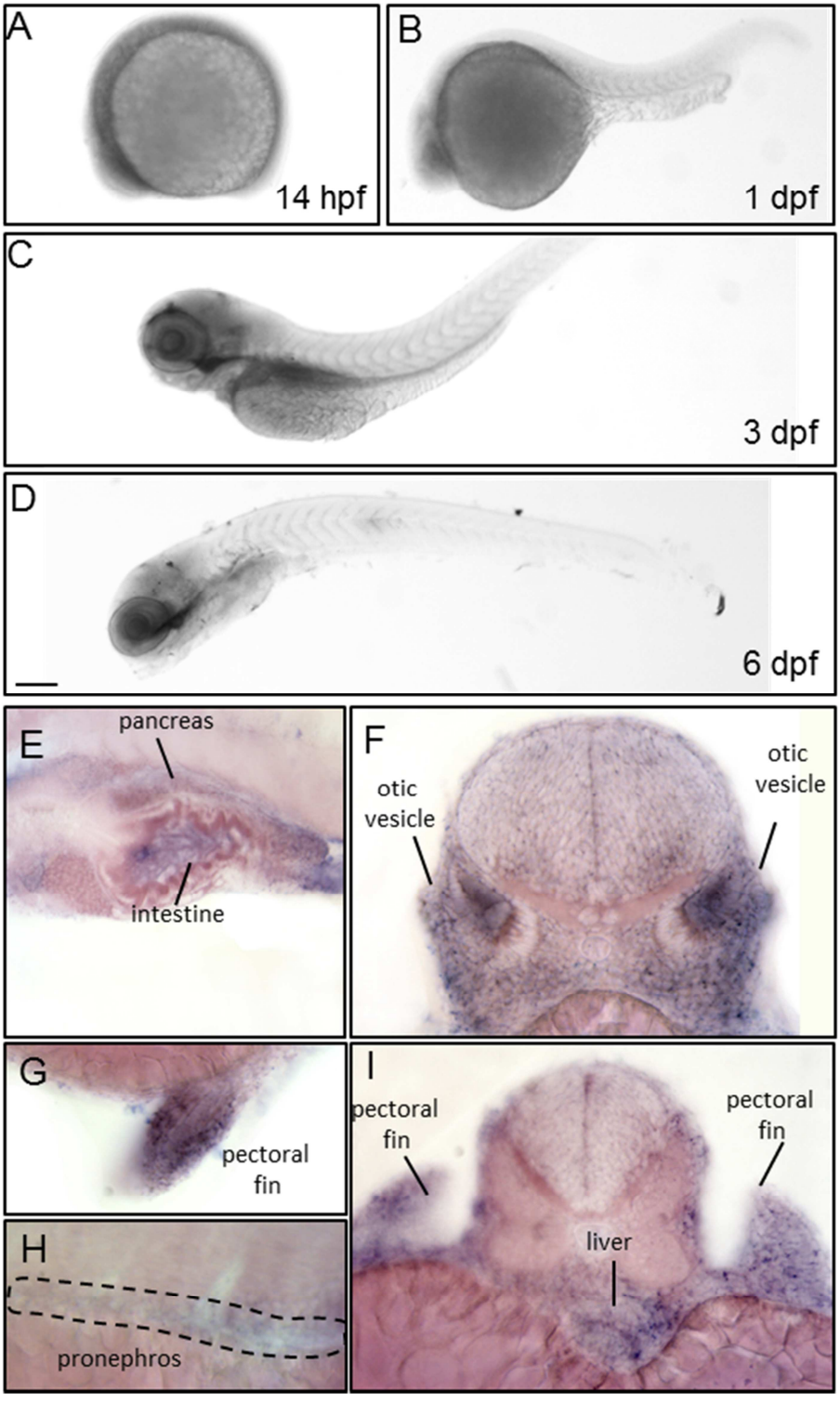

Fig. 19. WMISH of *gr* transcripts performed at the same stages as figures 15 and 17. A-D) Light microscopy lateral views of zebrafish embryos and larvae at 14 hpf (A), 1 dpf (B), 3 dpf (C) and 6 dpf (D) displaying *gr* mRNA localization during development. E-I) Details of *gr* positive structures of 2 dpf (F-I) an 5 dpf (E) larvae embryos analysed by WMISH. Scale bar: 200 μM.

6.3. The ia20 line responds to pharmacological treatment with GCs

Our next goal was the demonstration of the transgenic line responsiveness to exogenous GCs, in order to further validate the ia20 transgenic line and assess its power as new tool. Thus, we outcrossed transgenic ia20 males with WT females and we treated their fluorescent progeny with nine different concentrations of the synthetic GC dexamethasone, DEX (10, 50, 100, 250 nM, 1, 2.5, 5, 10 and 25 μM) for 24 h, from 48 hpf to 72 hpf. We observed that the larvae treated with 100 nM concentration of DEX or more, displayed, *in vivo,* a fluorescence intensification when compared to vehicle-treated controls. In larvae treated with higher DEX concentration this expression increase became more evident, thus suggesting a dose-dependent response. Saturation was reached at 10 and 25 μM. This dose-response effect was also confirmed by WMISH (Fig. 20).

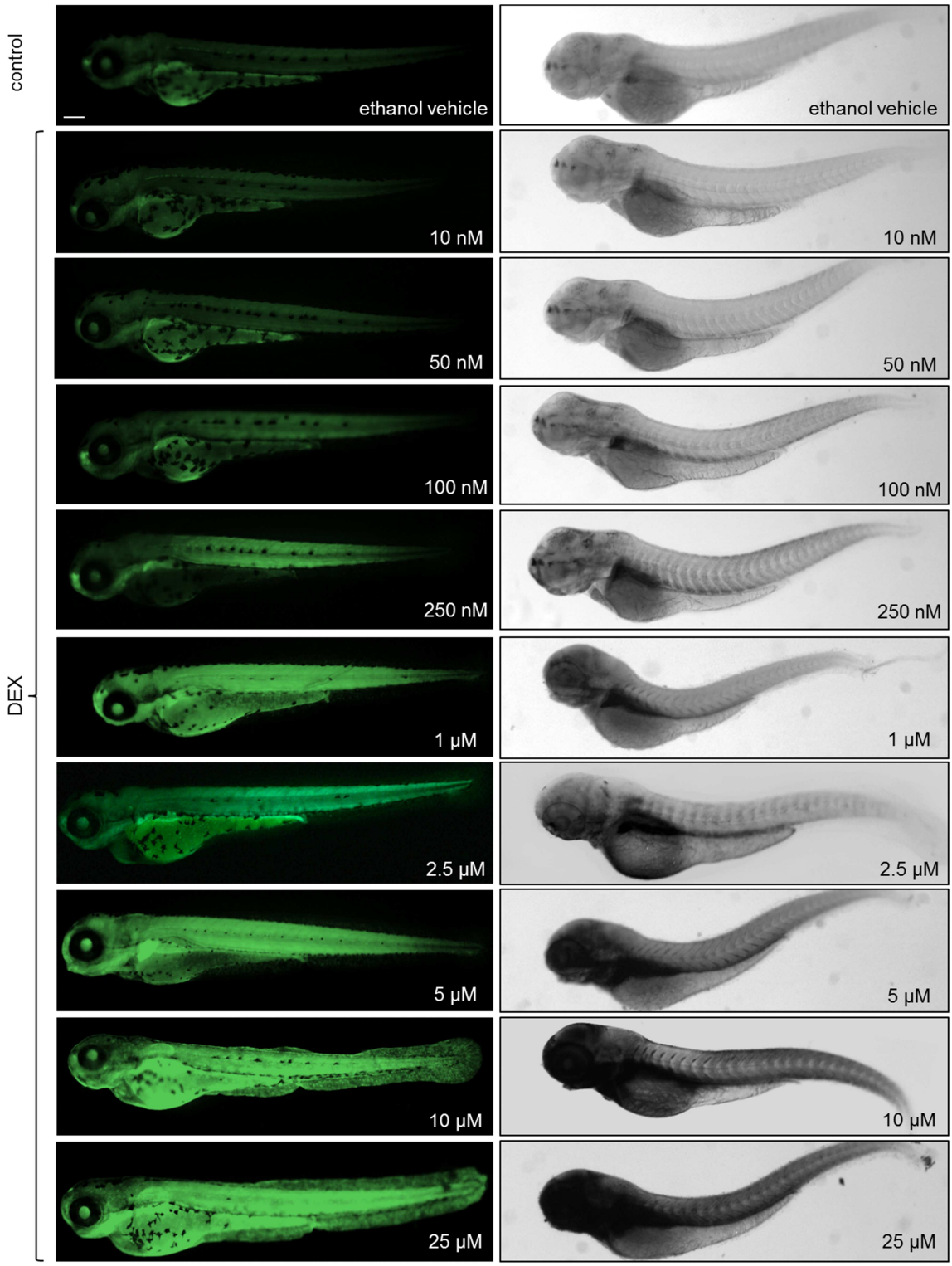

Fig. 20. DEX-induced fluorescence in Tg(9xGCRE-HSV.Ul23:EGFP)ia20 zebrafish line is dose-dependent. EGFP protein (on the left) and mRNA (on the right) distribution after treatment of transgenics with 10, 50, 100, 250 nM and 1, 2.5, 5, 10 and 25 µM DEX for 24 h. Treated embryos display a dose-dependent increase as compared to their ethanol vehicle-treated siblings. Scale bar: 200 µM.

To verify whether the transgene was responding to the treatment with the GC agonist in a dose-dependent manner similar to that of an endogenous gene, qPCR analysis was carried out for *egfp* and *fkbp5* transcripts. *fkbp5* is a ubiquitous gene belonging to the family of immunophilins. It is part of the multimeric complex that binds the glucocorticoid receptor in the absence of ligand (see chapter 2.3.1). *fkbp5* expression is enhanced by Gr and regulates negatively Gr activity, thus forming a negative feed-back loop (Jääskeläinen et al., 2011). As Jääskeläinen and colleagues demonstrated that *fkbp5* is a sensitive biomarker of *in vivo* responses to GCs (Jääskeläinen et al., 2011), we selected this gene as an endogenous biomarker of GCs response in our experiments.

After 24h DEX treatment, both *egfp* and *fkbp5* expression are significantly increased in ia20 larvae. In Figure 21, where the control expression value is set at 1, the comparison among the expression levels at different DEX concentrations shows that for both genes this expression increase is dose-dependent. Transcripts were significantly higher after DEX treatment, starting from 1 μM for *egfp* and 2.5 μM for *fkbp5*. Moreover, *egfp* was significantly more expressed with respect to *fkbp*5 in larvae treated with DEX at 1 μM upwards.

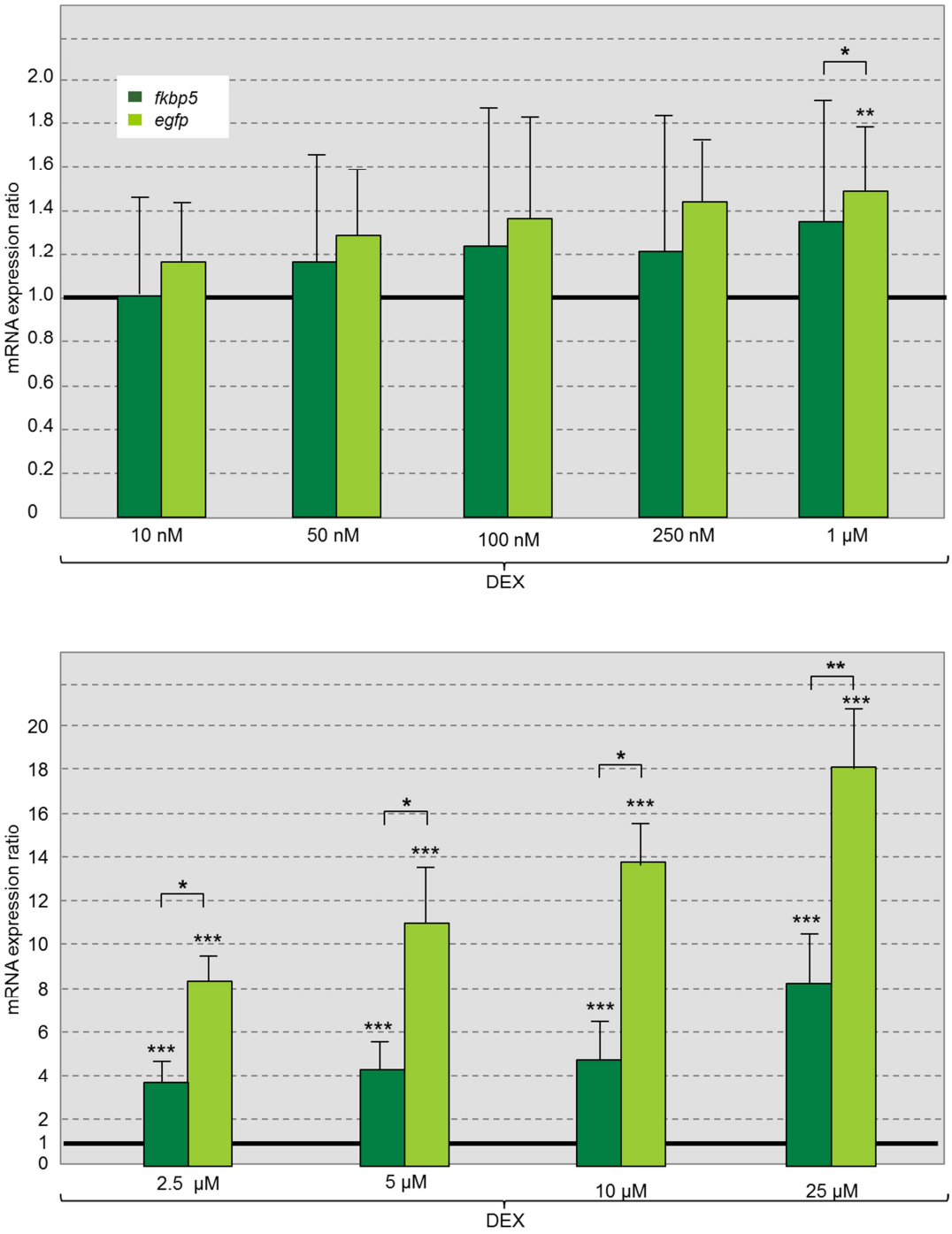

Fig. 21. Fold changes in gene expression of *fkbp5* and *egfp*, in 10, 50, 100, 250 nM and 1 µM (upper panel) and 2.5, 5, 10 and 25 µM (lower panel) DEX-treated transgenics compared to controls (set at 1) with vehicle only. The expression levels of the target genes were normalized on *ef1a* as housekeeping gene. The experiment was repeated three times with 10 embryos for each treatment. Values represent the mean ± S.E. Asterisks indicate that expression levels are significantly different from the control: **P<0.01, ***P < 0.001.

A more detailed analysis of the DEX-dependent responsiveness at the 10 μM concentration in the transgenic line was performed by confocal microscopy. A strong fluorescence enhancement with respect to control was detected in many tissues such as the pectoral fin epithelium (Fig. 22, A-A'), mesenchymal-like cells of the skin (Fig. 22, B-B'), skeletal muscle fibers (Fig. 22, C-C'), KA'' interneuron cells (Fig. 22, D-D'), as well as in the pituitary (Fig. 22, E-E' and arrowhead in G'). Moreover, EGFP signal also appeared in novel sites like blood cells (Fig. 22, arrows panel D') and in the vessel endothelium (Fig. 22, arrows in panel B'). Notably, in these cell types, the transgene was not expressed in the absence of GC agonist treatment. Moreover, with at least 10 μM DEX, a clear signal appeared also in the pineal gland (Fig. 22, F-F' and arrow in panel G'). This localization was confirmed by double WMISH of *egfp* and *otx5,* a specific marker of the pineal gland (see figure 18, chapter 5.3.1).

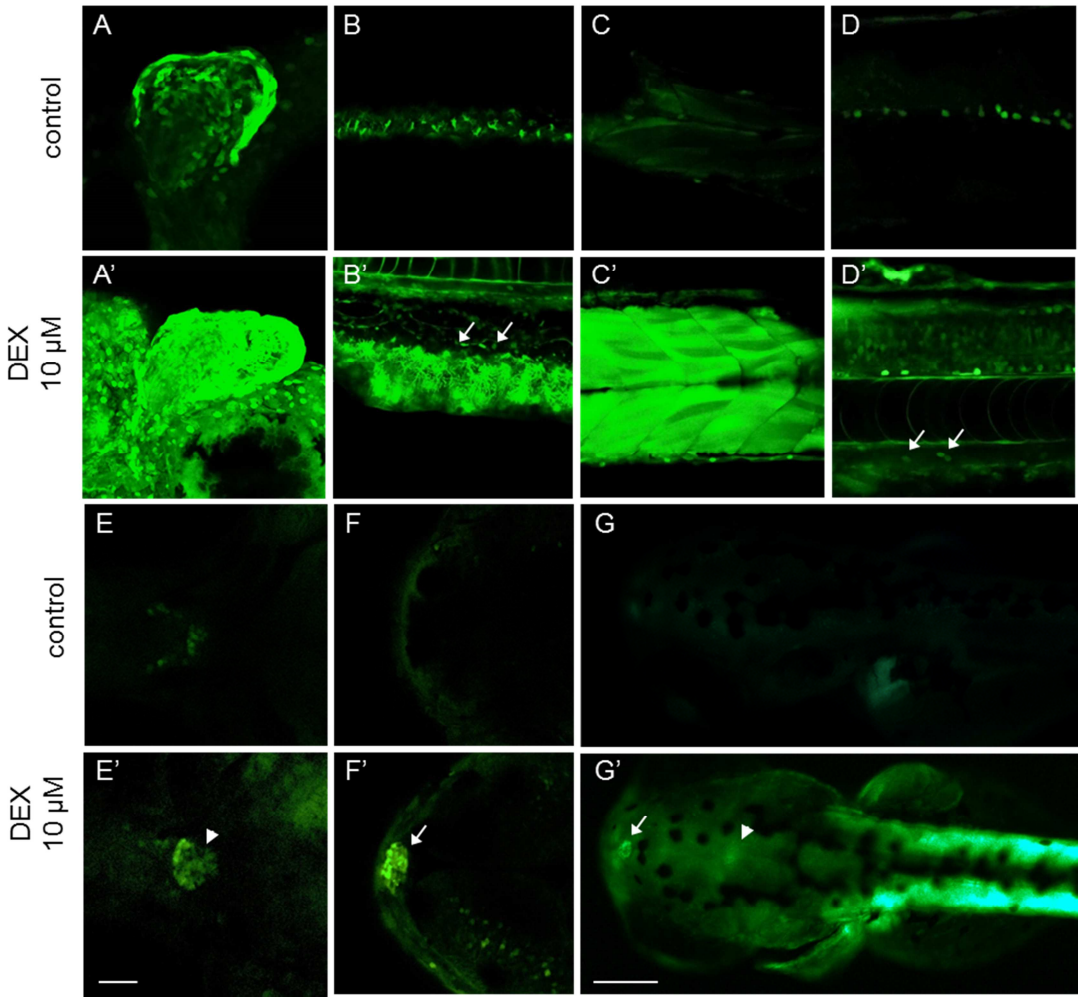

Fig. 22. Fluorescence increase after DEX treatment and visualization of new responding districts. Confocal microscopy (A-F and A'-F') and fluorescence microscopy (G-G') images of a Tg(9xGCRE-HSV.UI23:EGFP)ia20 larva treated with 10 µM DEX compared to control. DEX incubation caused a strong EGFP increase in pectoral fins (A', lateral view), dermal mesenchymal-like cells (B', lateral view), muscle fibers (C', lateral view), pituitary (arrowhead in E' and in G', dorsal view) in blood cells and vessels (arrows in B' and in D', lateral view) and in the pineal gland (arrow in F' and in G'). Scale bar: 200 µM.

6.4. Selective response of the ia20 line to different steroids

As different steroid receptors share the same HREs (see chapter 2.1), there might be a possible crosstalk among their pathways, causing a non-specific GCs responsiveness. For this reason, a screening was carried out to evaluate the responsiveness, during the first developmental stages, of the ia20 transgenic line to different glucocorticoids (cortisol, corticosterone, prednisolone,

dexamethasone), mineralocorticoids (11-deoxycorticosterone, aldosterone), progestins (progesterone), androgens (11-ketotestosterone) and estrogens (17β-estradiol). All steroid treatments were performed at the same concentration (5 μM) and started at 10 hpf. The effects on reporter expression were evaluated by WMISH at 1, 2 (not shown) and 3 dpf and by fluorescence microscopy analysis (Fig. 23). Incubation with cortisol led to the same results obtained with DEX: a sharp increase of *egfp* mRNA was already visible at 2 dpf in the same tissues. A modest effect on reporter activity was detected with corticosterone. The incubation with progesterone and prednisolone led to a clear increase of reporter transcription. Progesterone responsiveness is probably not due to Gr and Pr crosstalk, but to the conversion of progesterone to cortisol. As demonstrated by Parajes and colleagues, at 3 dpf *cyp11a2*, a key enzyme in cortisol biosynthesis, is already active (Parajes *et al.*, 2013). Instead, embryos treated with 11β-deoxycorticosterone (DOC), aldosterone, 11-ketotestosterone as well as 17β-estradiol displayed expression levels comparable to controls (Fig. 23). Thus, until this stage, the ia20 line selectively responds to glucocorticoids, as no response to mineral corticoids, androgens and estrogens was detected.

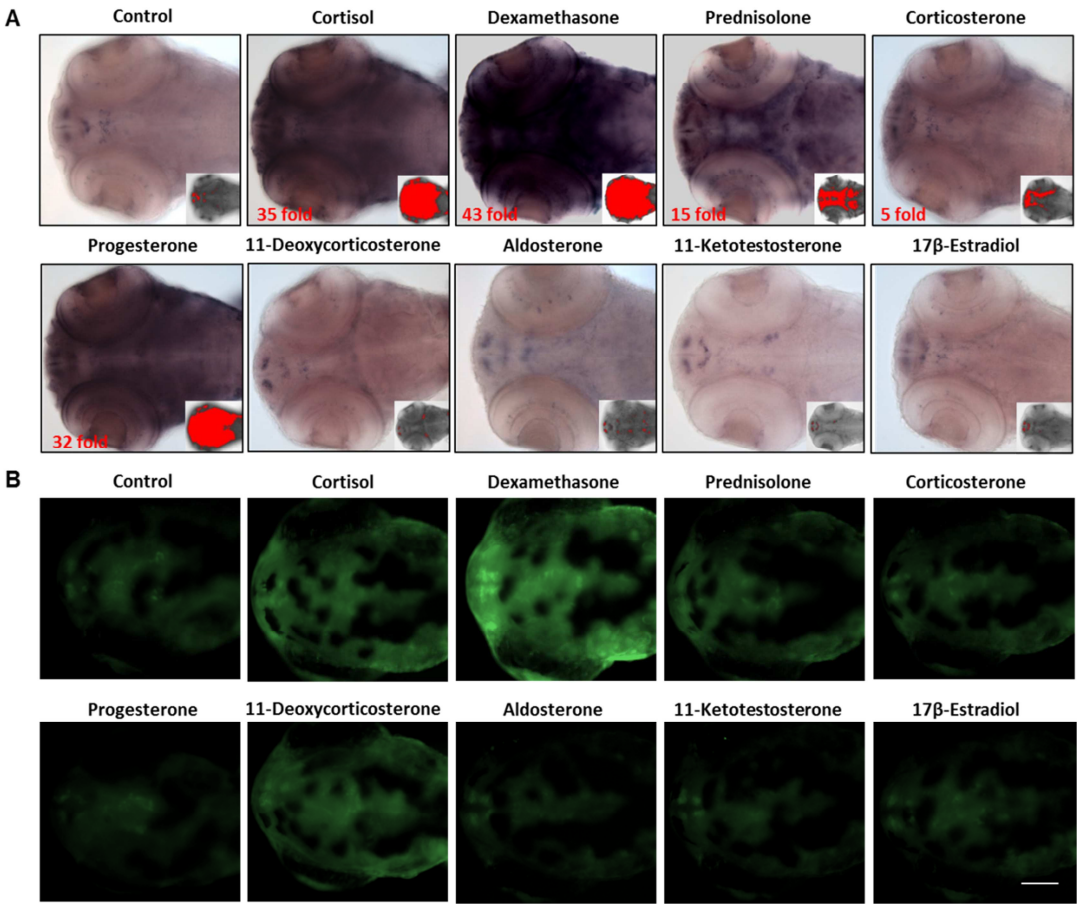

Fig. 23. Transgenic line responses to different steroid treatments. A) Light microscopy dorsal view and B) fluorescence microscopy images of 3-dpf transgenic zebrafish treated for 48 h with the indicated compounds at the same concentration (5 μM). Responses were visualized both by WMISH of *egfp* mRNA and *in vivo* by EGFP fluorescence. Cortisol, dexamethasone, prednisolone, progesterone and corticosterone treatments increased reporter activity compared to control, while no changes were detectable with 11β-deoxycorticosterone (DOC), aldosterone, 11-ketotestosterone and 17β-estradiol (E2). Threshold areas, highlighted in red and corresponding to egfp positive regions, are shown in small boxes on the bottom-right of single images in each WMISH picture. Threshold was set at 201. . Scale bar: 200 μM.

Dose-dependent responsiveness of the transgenic line to five different concentrations (10 nM, 100 nM, 1 μM, 5 μM and 25 μM) of cortisol, corticosterone and prednisolone were analyzed by qPCR of *egfp* and *fkbp5* transcripts. As reported in Figure 24 and in agreement with the WMISH results, the highest reporter induction was obtained with cortisol (Fig. 24A), followed by prednisolone (Fig.24B) and corticosterone (Fig. 24C). Moreover, the transgenic line

appeared sensitive to low doses of prednisolone, as the corresponding *egfp* increase was statistically significant at 100 nM and 1 μM for *fkbp5* (Fig. 24B). Cortisol produced a significant *egfp* expression increase starting from 1 μM, while *fkbp5* was significantly augmented from 5 μM. Finally, the ia20 line was less sensitive to corticosterone, as both genes reached significance at 5 μM.

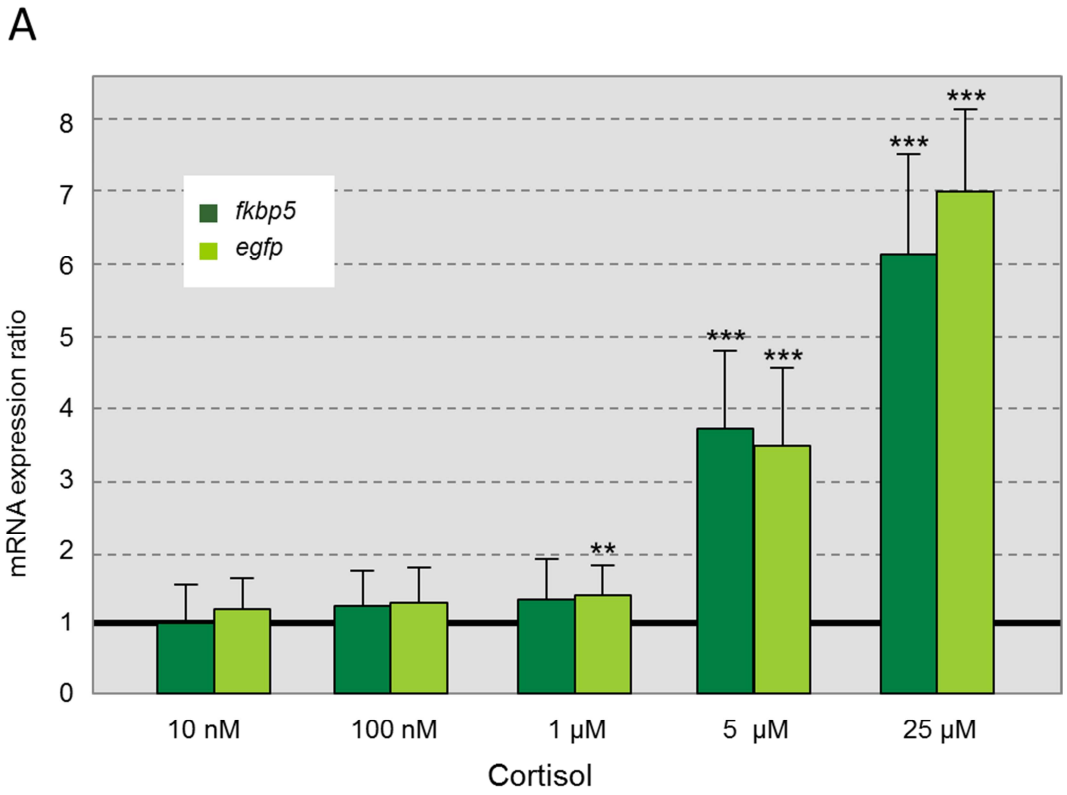

B

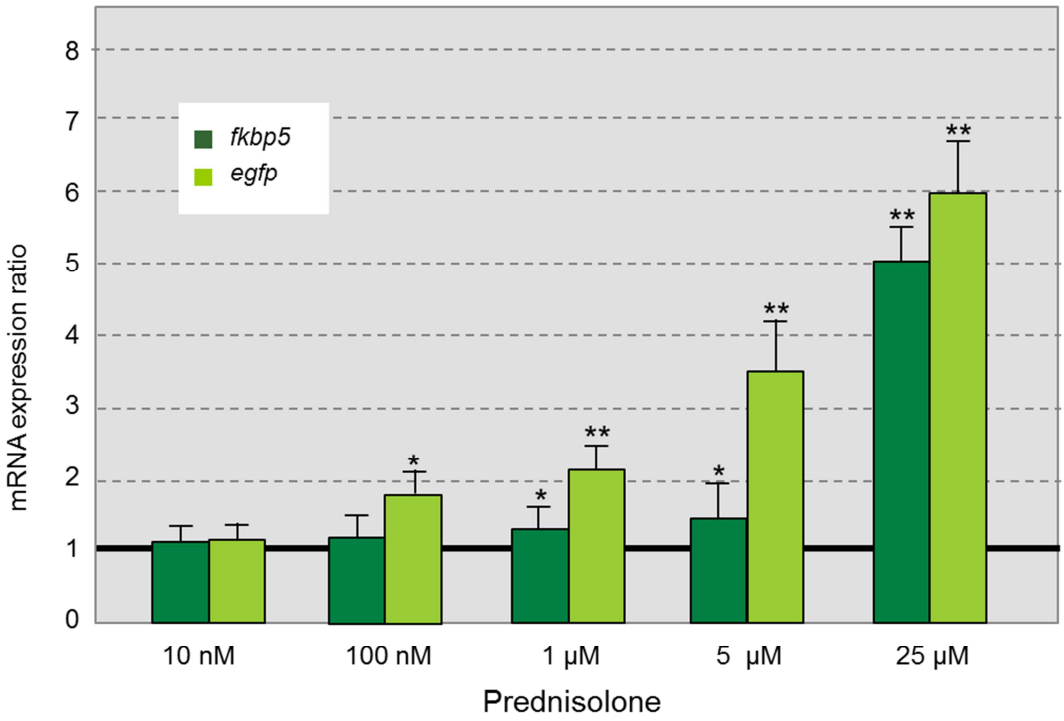
mRNA expression ratio
0
1
2
3
4
5
6
7
8
fkbp5
egfp
*
*
**
*
**
**
**
10 nM
100 nM
1 µM
5 µM
25 µM
Prednisolone

C

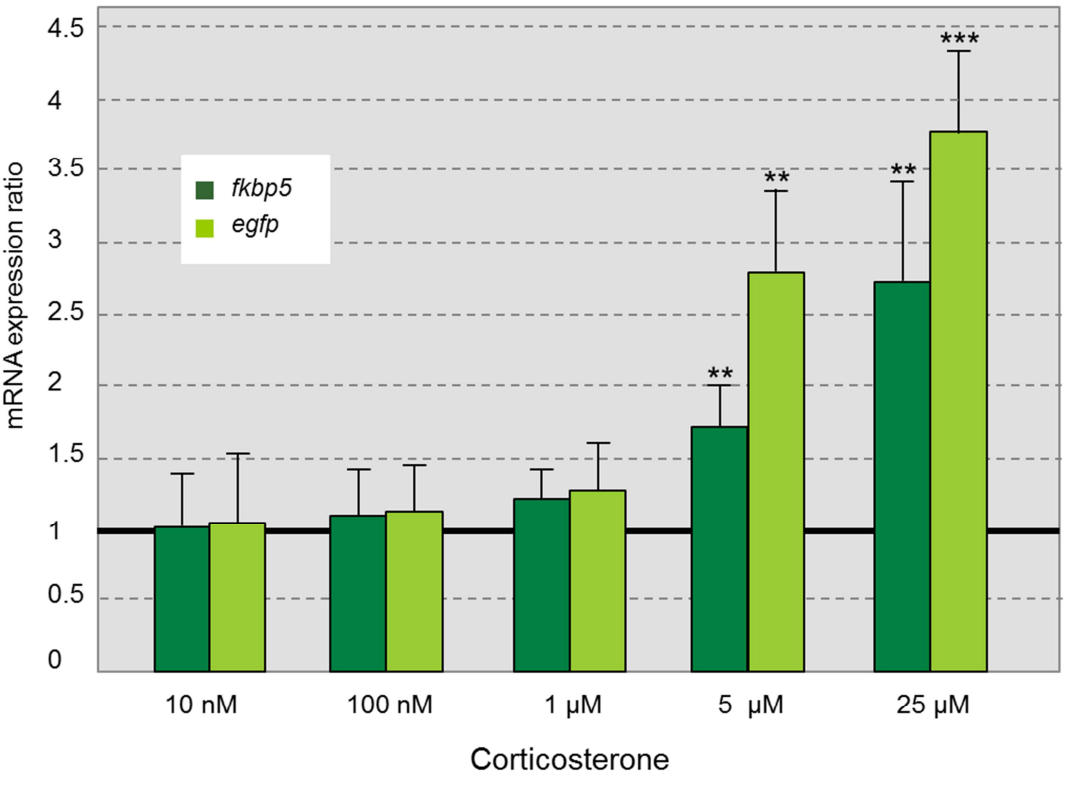
mRNA expression ratio
0
0.5
1
1.5
2
2.5
3
3.5
4
4.5
fkbp5
egfp
**
**
**
***
10 nM
100 nM
1 µM
5 µM
25 µM
Corticosterone

Fig. 24. Fold changes in gene expression of *fkbp5* and *egfp*, in 10 and 100 nM, 1, 5 and 25 μM cortisol (upper panel), prednisolone (intermediate panel) and corticosterone (bottom panel) treated transgenics compared to controls (set at 1) with vehicle only. The expression levels of the target genes were normalized on *ef1a* as housekeeping gene. Values represent the mean ± S.E. Asterisks indicate that expression levels are significantly different from the control: *P <0.05, **P<0.01, ***P < 0.001.

6.5. Reporter activity in ia20 fish decreases by GR knockdown and RU486 treatment

For a further validation of transgene expression specificity, we knocked-down *gr* by morpholino microinjection (see chapter 4.2.2) in ia20 embryos. One-cell stage embryos were microinjected with three different MOs: *gr*^{ATG1}MO (MO2-*nr3c1*) to block the translation of both maternal and zygotic *gr* transcripts; *gr*^{splic}MO (MO4-*nr3c1*), a splicing MO to block post-transcriptionally the zygotic *gr* transcripts alone and *gr*^{mism}MO (MO2-*nr3c1*-5m), as a mismatched control MO. The efficacy of *gr*^{ATG1}MO in targeting and blocking protein translation was determined in a previous work using an *in vitro* transcription/translation coupled system, whereas the effectiveness of *gr*^{splic}MO was analyzed by RT-PCR in the same work (Pikulkaew et al., 2011).

We performed a detailed confocal microscopy analysis in *gr*^{ATG1}MOs, displaying a completely abolished or strongly reduced fluorescence of transgenic fish in the target tissues for glucocorticoids previously shown in Figure 16 (Fig. 25). Similarly, *gr*^{splic}MOs analysis revealed a consistent or complete fluorescence reduction, while in control *gr*^{mism}MOs fluorescence intensity was not altered with respect to non-microinjected controls (data not shown).

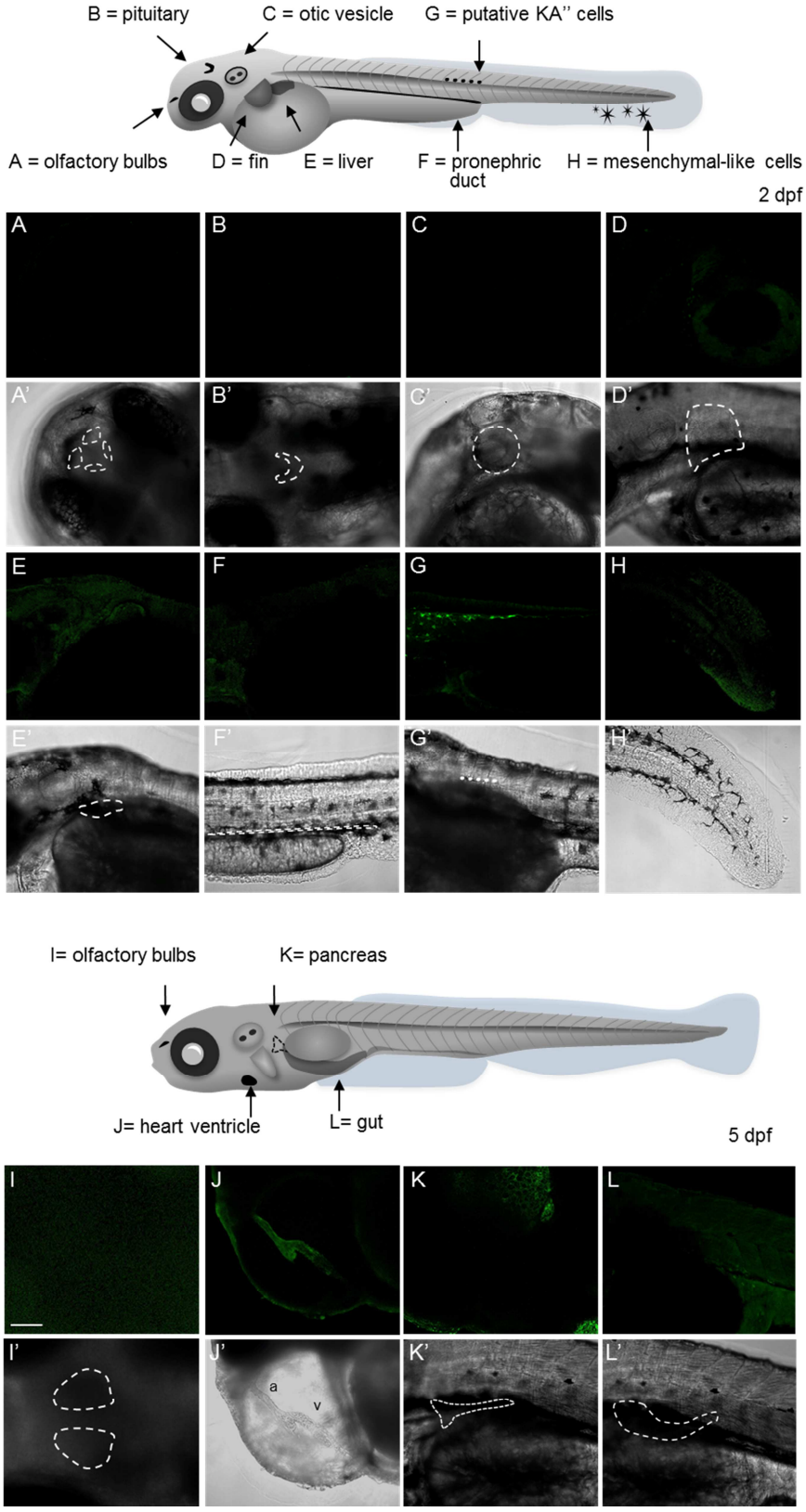

Fig. 25. Reporter expression in untreated 2- and 5-dpf transgenic zebrafish following *gr* MOs injections. Top panel: schematic representation of a 2-dpf embryo indicating the EGFP positive cells and tissues, as reported in Fig. 2. Below: 20x confocal microscopy pictures showing EGFP fluorescence reduction in olfactory bulbs and tracts (A, dorsal view, A', bright field), pituitary (B, dorsal view, B', bright field), otic vesicle (C, lateral view, C', bright field), pectoral fin (D, dorsal

view, D', bright field), liver (E, lateral view, E', bright field), pronephros (F, lateral view, E', bright field), putative KA'' interneurons (G, lateral view, G', bright field) and dermal mesenchymal-like cells (H, lateral view, H', bright field). Bottom panel: schematic representation of a 5-dpf larva indicating the newly detectable EGFP-positive districts in addition to those already revealed at 2 dpf in transgenic zebrafish, as reported in Fig. 2. Below: 20x confocal images showing EGFP fluorescence reduction in the olfactory bulbs (I, dorsal view, I', bright field), heart (J, lateral view, J', bright field), pancreas (K, lateral view, K', bright field) and gut (L, lateral view, L', bright field). Scale bar: 200 μM.

To detect GCs responsiveness, morphants and controls were incubated with or without 10 mM DEX for 24 h (from 2 to 3 dpf). As shown in Figure 26, no EGFP signal enhancement was detected after DEX treatment in both ATG and splicing morphants while in *gr*^{mism}MOs DEX responsiveness was not altered with respect to non-microinjected control.

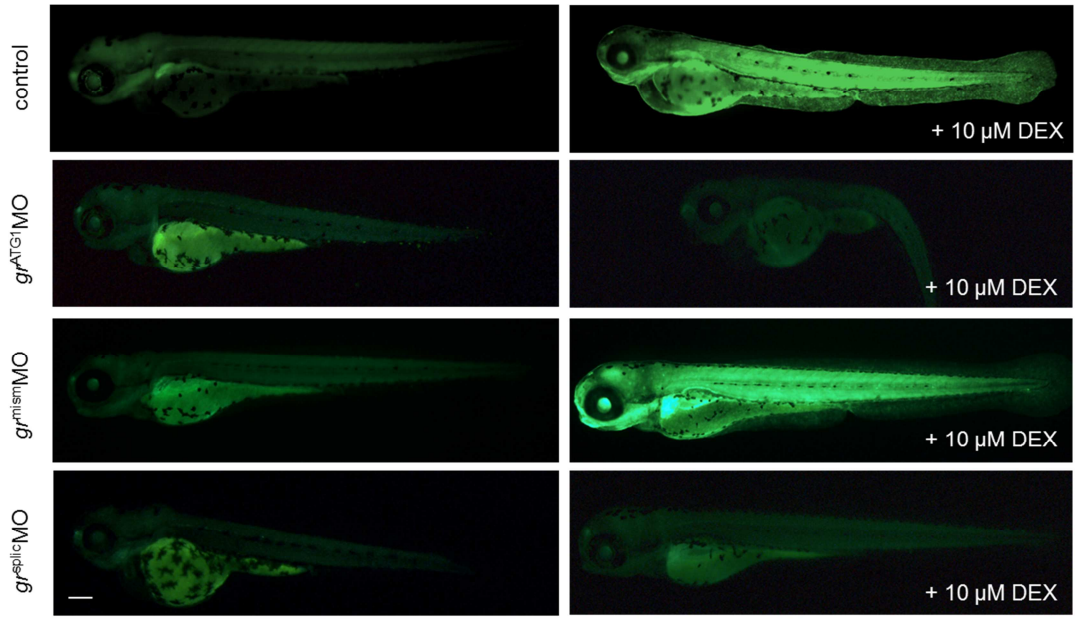

Fig. 26. Reduced GRE activity following *gr* MOs injections alone or combined with 10 μM DEX treatment of 2-dpf transgenics for 24 h. EGFP protein localization in controls (ia20 embryos) and after translation-blocking MO (*gr*^{ATG1}MO), missplicing MO (*gr*^{splic}MO) and mismatched control MO (gr^{mism}MO) injections alone (on the left) or combined with DEX treatment (on the right). Scale bar: 200 μM.

Moreover, *gr*^{mism}MO microinjection did not modify either *egfp* or *fkbp5* transcription levels, as assessed by qPCR (Fig. 27) confirming the presence of an active Gr. Instead, microinjections with either *gr*^{ATG1}MO or *gr*^{splic}MO significantly reduced GC signaling as indicated by strong decrease of fluorescence and significant reduction of basal *fkbp5* gene expression. DEX treatment of the *gr*-morphants caused an increase of the *fkbp5* transcripts, suggesting incomplete penetrance of the two MOs. Analogously, the *egfp* transcripts were also increased by DEX treatment and this increase was statistically significant with respect to control (transgenic ia20 zebrafish without DEX) in *gr*^{splic}MO injected embryos (Fig. 27).

Moreover, increase of both *egfp* and *fkbp5* transcripts after DEX

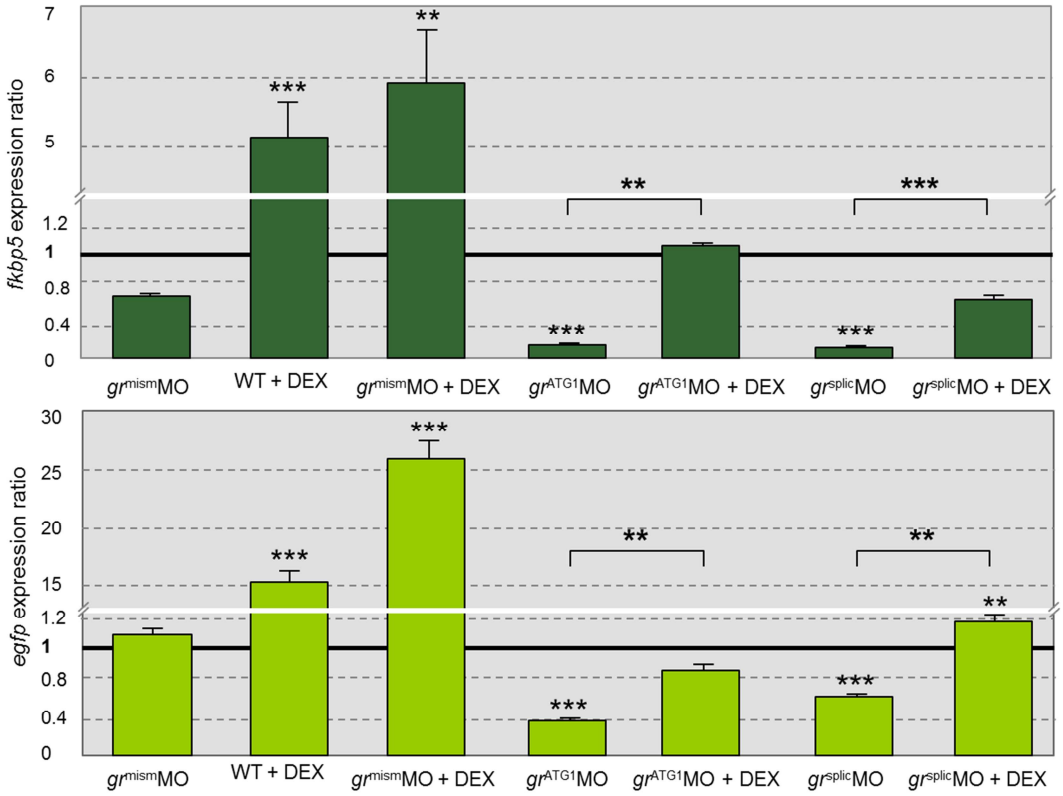

treatment was statistically significant compared to *gr*-morphants.

Fig. 27. Fold changes in gene expression of *fkbp5* (top panel) and *egfp* (bottom panel) in embryos injected with *gr*^{mism}MO, *gr*^{ATG1}MO and *gr*^{splic}MO w/wo DEX treatment as compared to non- injected/non-treated control (set at 1). The

expression levels of the target genes were normalized on *ef1α* as housekeeping gene. Values represent the mean ± S.E. Asterisks indicate expression levels that are significantly different from control (ia20 embryos) or between samples as indicated by the horizontal line: **P < 0.01; ***P < 0.001.

The specificity of transgene expression was further confirmed by treatment of embryos with DEX (10 μM) alone or together with the GR antagonist RU486 (50 nM, 250 nM and 1250 nM) for 24 h (from 2 to 3 dpf). Co-treatment with RU486 caused a significant and dose-dependent decrease of *egfp* and *fkbp5* mRNA levels compared to those in embryos treated with DEX alone (Fig. 28), in agreement to the blocking of DEX responsiveness observed by Weger and colleagues in the GRIZLY assay (Weger *et al.*, 2012).

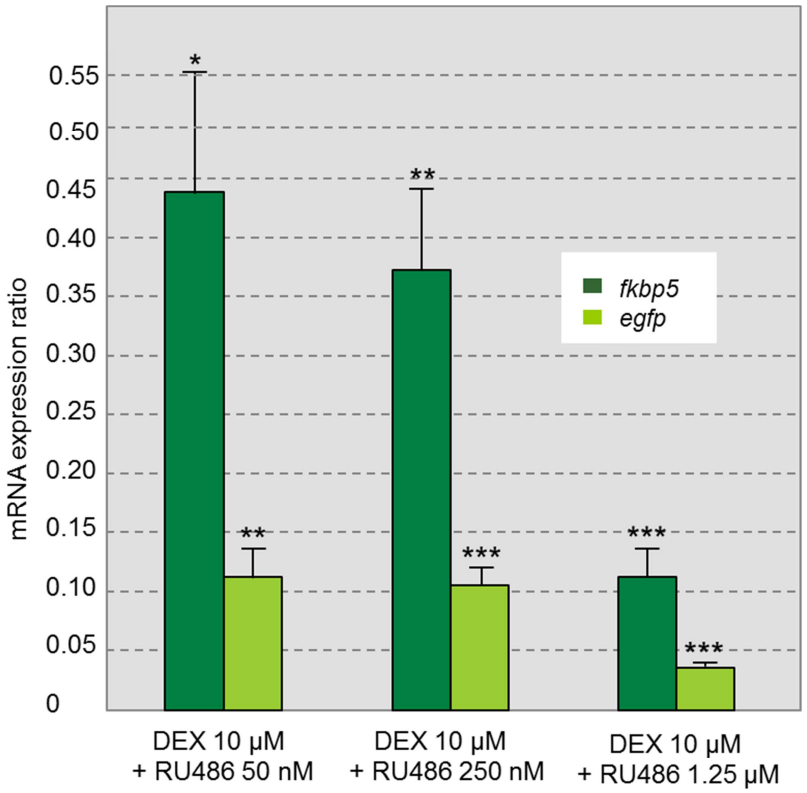
mRNA expression ratio
0.55
0.50
0.45
0.40
0.35
0.30
0.25
0.20
0.15
0.10
0.05
0
*
**
**
***
***
***
fkbp5
egfp
DEX 10 µM
+ RU486 50 nM
DEX 10 µM
+ RU486 250 nM
DEX 10 µM
+ RU486 1.25 µM

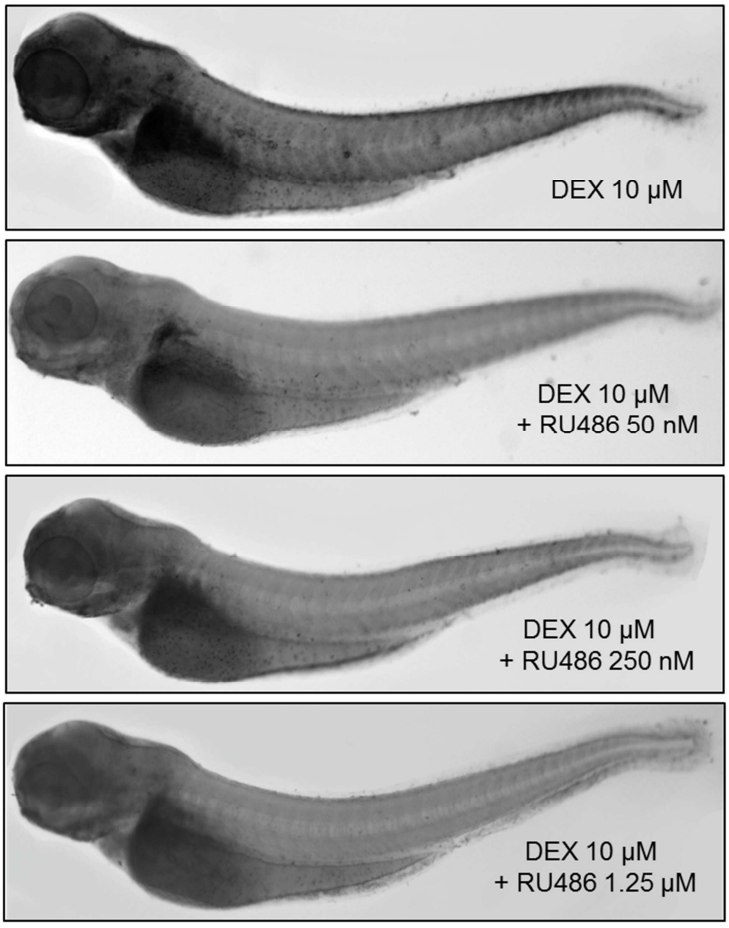
DEX 10 µM
DEX 10 µM
+ RU486 50 nM
DEX 10 µM
+ RU486 250 nM
DEX 10 µM
+ RU486 1.25 µM

Fig. 28. Reduced GRE activity following treatment with the Gr antagonist RU486. Two-dpf transgenic embryos were treated for 24 h with 10 μM DEX alone or combined with three different RU486 concentrations (50, 250 and 1250 nM). Left panel: fold changes in gene expression of *fkbp5* and *egfp* in treated embryos as compared to only DEX-treated control (set at 1). The expression levels of the target genes were normalized on *ef1α* as housekeeping gene. Values represent the mean ± S.E. Asterisks indicate expression levels that are significantly different from control (DEX-treated ia20): *P<0.05; **P < 0.01; ***P < 0.001. Right panel: WMISH of *egfp* mRNA after DEX treatment alone or combined with RU486 at different concentrations.

Moreover, when morphants were treated with 5 μM progesterone for 24 h (from 2 dpf to 3 dpf), they did not display any fluorescence increase (Fig. 29). The increase was instead seen in control fish. Therefore, we validated he hypothesis that the progesterone effect was dependent on the metabolic conversion of progesterone to cortisol as previously suggested in chapter 6.4. We also demonstrated that a functional GR receptor is needed for the hormone-dependent induction of transgene activation.

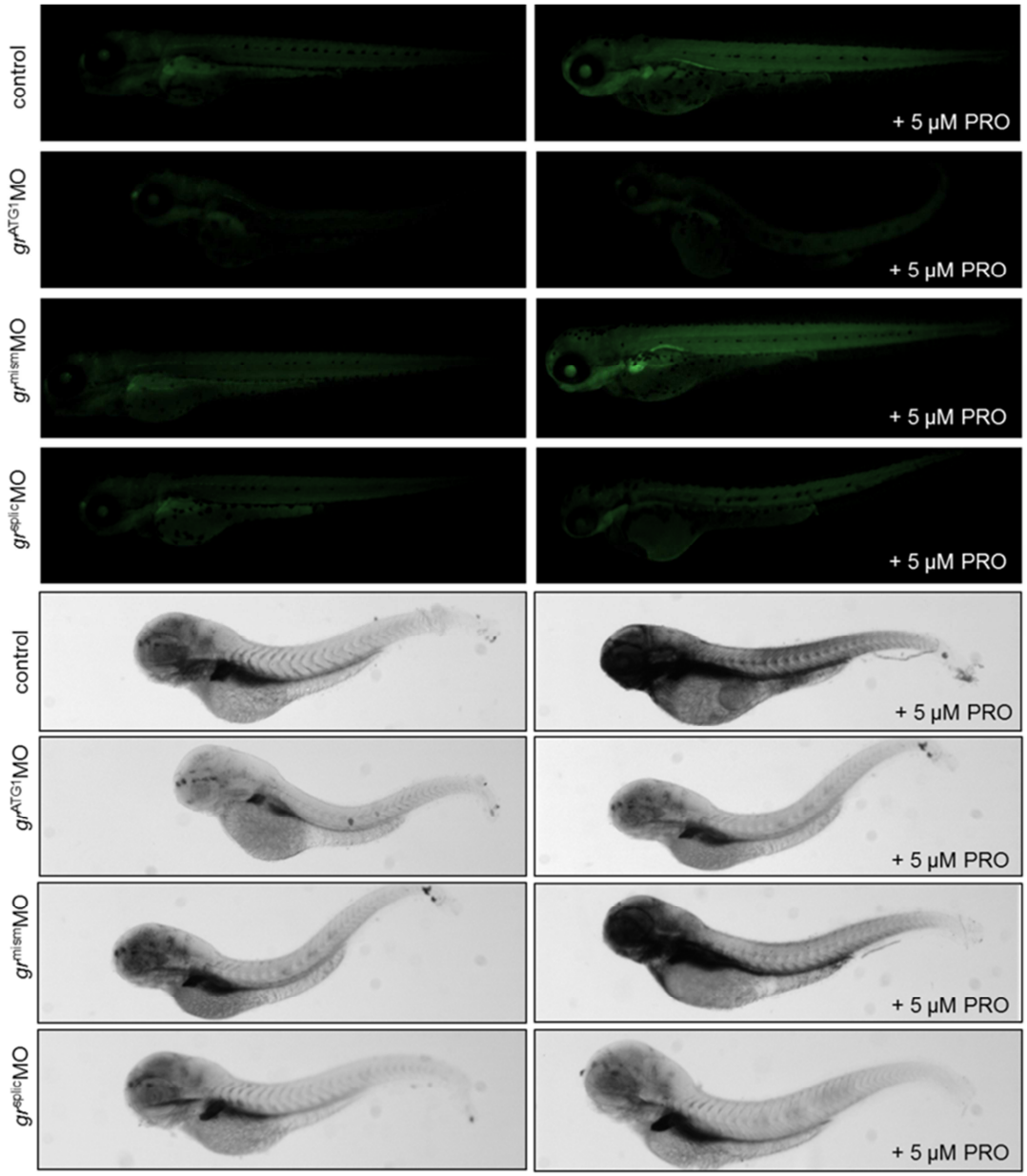

Fig. 29. Reduced GRE activity following *gr* MOs injections alone or combined with 5 µM progesterone treatment of 2 dpf transgenics for 24 h. EGFP fluorescence and messenger WMISH localization after translation-blocking MO (*gr*^{ATG1}MO), missplicing MO (*gr*^{splic}MO) and mismatched control MO (gr^{mism}MO) injections alone (on the left) or combined with progesterone treatment. Scale bar: 200 µM.

6.6. Adult fish of the ia20 line show endogenous GR transcriptional activity

After analysing transgene expression at embryonic and larval stages, we characterized its persistence and GCs responsiveness during adult life (Fig. 30).

Interestingly, in the ia20 line endogenous fluorescence is still detectable during adult life. In untreated adult males and females, transgene fluorescence was observed in many tissues, such as the esophageal sacs mucosa (Fig. 30A, 30K), ventricular epicardium (Fig. 30B, 30L), liver (Fig. 30C, 30M), intestinal mucosa (Fig. 30D, 30N), testis (Fig. 30E) and ovary (Fig. 30O). A lower fluorescence signal was also detected in the brain, skeletal muscle and kidney (not shown). In order to analyse the capability of the adult ia20 fish, male and female, to respond to exogenous GCs we decided to perform a 24h treatment with 10 μM DEX. After the treatment, both male and female transgenic fish showed an increase of the fluorescence in the brain, liver, intestinal mucosa and kidney (not shown) as well as detectable transgene expression in the skeletal elements of the splanchnocranium (Fig. 30 H', R'), spinal cord (Fig. 30 J', T'), eye (Fig. 30 F', G', P', Q') and skin (Fig. 30 I', S').

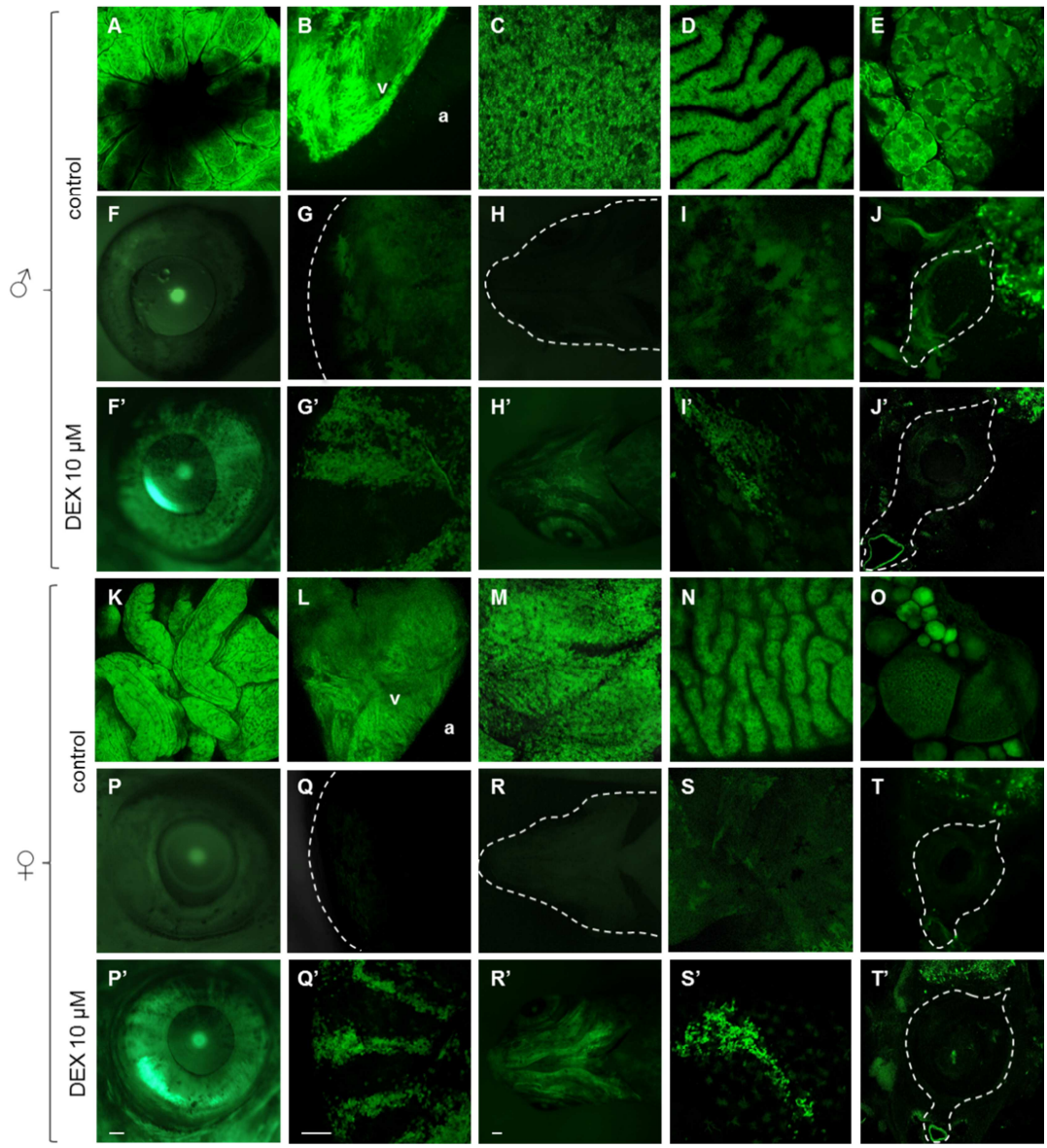

Fig. 30. 20x confocal microscopy pictures showing EGFP in control and 10 µM DEX-treated adult zebrafish males and females: esophageal sacs (A, K), ventricular epicardium (B, L; v = ventricle; a = atrium), liver (C, M), intestinal mucosa (D, N), testis (E), ovary (O), eye (F-G, F'-G'; P-Q, P'-Q'), skeletal elements of the splanchnocranium (H', R'), skin (I, I', S, S') and spinal cord (J, J', T, T'). Scale bars: 200 µM.

6.7. Transgene expression shows variations in tissues specificity and intensity with respect to the light cycle

The endogenous circulating GCs are not constant during the day, but their amount fluctuates according to the light/dark (LD) rhythm (see chapter 1.2). In order to evaluate the sensitivity of the ia20

transgenic line to the circadian variations of the concentration of endogenous GCs, we analyzed *egfp* transcription by WMISH in 5 dpf transgenic larvae exposed to standard photoperiodic regimen (14 h light/10 h dark) at 15 time points. Larvae were collected at 2 h intervals starting from 2 h before light onset (8 am) for 28 h.

The analysis of the fluorescence revealed that during the dark period, reporter activity was low and mainly limited to the digestive tract (from 20 pm to 6 am), but it increased just before the light onset (8 am), especially in the liver and intestine, where it remained high till 12 am to decrease later on (Fig. 31A). In the eye and brain, the signal increased from 10 to 12 am, and then decreased. The pattern observed in 5 dpf larvae was repeated in their 6 dpf siblings collected at 6 am, 8 am and 10 am the following day, thus denoting that the messenger variations are due to GCs circadian fluctuation and not to the different developmental stage.

For a more detailed analysis of *egfp* expression close to light onset, we also collected 5 dpf larvae once an hour from 3 hours before light onset (5 am) to 5 hours post light onset (1 pm) and performed egfp WMISH, shown in Figure 32 B. The *egfp* and *fkbp5* messenger expression pattern were studied by means of real time PCR of both transcripts at 5, 8 and 11 am. This assay showed a significant up-regulation of both transcripts at 8 am (Fig. 32). Moreover, the same expression pattern observed for *egfp* was obtained by WMISH also for *fkbp5* expression in wild-type fish (Fig. 31C). Fluorescence analysis of transgenic fish showed a similar circadian modulation of transgene expression with an EGFP signal delay consistent with the time required for translation (Fig. 31A). The decrease of fluorescence was slower with respect to the mRNA decrease due to the higher protein stability. Finally, WMISH of *gr* expression (Fig. 31D) did not show substantial variations as also reported by Dickmeis and colleagues, who did not detect any significant variation of *gr* mRNA during the LD cycle (Dickmeis *et al.*, 2007). This result confirms the hypothesis that

the observed variations of *egfp* and *fkbp5* mRNA and of EGFP fluorescence depend on the oscillation of GCs concentration, thus validating the ia20 line sensitivity to endogenous GCs fluctuations during day time.

A

EGFP fluorescence

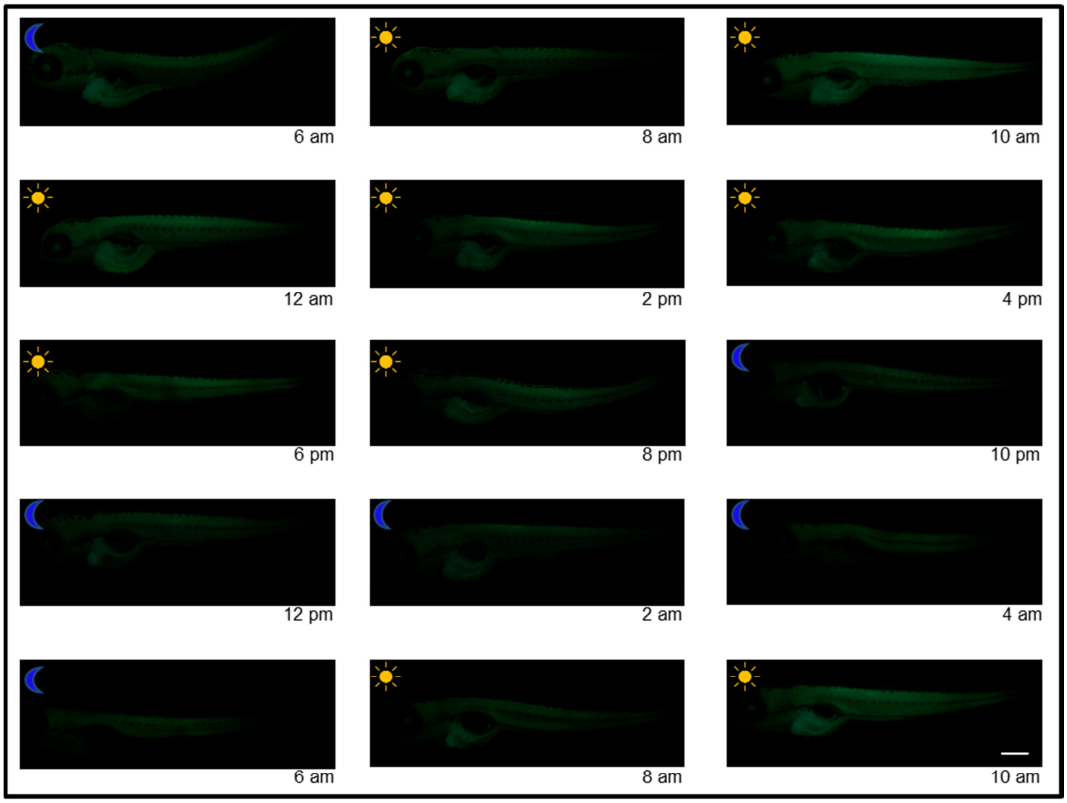

B

WMISH: *egfp*

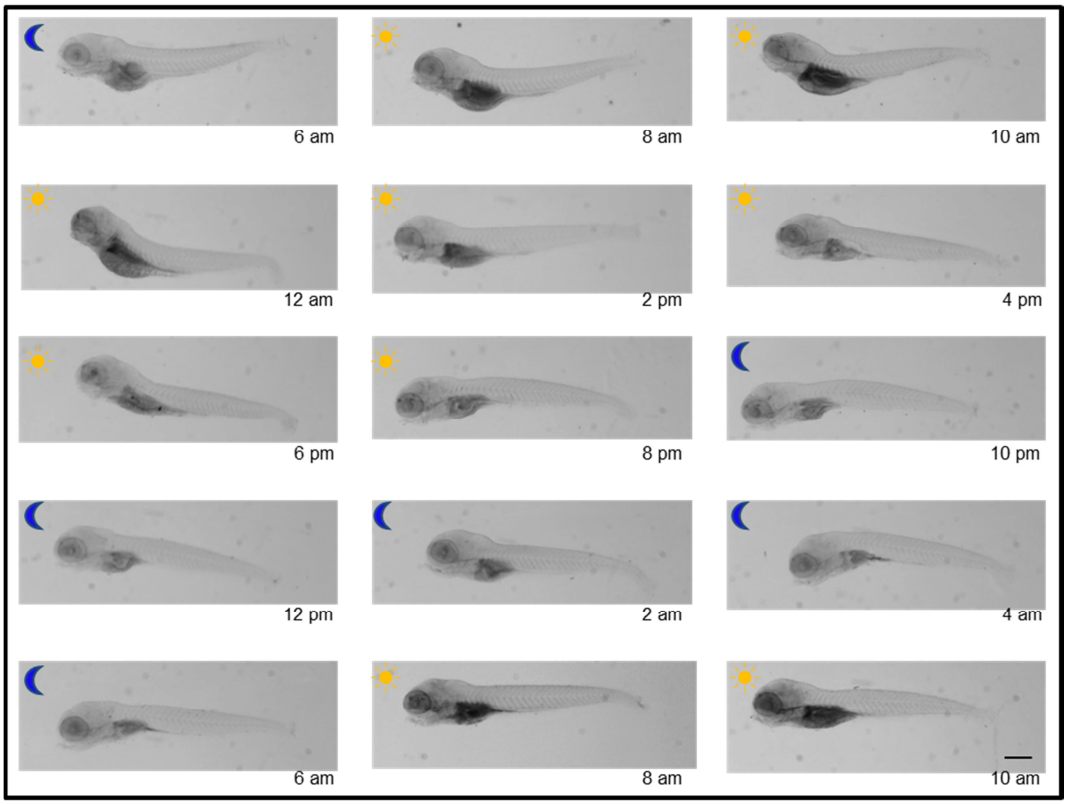

C

WMISH: *fkbp5*

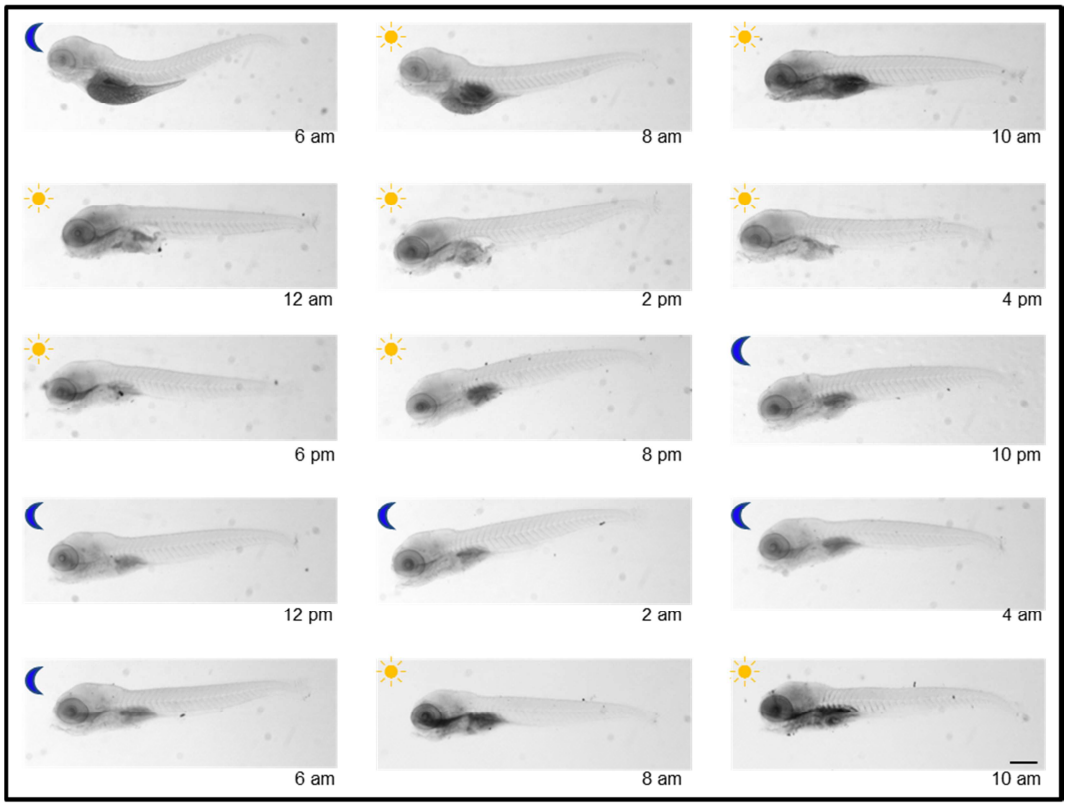

D

WMISH: *gr*

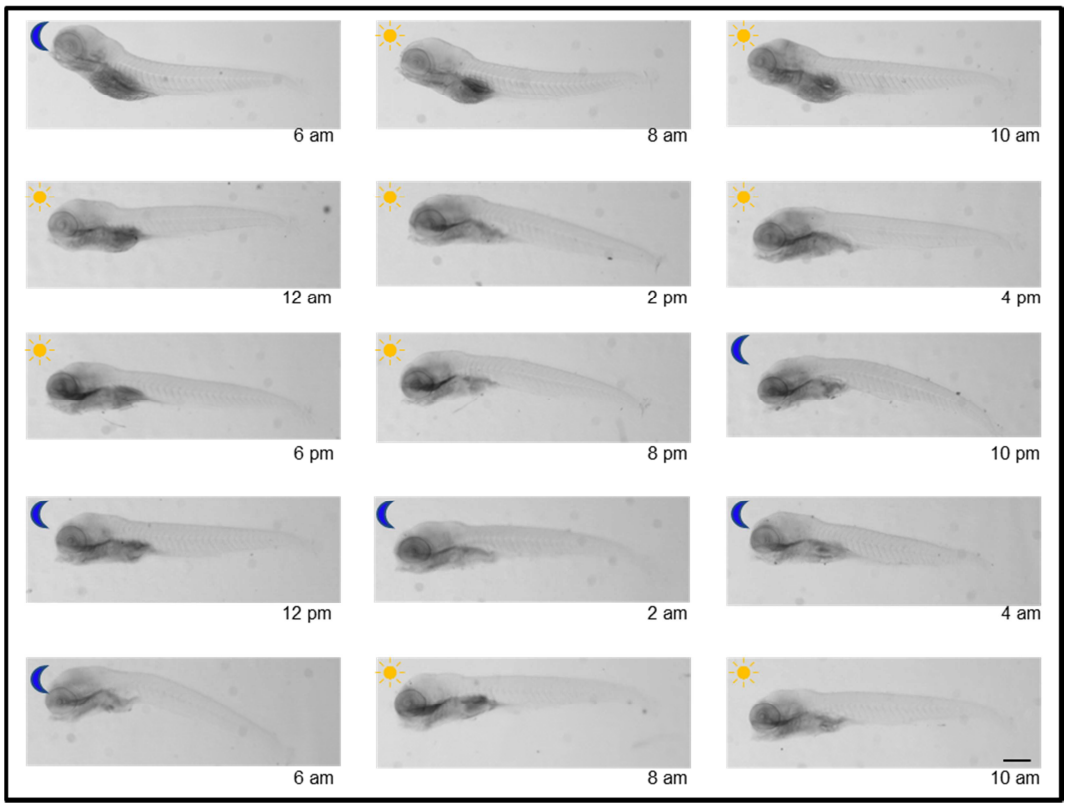

Fig. 31. A) Fluorescence microscopy lateral view, B) WMISH of *egfp* mRNA of 5 dpf transgenic larvae and C) WMISH of *fkpb5* mRNA, D) WMISH of *gr* mRNA of 5 dpf WT larvae exposed to standard photoperiodic regime and analysed from 2 h before light onset for 28 h.

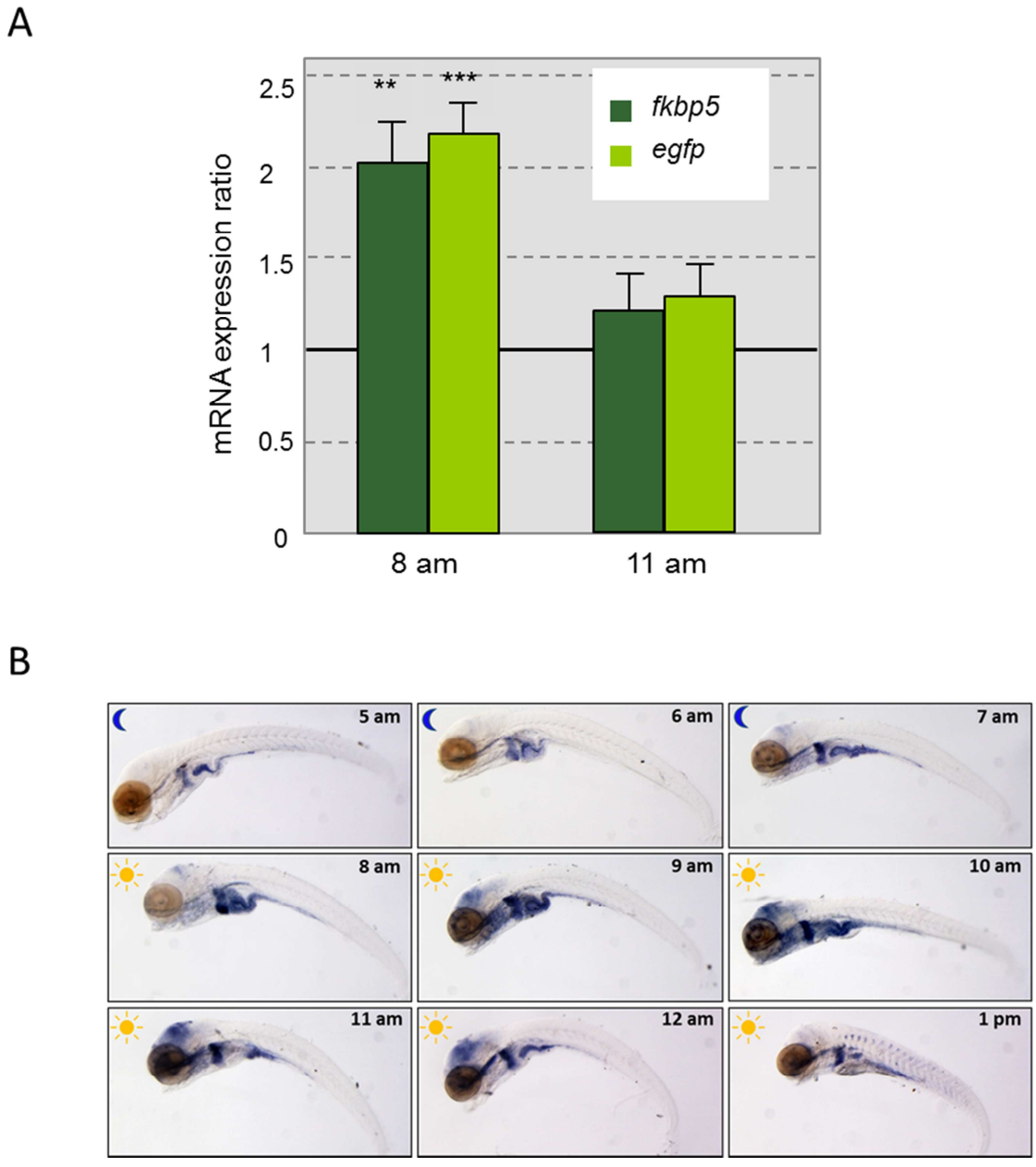

Fig. 32. A) fold changes in gene expression of *fkbp5* and *egfp* in 5-dpf larvae exposed to standard photoperiodic regime and analysed at 5, 8 and 11 am. Expression levels at 8 and 11 am were compared to those at 5 am (set at 1). The expression levels of the target genes were normalized on *ef1a* as housekeeping gene. Values represent the mean ± S.E. Asterisks indicate expression levels that are significantly different: **P < 0.01; ***P < 0.001. B) *egfp* WMISH performed on

5 dpf larvae collected every hour from 3 hours prior to light onset (5 am) to 5 hours after light onset (1 pm). Scale bar: 200 μM.

6.8. Generation and expression analysis of a ia20 line in *gr*^{s357} background

The glucocorticoid receptor shares, with other members of the steroid hormone receptors family, (including mineralocorticoid, progesterone and androgens receptors), the ability to bind to the same response element: the glucocorticoid responsive elements (GREs). For this reasons these responsive elements are also called "hormone responsive elements" (HREs) (see chapter 2.1). In our previous work (Benato *et al.,* 2014), we excluded the presence of significant cross-reactivity until 3 dpf (see chapter 6.4), but we did not characterize its possible occurrence at later stages, when progestogens, androgens and mineralocorticoids receptors expression could reach higher levels. For this reason, in order to characterize the steroid response and possible cross-reactivity through binding to HREs, we generated a zebrafish glucocorticoid responsive line (ia20 line; Benato *et al.*, 2014) in *gr*^{s357} background, in which Gr transcriptional activity is disrupted (Muto et al., 2005; Ziv et al., 2013; see chapter 3.3).
A detailed confocal microscopy (Fig. 33) analysis of 2 and 5 dpf larvae, heterozygous or homozygous for the s357 mutation, revealed a clear decrease of the endogenous fluorescence in homozygous mutants (ia20/*gr*$^{s357-/-}$), as expected by the very low occurrence of steroid hormone receptors except for Gr. The fluorescence signal was very low or absent, with respect to ia20 zebrafish, in some discrete sites such as otic vesicle (Fig. 33, A, A', A"), pectoral fin (Fig. 33, B, B', B") and putative KA" interneurons (Fig. 33, C, C', C") in 2 dpf embryos or dermal mesenchymal cells (Fig. 33, H, H', H") in 5 dpf larvae. In olfactory bulbs (Fig. 33, D, D', D"), liver (Fig. 33, E, E', E"), gut (Fig. 32, F, F' F") and muscle (Fig. 33 G, G', G") of 5 dpf larvae

the decrease was consistent although a lower fluorescence signal is still present.

A slight fluorescence decrease was detectable in heterozygous larvae (ia20/*gr*$^{s357+/-}$) when compared to WT (ia20/*gr*$^{s357+/+}$), but this was much less remarkable than the decrease observed in ia20/*gr*$^{s357+/-}$.

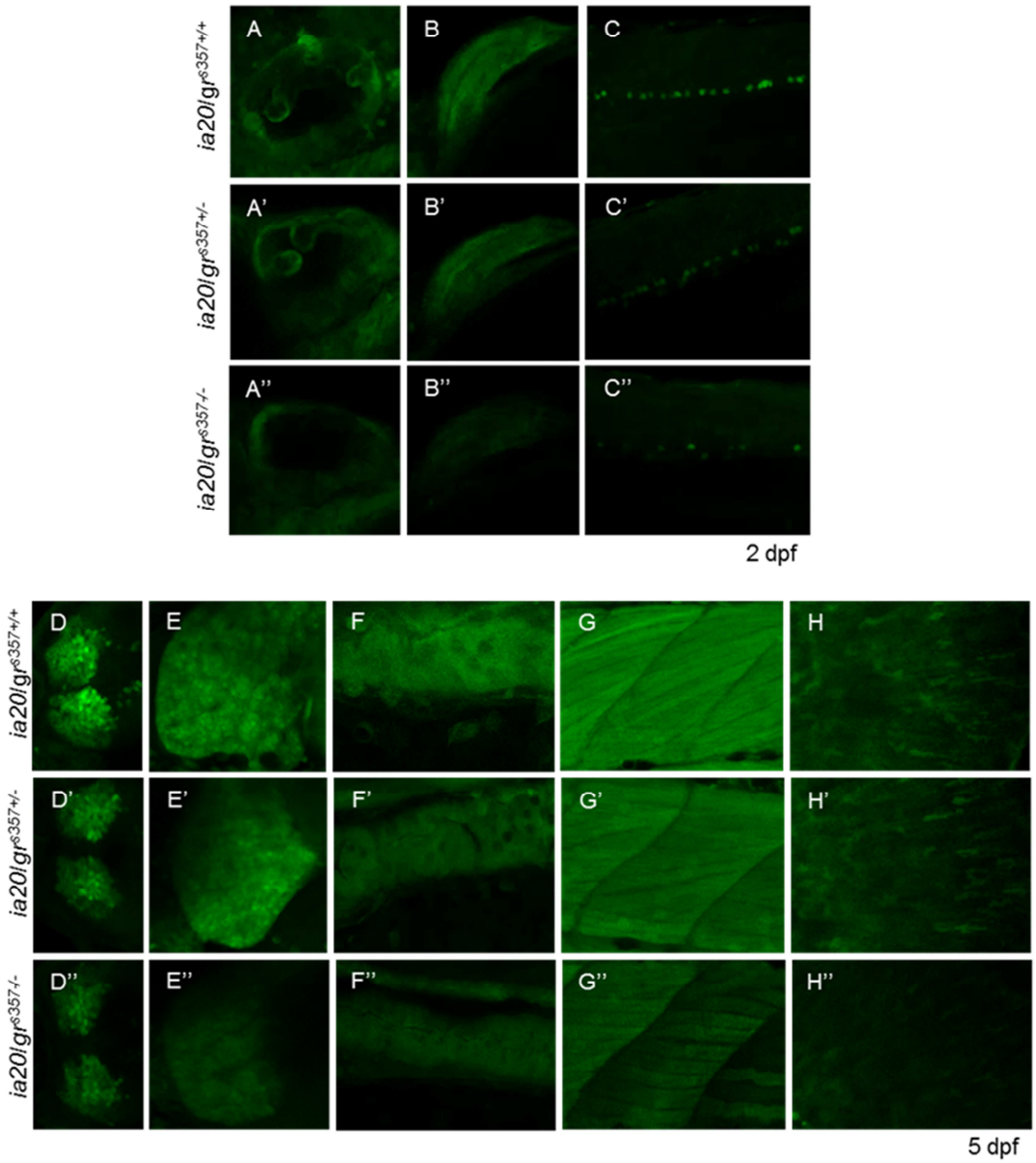

Fig. 33. Confocal images of otic vesicle (A, A', A"), pectoral fin (B, B', B") and putative KA" interneurons (C, C', C") in 2 dpf embryos (upper panel) and olfactory bulbs (D, D', D"), liver (E, E', E"), gut (F, F' F"), muscle (G, G', G") and dermal mesenchymal cells (H, H', H") in 5 dpf larvae (bottom panel) of WT (ia20/*gr*$^{s357+/+}$),

heterozygous (ia20/*gr*$^{s357\ +/-}$) and homozygous (ia20/*gr*$^{s357-/-}$). Homozygous *gr*^{s357} mutants (ia20/*gr*$^{s357-/-}$) display a less intense endogenous fluorescence with respect to heterozygous (ia20/*gr*$^{s357\ +/-}$) and wild type (ia20/*gr*$^{s357\ +/+}$) fish. Heterozygous larvae seem to display an intermediate phenotype between WT and homozygous fish.

6.9 Steroid responsiveness to glucocorticoids is lacking in *gr*^{s357} homozygous mutants

In order to characterize the steroid responsiveness of *gr*^{s357} homozygous mutants at early stages, we repeated the 5 μM steroid treatments described in chapter 6.4, from 10 hpf to 3 dpf. The results obtained show that, differently from wild type fish, 3 dpf *gr*^{s357} homozygous mutants lost almost entirely their steroid responsiveness (Fig. 34).

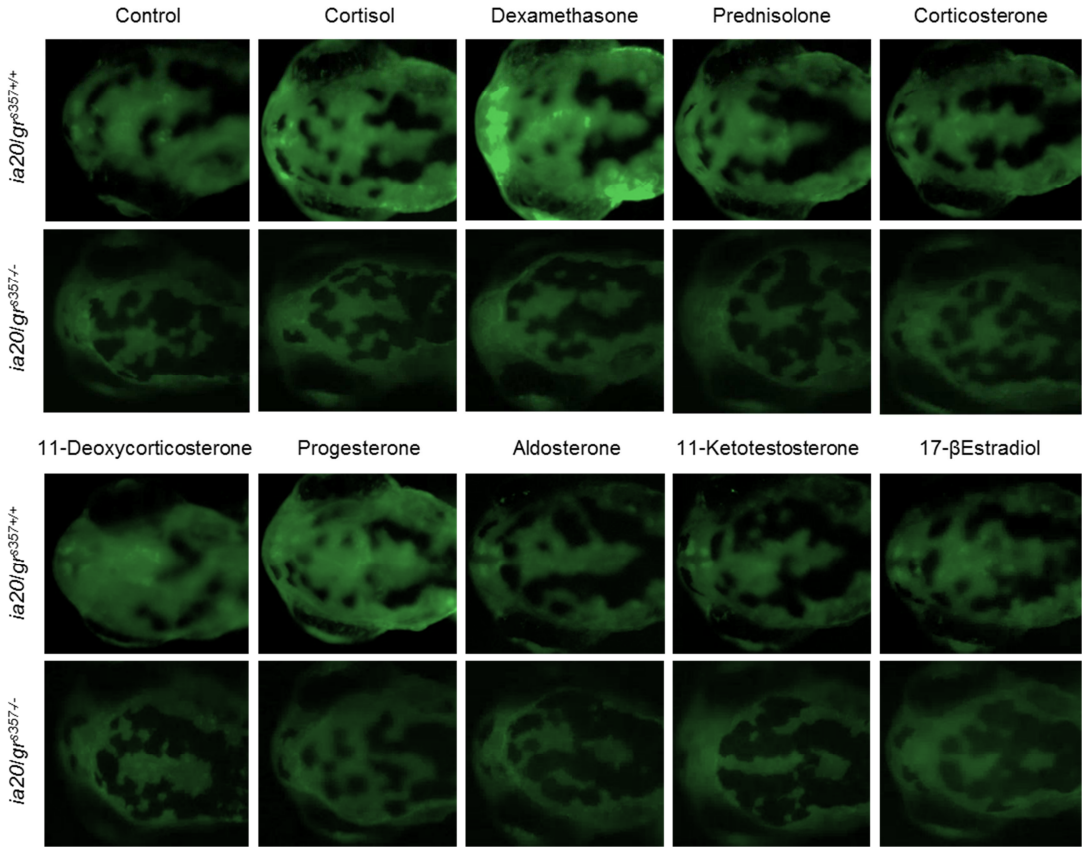

Fig. 34. Fluorescence images of the head region of 3 dpf *gr*$^{s357-/-}$ larvae treated with 5 μM steroids from 10 hpf until 3 dpf. For comparison, the fluorescence images

relative to the same treatment performed on ia20 embryos in WT background are also reported (Benato *et al.*, 2014; see Fig. 22). Wild type larvae (*ia20*/*gr*$^{s357+/+}$) display a cortisol, dexamethasone, corticosterone and progesterone response, whereas *ia20*/*gr*$^{s357-/-}$ mutants do not show any GCs response.

Moreover, we performed a 10 μM DEX treatment for 24 h (from 48 hpf to 72 hpf) on ia20 and ia20/*gr*^{s357} heterozygous and homozygous larvae. As previously demonstrated *in vitro* by Ziv and colleagues (Ziv *et al.*, 2013), we here show *in vivo* that *gr*$^{s375-/-}$ mutants do not respond to DEX (Fig. 35).

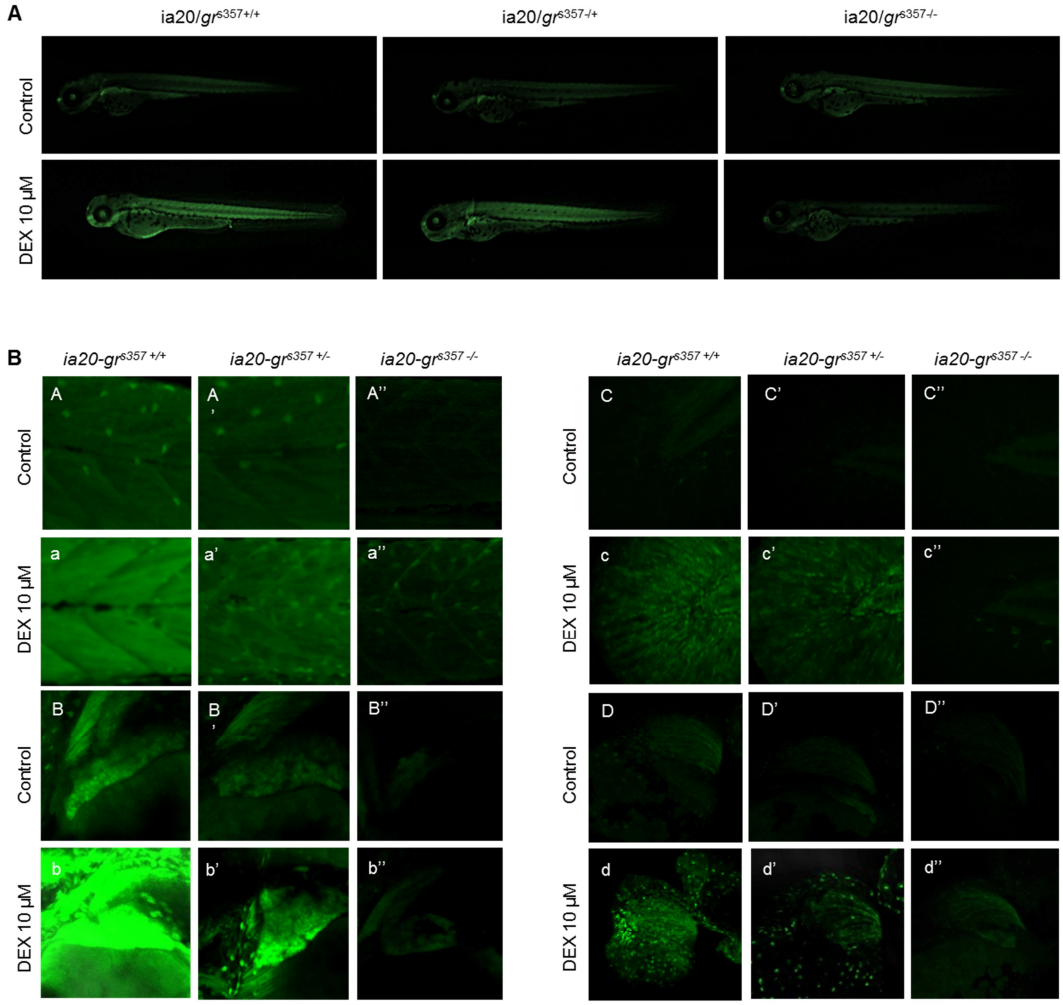

Fig. 35. Embryos were treated with 10 μM dexamethasone from 48 hpf and observed at 72 dpf. Dexamethasone response was completely lost in ia20/gr$^{s357\ -/-}$ mutants. A) Fluorescence images of whole 3 dpf larvae. B) Confocal magnification

of muscle (A, A', A", a, a', a"), liver (B, B', B", b, b', b"), dermal mesenchymal cells (C, C', C", c, c', c") and pectoral fin (D, D', D", d, d', d") of 3 dpf larvae.

6.10. Characterization of ia20/*gr*^{s357} endogenous EGFP signal at later stages

In our previous work (Benato *et al*., 2014), we demonstrated that in the ia20 line fluorescence is not limited to early development, but it persists in later stages (see chapter 6.6 and Fig. 30). In order to characterize the specificity of EGFP signal, we compared the fluorescence of ia20/*gr*$^{s357+/+}$ (WT) and ia20/*gr*$^{s357-/-}$ in discrete sites at late larval stages (21 dpf): lower jaw (Fig. 36 A, A'), pectoral fin (Fig. 36 B, B'), pronephros (Fig. 36 C, C'), liver and skeletal elements of the splanchnocranium (Fig. 36 D, D'), muscle and gut (Fig. 36 E, E'). As shown in Figure 36, homozygous mutants display a sharp fluorescence reduction or elimination in all the districts we took into consideration in our analysis.

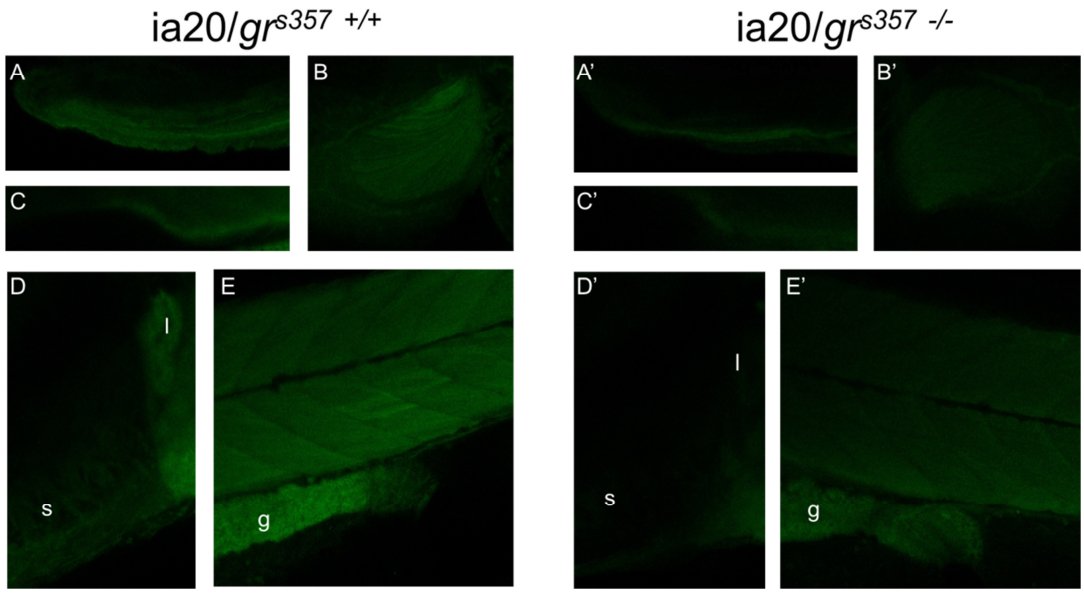

Fig. 36. Confocal analysis of lower jaw (A, A'), pectoral fin (B, B'), pronephros (C, C'), liver (l) and skeletal elements of the splanchnocranium (s) (D, D'), muscle and gut (g) (36 E, E') showing a strong fluorescence decrease in homozygous mutants when compared to ia20 larvae.

6.11. Adult *gr*$^{s357-/-}$ fish do not respond to exogenous glucocorticoids

In order to characterize the adult zebrafish glucocorticoids responsiveness in the absence of Gr transcriptional activity, we performed a DEX treatment (5 μM for 24 h) on male and female adult ia20/*gr*$^{s357+/+}$ (WT) and ia20/*gr*$^{s357-/-}$. Previous treatments (see Fig. 34 and 35, chapter 6.9) were performed during early development, when the other steroid receptors are expressed at very low levels.
We analyzed through confocal microscopy four representative sites (gut, ovary/testis, muscle and liver), revealing that DEX responsiveness is lost in most sites in homozygous mutants, as shown in Figure 37: gut (female: Fig. 37 A, A', A'', A'''; male: Fig. 37 B, B', B'', B''') and liver (female: Fig. 37 G, G', G'', G'''; male: Fig. 37 H, H', H'', H'''). In muscle (female: Fig. 37 E, E', E'', E'''; male: Fig. 37 F, F', F'', F'''), we detected a fluorescence decrease in homozygous mutants, with remaining signal mostly concentrated in the lateral region. Moreover, fluorescence seems to be more intense in males. As androgen receptor is known to be expressed in muscle at a lower rate in females with respect to males (Hossain *et al*., 2008) and no DEX response was observed, this result suggests that muscle is also responding to androgens. Conversely, we did not observe any fluorescence differences between ia20/*gr*$^{s357+/+}$ and ia20/*gr*$^{s357-/-}$ fish in gonads, indicating that these structures are likely responding to endogenous steroids by means of progesterone and androgen receptors (Fig. 37 D, D', D'', D''') and (Fig. 37 C, C', C'', C''').
This was only a preliminary experiment performed in order to have an indication of glucocorticoids responsiveness in adult homozygous mutants. We will now need to perform further treatments with androgens, progesterone and mineralocorticoids in order to finely

characterize the cross-reactivity of different steroid receptors in the absence of Gr transcriptional activity.

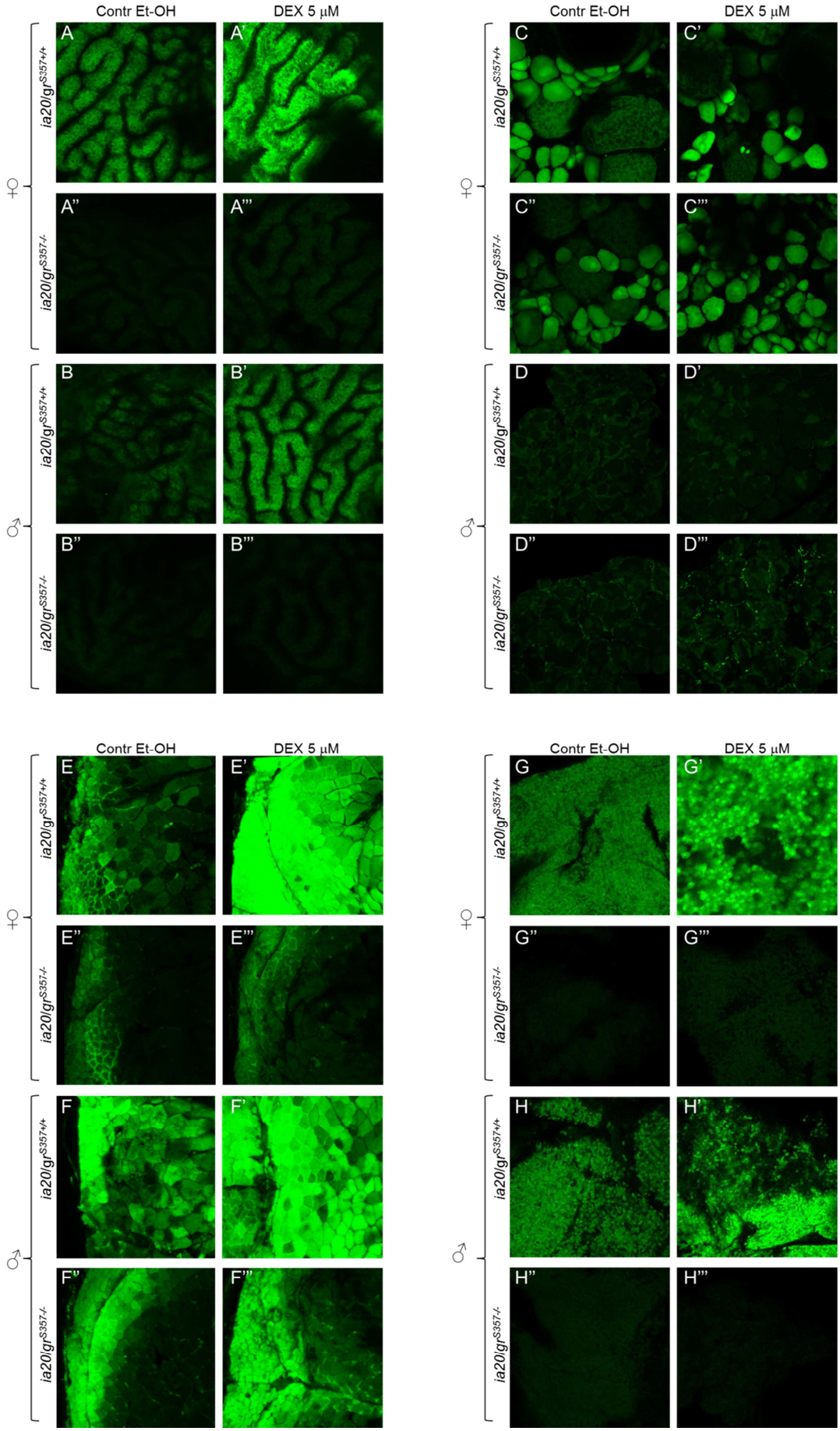
Contr Et-OH
DEX 5 µM
♀
♂
ia20/gr^S357+/+
ia20/gr^S357-/-
A
A'
A''
A'''
B
B'
B''
B'''
C
C'
C''
C'''
D
D'
D''
D'''
E
E'
E''
E'''
F
F'
F''
F'''
G
G'
G''
G'''
H
H'
H''
H'''

Fig. 37. Adult male and female ia20/*gr*$^{s357+/+}$ (WT) and ia20/*gr*$^{s357-/-}$ (homozygous mutants) were treated with 5 μM DEX for 24 h. We observed no DEX response in homozygous mutant in gut (female: Fig. 37 A, A', A'', A'''; male: Fig. 37 B, B', B'', B''') and liver (female: Fig. 37 G, G', G'', G'''; male: Fig. 37 H, H', H'', H'''). No appreciable differences were observed between ia20/*gr*$^{s357+/+}$ and ia20/*gr*$^{s357-/-}$ in gonads (ovary: Fig. 37 C, C', C'', C'''; testis: Fig. 37 D, D', D'', D'''). In muscle (female: Fig. 37 E, E', E'', E'''; male: Fig. 37 F, F', F'', F'''), fluorescence decreases in ia20/*gr*$^{s357-/-}$ mutants, where it is concentrated in the lateral region.

7. DISCUSSION

Most of this PhD thesis is dealing with the setting, description and validation of a transgenic zebrafish line, "ia20", in which the activation of the GCs signaling pathway can be monitored *in vivo*. The transcriptional activity of the glucocorticoid receptor can be thoroughly analyzed not only from a spatial point of view, but it can also be followed during development and adult life. The integrated reporter transgene incorporates a conserved GRE tandem repeat that has been multiplied nine-fold to increase cooperative binding of ligand-activated Gr to GRE and boost transcription initiation of the *egfp* transgene (Jantzen et al., 1987). The *egfp* transgene is located downstream of these nine GRE repeats, which drive and strongly activate its transcription. As a result, a massive EGFP production occurs in all the cells where the glucocorticoid receptor is activated.

One current issue in the generation of transgenic lines is positional effect, i.e. a different transgene expression pattern according to the genomic contest in which the transgene has been inserted. As recommended by Fisher and colleagues, we analyzed the offspring generated by several independent founders (Fisher *et al*., 2006). They showed the same EGFP expression pattern, thus ruling out positional effects.

The transgenic line exhibits a high sensitivity, as evidenced by the detection of regionalized fluorescence in embryonic head and tail driven by endogenous GCs already at 14 hpf. Recently, Weger and colleagues set an *in vivo* GCs responsive line where four GRE repeats drive the expression of luciferase (Glucocorticoid Responsive In vivo Zebrafish Luciferase Activity, GRIZLY, assay) (Weger *et al*., 2012; Weger *et al*., 2013). In the GRIZLY assay, response was demonstrated to start at 1 dpf and only under DEX stimulation. This line represents an effective tool for GREs-mediated chemical screenings, but does not enable a detailed spatial analysis of GCs

activity. The ia20 line, instead, allowed us to have a thorough dissection of the spatio-temporal GCs activity *in vivo* (see results in chapter 6.2). The use of a fluorescent molecule as reporter provides a higher spatial resolution, as shown by clear EGFP signaling in isolated dermal mesenchymal-like cells, blood and two rows of cells located above the notochord, possibly corresponding to the KA'' interneurons. These cells are distributed irregularly along the lateral floor plate domain and, after differentiation, lose the ability to respond to the Hedgehog (Hh) signal (Huang et al., 2012). This could explain the lack of total co-localization between GRE and Hh activity in the cells when we outcrossed the ia20 line with a floor plate reporter (see chapter 6.2).

The human glucocorticoid receptor expression has been finely described by Pujols and colleagues and the overall expression pattern of our zebrafish transgenic line is extended to all sites of potential GCs activity (Pujols et al., 2002). Steroid selectivity of the reporter demonstrated high responsiveness to cortisol, DEX and prednisolone, low responsiveness to corticosterone, and ineffectiveness of mineralocorticoids, androgens and estrogens. The low corticosterone responsiveness is not surprising as the physiologically most relevant glucocorticoid in teleosts is cortisol, and corticosterone activity as an agonist is weaker with respect to cortisol and dexamethasone (Stolte *et al*., 2008).

The intense GRE-driven transcription induced by progesterone may be partly ascribed to its greater high cellular permeability as compared to GCs and to the conversion of progesterone into cortisol. In fact the steroidogenic enzymes involved are already active in larvae, as demonstrated by a 90% reduction of cortisol concentrations in morphants of *cyp11a2*, at 72 hpf with respect to controls (Parajes et al., 2013). Moreover, progesterone responsiveness could also reflect some affinity of this steroid for GR, as reported in dog (Selman et al., 1996) and humans, where it acts

as a low potency agonist (Koubovec et al., 2005). Interference by binding of progesterone to its specific receptor (Pr) is unlikely because *pr* mRNA levels are very low till 2 dpf in zebrafish (Pikulkaew et al., 2010). The hypothesis that the strong progesterone response might be caused by binding of the Pr to the reporter transgene was also excluded by incubating the *gr*-morphants (gr^{ATG1}MO and gr^{splic}MO) with 5 μM progesterone (see Fig. 29). While in control fish the hormone treatment induced an increase of transgene activity, in *gr*-morphants we did not detect evident effects. Therefore, we validated the hypothesis that the progesterone effect was dependent on Gr and, thus, on the metabolic conversion of progesterone to cortisol. Consequently, we can assume that, at least until 3 dpf, the ia20 line steroid responsiveness is selectively restricted to glucocorticoids. This conclusion is also supported by the clear and strong reduction of GCs responsiveness observed at 3 dpf in the ia20/$gr^{s357-/-}$ line, where the transcriptional activity of Gr is disrupted by a single amino acid substitution affecting DNA binding that impairs both transactivation and trans-repression (Ziv *et al.,* 2013; see chapter 3.3). Our data, put together, suggest that, at least until 3 dpf, the ia20 transgenic line is only reporting GCs activity.

In the ia20 line, dose-dependent responsiveness to DEX was established after exposure to increasing DEX concentrations, concomitantly with enhanced expression of *egfp* and *fkbp5* mRNAs. Similarly, signaling driven by endogenous GCs in target organs was strongly magnified by exogenous DEX. Although the activity of GCs *in vivo* was normally enhanced using micromolar concentrations of DEX, as also reported for the GRE-Luc line (Weger *et al*., 2012), in the ia20 line the *egfp* mRNA increase, analyzed by qPCR, was statistically significant already at 1 μM. However, differences in the fluorescence levels and the hybridization signals were already appreciated at 100 nM of DEX. Similarly, signaling driven by endogenous GCs was highly amplified by adding DEX and the ia20 line has been found to respond

in a dose-dependent manner also to GCs agonists such as cortisol, prednisolone and corticosterone.

Knockdown of maternal and/or zygotic *gr* mRNAs determined a strong reduction of reporter activity induced by DEX and curtailed expressions of *egfp* and *fkbp5* mRNAs. The fact that these mRNAs were more reduced in morphant larvae not exposed to DEX suggests that DEX over-induced reporter activity, largely compensating for the knockdown effect. A similar decrease of fluorescence was obtained by co-treatment of transgenic embryos with the GR antagonist RU486 suggesting that, at early stages, the fish line is only reporting GC activity.

The similar modulation of *egfp* and *fkbp5* expression under different treatments is remarkable, because it demonstrates that, despite its artificial assemblage, the transgene is operating like an endogenous promoter. This matching, however, is only partial, because it does not cover indirect transactivation and transrepression due to crosstalk between GR and other transcription factors, given the absence of additional docking sites for them in the transgene promoter (Kassel and Herrlich, 2007).

From a quantitative point of view, the increased number of responsive elements with respect to the ones located upstream to the *fkbp5* gene makes the transgene more prone to cooperativity and transcription, and the increased sensitivity enables the detection of new GC responsive targets, as the cristae and lateral canals of the otic vesicles, and scattered mesenchymal-like cells and putative KA'' cells.

Notably, we first detected an ascending rostro-caudal gradient of transgene, with the highest levels of GRE-reporter activity in the caudal portion of 24-hpf larvae. This expression pattern could be related to the key action of Gr signaling in axial mesoderm development, which is disrupted when *gr* expression is perturbed (Wang *et al*., 1999; Nesan *et al*., 2012).

Interestingly, similarly to the well-known morphogen retinoic acid, also GCs play a function in modulating Wnt antagonists, in particular during differentiation of mesenchymal stem cells (Beildeck *et a*l., 2010). Moreover, mouse skeletal development and mesenchymal progenitor cells are committed to osteoblastic lineage via a GC-dependent Wnt signaling (Zhou *et al*., 2009).

Relevant is our finding of localized transgene expression in the cardiac district of 2-dpf embryos and in the heart of 5-dpf larvae as well as in adult fish, where it is particularly intense in the ventricular epicardium. In mice, GC signaling is required for fetal heart maturation (Rog-Zielinska *et al*., 2013) and its over-activation through GR conditional expression perturbs adult cardiac physiology through conduction defects (Sainte-Marie *et al*., 2007). Given the persistence of transgene expression in the adult zebrafish heart, it is plausible that also in teleosts GC signaling plays a critical role in cardiomyocyte function and remodelling after insults, as shown in mice (De *et al*., 2011; Ren *et al*., 2012). We also found that the esophageal sacs mucosa expressed, particularly at adulthood, a high level of reporter transgene. A key role of GCs signaling in promoting cell proliferation and apoptosis in the esophageal epithelium was already demonstrated in medaka (Takagi *et al*., 2011). Moreover, adrenalectomy has been reported to result in reduced cell proliferation in the rat small intestine (Foligne *et al*., 2001). Pleiotropic effects of GCs have been proposed in the small intestine where, at least in mouse and human, an autonomous synthesis of these steroids has been recently documented (Mueller *et al.*, 2007). In this organ, GCs are involved not only in the regulation of locally confined immune responses (Mueller *et al*., 2007), but also in intestinal cell maturation and transcriptional activation of genes involved in the absorptive function (Quaroni *et al*., 1999). Thus, it may be envisaged an involvement of GCs in tissue renewal and support of digestive function in the esophageal sacs and intestinal

tract. DEX treatment in adult ia20/*gr*$^{s357-/-}$ seems to confirm the GCs specificity of the EGFP signal in the digestive system observed in the ia20 line. Indeed, liver and gut displayed a consistent decrease of endogenous fluorescence and a loss of DEX responsiveness in the absence of Gr transcriptional activity, suggesting that, in these adult tissues, the transgenic line is only reporting GCs activity. However, this was only a preliminary experiment and further treatments with progesterone, androgens and mineralocorticoids will be necessary in order to confirm this result.

The expression of the transgene in adult muscle and its DEX responsiveness suggest that this tissue responds to GCs, but the incomplete fluorescence elimination in ia20/*gr*$^{s357-/-}$ mutants indicates that muscle is likely responding also to androgens. Moreover, in agreement with our findings, it was previously demonstrated by Hossain and colleagues that the androgen receptor is expressed in zebrafish muscle at a higher rate in males than females (Hossain *et al.*, 2008).

Fluorescence was observed also in the ovary of ia20 transgenic females. Confocal analysis of this organ demonstrated localized EGFP expression in follicular cells and in the ooplasmic and nuclear regions of developing oocytes. A modulation of ovarian functions by GCs as well as the presence of their receptor have been demonstrated in human, where it limits inflammation and tissue injury during ovulation (Rae *et a*l., 2004), rat (Tetsuka *et al*., 1999) and teleost, with a possible role in the diversion of energy resources from ovarian growth to other tissues during chronic stressful situations (Leatherlan *et al.*, 2010). Actually, fluorescence showed by ovulated oocytes and RT-PCR detection of maternal *egfp* mRNA starting from one-cell stage suggest the possibility of a continual activation of the GC signaling pathway throughout female gametogenesis. On the other hand, *pr* transcripts and proteins have been found at high concentrations in zebrafish ovaries, both in follicular cells and early-stage oocytes

(Hanna *et al*., 2010). Since the GRE sequence is shared as responsive element by the progesterone-Pr complex, an involvement of the latter in transgene ovarian activation cannot be excluded. Similarly, given GRE responsiveness also to Ar, transgene activation in the testis of adult zebrafish could be related to androgen receptor present in Sertoli cells contacting spermatogonia (de Waal *et al*., 2008) as well as to the occurrence of Pr in Leydig and Sertoli cells (Chen *et al*., 2010). In fact, when we treated with DEX adult ia20 and ia20/*gr*$^{s357-/-}$, we did not observe any appreciable difference between wild type and mutant background in these tissues, thus suggesting that the EGFP signal did not result from the glucocorticoid activity alone and that Pr in ovary and Pr and Ar in testis might bind to GREs and contribute to transgene expression. Further treatments with progesterone and androgens will enable us to shed light on the contribution of these steroids in the GREs-mediated transcriptional activation in gonads.

Albeit only *gr* mRNA is present at high concentrations in ovulated eggs and during early developmental stages (Pikulkaew *et al*., 2010), thus validating the relevance of GC transgene activation in embryogenesis, this does not hold at adulthood, when all steroid hormone pathways are operative. In order to rule out potential modulation of the reporter by other steroid hormones in adult stage, specific mutant lines for the different GRE-sharing steroid receptors should be adopted. As preliminary DEX treatments of *gr* mutant line suggest that Gr is not the only receptor interacting with GREs in gonads, our next goal will be the characterization of Pr and Ar contribution in the GREs-mediated transcriptional regulation, by means of progesterone and androgens treatments in ia20 and ia20/*gr*$^{s357-/-}$adults.

The paternally acquired transgene was transcribed in the progeny already at 2 hpf, which is strikingly precocious, being timed at the cleavage stage, when the synchronous divisions of the blastomeres

every 14-15 min limit the window for zygotic transcription (Tadros and Lipshitz, 2009). The embryonic content of *egfp* mRNA increased at 3 hpf with mid-blastula transition and remained high from 4 hpf onwards. The very early activation of the transgene promoter points to a fundamental developmental role of GCs and their receptor in zebrafish ontogenesis, as previously speculated (Pikulkaew et al., 2011; see chapter 3.2). However, this observation is in contrast with the viability of the mutant zebrafish strain, $gr^{s357-/-}$ (Ziv et al., 2013). The R443C mutant Gr protein of this line can bind cortisol but cannot perform DNA binding activity due to a missense mutation located in the DNA-binding domain (Ziv et al., 2013) that impairs both transactivation and trans-repression. Although morpholino off-target effects have been excluded by co-injection of p53-MO, we cannot rule out that some developmental defects as well as the reduced viability of the *gr*-morphants could be partially ascribed to this problem. In mouse a complete inactivation of the glucocorticoid receptor has been demonstrated to be inconsistent with life as $GR^{null/null}$ mice show severe abnormalities and die just after birth (Cole et al., 1995). In contrast, mice carrying the $GR^{dim/dim}$ (Reichardt et al., 1998), that impairs homodimerization and DNA binding of the receptor (A458T), are viable. In these mutants the GRE-dependent gene transcription is absent whereas other DNA-binding independent activities of the GR receptor, such as cross-talk with other transcription factors are allowed. Thus, we can speculate that, in zebrafish $gr^{s357-/-}$ mutants, similarly to the corresponding human GR R477H mutant that maintains full capacity to repress TNFα-induced NF-κB activity, some genomic functions not mediated by binding to GREs are still present (Ruiz et al., 2013).

Our results suggest that the GC signaling pathway exerts a basic integrative function by targeting genes that confer priority for resource access and consumption. Specifically, during embryonic and larval development, EGFP was expressed in organs and body parts

undergoing fast proliferation and differentiation, like head, tail, fins and primitive intestine with its hepatic and pancreatic offshoots.
In the ia20 line fluorescence was also precociously detected in fast developing sensory organs, like the eyes, the olfactory bulbs and tracts, and in other structures such as otic vesicles, pituitary and epiphysis. Energy allocation to these structures is justified by the immediate need of the larva to scan and process environmental cues into adaptive responses.
Furthermore, the role of activated GR in timing resource assignment is supported by the responses in terms of *egfp* transcript and protein disclosed by WMISH and fluorescence analysis in larvae exposed to standard photoperiodic regime as well as *fkbp5* expression. The trend of EGFP expression and its prevalent gastro-intestinal localization are interpretable as a functional predisposition for food seizing and digestion after nighttime fasting. GC signaling appears to harmonize the metabolic pre-activation of those organs that are expected to be soon functionally active, possibly by entraining local clocks. This hypothesis may be supported by the well-known surge in HPA axis activity before awakening in humans and other mammals (Chung *et al*., 2011). Of interest is the report that circadian cell proliferation rhythms were severely compromised by shutting down GC signaling in mutant zebrafish larvae with corticotrope deficiency whereas circadian rhythm effects were rescued by DEX treatment (Dickmeis et al., 2007). Dickmeis and colleagues (2007) hypothesized that GCs fluctuations during day time might lead to an involvement of peripheral circadian clock in the regulation of cell proliferation. Moreover, in mammals, regulation of a large proportion of the hepatic circadian transcriptome by GC signaling has been recently reported (Reddy et al., 2007).

8. FINAL CONCLUSIONS

In this thesis we described the setting and validation of a new transgenic GCs responsive line. Not only we detected transgene activation in well-known GC targets such as liver, bone, muscle or brain as we expected, but we also found positivity in other structures, like olfactory complex, otic vesicles or putative KA'' cells, which was actually a novelty. We showed that the ia20 line responds to glucocorticoids in a very selective way, at least during early development. Moreover, preliminary experiments on *gr*^{s357} mutants seem to confirm the specificity of this responsiveness in some tissues during adulthood.

GCs response was dose-dependent and exogenous GCs responsiveness was maintained until adult life. These results illustrate the potential of this transgenic line for deepening knowledge on GCs functions during both development and adult life. Due to its sensitivity to slight GCs concentration fluctuation, the ia20 line can be assumed to be suitable for pharmacology and toxicology studies, in order to detect the GREs-mediated Gr involvement in the response to drugs or toxic compounds even at very low concentrations.

Further experiments will be necessary to characterize the cross-reactivity of the transgenic line among different steroid receptors during adult life. In particular, we will perform several steroid (progesterone, androgens and mineralocorticoids) treatments on adult ia20 and ia20/*gr*$^{s357-/-}$ fish, in order to understand if and in which tissues the related receptors can regulate gene transcription by binding to GREs. As well as *gr*^{s357}, the transgenic line could be, in the future, put under any mutant background, acting as a potent *in vivo* tool to unravel Gr involvement in a huge number of biological processes.

9. REFERENCES

Alsop, D., Vijayan, M.M., 2008. Development of the corticosteroid stress axis and receptor expression in zebrafish. The American Journal of Physiology - Regulatory, Integrative and Comparative Physiology, 294: R711-R719.

Alsop, D.,Vijayan, M., 2009. The Zebrafish stress axis: molecular fallout from the teleost-specific genome duplication event. General and Comparative Endocrinology, 161: 62-66.

Beildeck, M.E., Gelmann, E.P., Byers, S.W., 2010. Cross-regulation of signaling pathways: an example of nuclear hormone receptors and the canonical Wnt pathway. Experimental Cell Research, 316: 1763-1772.

Benato, F., Colletti, E., Skobo, T., Moro, E., Colombo, L., Argenton, F., Dalla Valle, L., 2014. A living biosensor model to dynamically trace glucocorticoid transcriptional activity during development and adult life in zebrafish. Molecular and Cellular Endocrinology, 392: 60-72.

Buckingham, J.C., 2006. Glucocorticoids: exemplars of multi-tasking. British Journal of Pharmacology, 147 Suppl 1: S258-S268.

Bury, N.R., Sturm, A., 2007. Evolution of the corticosteroid receptor signalling pathway in fish. General and Comparative Endocrinolology, 153: 47-56.

Charmandari, E., Tsigos, C., Chrousos, G., 2005. Endocrinology of the stress response. Annual Review of Physiology, 67: 259-284

Chen, S.X., Bogerd, J., García-López, A., de Jonge, H., de Waal, P.P., Hong, W.S., Schulz, R.W., 2010. Molecular cloning and functional characterization of a zebrafish nuclear progesterone receptor. Biology of Reproduction, 82: 171-181.

Chrousos, G.P., 2009. Stress and disorders of the stress system. Nature Reviews Endocrinology, 5: 374-381.

Chung, S., Son, G.H., Kim, K., 2011. Circadian rhythm of adrenal glucocorticoid: its regulation and clinical implications. Biochimica et Biophysica Acta, 1812: 581-591.

Cole, T.J., Blendy, J.A., Monaghan, A.P., Krieglstein, K., Schmid, W., Aguzzi, A., Fantuzzi, G., Hummler, E., Unsicker, K., Schutz G., 1995. Targeted disruption of the glucocorticoid receptor gene blocks adrenergic chromaffin cell development and severely retards lung maturation. Genes & Development, 9: 1608-1621.

Corallo, D., Schiavinato, A., Trapani, V., Moro, E., Argenton, F., Bonaldo, P., 2013. Emilin3 is required for notochord sheath integrity and interacts with Scube2 to regulate notochord-derived Hedgehog signals. Development, 140: 4594-4601.

Dahm R, Geisler R., 2006. Learning from small fry: the zebrafish as a genetic model organism for aquaculture fish species. Marine Biotechnology, 8: 329-45.

De Bosscher, K., VandenBerghe, W., Haegeman, G., 2003. The interplay between the glucocorticoid receptor and nuclear factor-κB or activator protein-1: molecular mechanisms for gene repression. Endocrinology Reviews, 24: 488-522.

de Waal, P.P., Wang, D.S., Nijenhuis, W.A., Schulz, R.W., Bogerd, J., 2008. Functional characterization and expression analysis of the androgen receptor in zebrafish (*Danio rerio*) testis. Reproduction, 136: 225-234.

De, P., Roy, S.G., Kar, D., Bandyopadhyay, A., 2011. Excess of glucocorticoid induces myocardial remodeling and alteration of calcium signaling in cardiomyocytes. Journal of Endocrinology, 209: 105-114.

Dickmeis, T., Lahiri, K., Nica, G., Vallone, D., Syantoriello, C., Neumann, C.J., Hammerschmidt, M., Foulkes, N.S., 2007. Glucocorticoids play a key role in circadian cell cycle rhythms. PLoS Biology, 5: e78.

Eisen, J.S., Smith J.C., 2008. Controlling morpholino experiments: don't stop making antisense. Development, 135: 1735-43.

Fisher, S., Grice, E.A., Vinton, R.M., Bessling S.L., Urasaki, A., Kawakami, K., McCallion, A.S., 2006. Evaluating the biological relevance of putative enhancers using Tol2 transposon-mediated transgenesis in zebrafish. Nature Protocols, 1: 1297-1305.

Foligne, B., Aissaoui, S., Senegas-Balas, F., Cayuela, C., Bernard, P., Antoine, J.M., Balas, D., 2001. Changes in cell proliferation and differentiation of adult rat small intestine epithelium after adrenalectomy: kinetic, biochemical, and morphological studies. Digestive Diseases and Sciences, 46: 1236-1246.

Germain, P., Staels, B., Dacquet, C., Spedding, M., Laudet, V., 2006. Overview of nomenclature of nuclear receptors. Pharmacological Reviews, 58: 685-704.

Grange, T., Roux, J., Rigaud, G., Pictet, R., 1991. Cell-type specific activity of two glucocorticoid responsive units of rat tyrosine aminotransferase gene is associated with multiple binding sites for

C/EBP and a novel liver-specific nuclear factor. Nucleic Acids Research, 19: 131-139.

Griffiths, B.B., Schoonheim, P.J., Ziv, L., Voelker, L., Baier, H., Gahtan, E., 2012. A zebrafish model of glucocorticoid resistance shows serotonergic modulation of the stress response. Frontiers in behavioral neuroscience, 6: 68.

Haffter, P., Granato, M., Brand, M., Mullins, M.C., Hammerschmidt, M., Kane, D.A., Odenthal, J., van Eeden, F.J., Jiang, Y.J., Heisenberg, C.P., Kelsh, R.N., Furutani-Seiki, M., Vogelsang, E., Beuchle, D., Schach, U., Fabian, C., Nüsslein-Volhard, C., 1996. The identification of genes with unique and essential functions in the development of the zebrafish, Danio rerio. Development, 123: 1-36.

Hanna, R.N., Daly, S.C., Pang, Y., Anglade, I., Kah, O., Thomas, P., Zhu, Y., 2010. Characterization and expression of the nuclear progestin receptor in zebrafish gonads and brain. Biology of Reproduction, 82: 112-122.

Heitzer, M.D., Wolf, I.M., Sanchez, E.R., Witchel, S.F., De Franco, D.B., 2007. Glucocorticoid receptor physiology. Reviews in Endocrine and Metabolic Disorders, 8: 321-330.

Hollenberg, S.M., Weinberger, C., Ong, E.S., Cerelli, G., Oro, A., Lebo, R., Thompson, E.B., Rosenfeld, M.G., Evans, R.M., 1985. Primary structure and expression of a functional human glucocorticoid receptor cDNA. Nature, Dec 19-1986 Jan 1; 318: 635-641.

Hossain, M.S., Larsson, A., Scherbak, N., Olsson P.E., Orban, L., 2008. Zebrafish androgen receptor: isolation, molecular, and biochemical characterization. Biology of reproduction, 78: 361-369.

Howe, K., Clark, M.D., Torroja, C.F., Torrance, J., Berthelot, C., Muffato, M., Collins, J.E., Humphray, S., McLaren, K., Matthews, L., McLaren, S., Sealy, I., Caccamo, M., Churcher, C., Scott, C., Barrett, J.C., Koch, R., Rauch, G.J., White, S., Chow, W., Kilian, B., Quintais, L.T., Guerra-Assunção, J.A., Zhou, Y., Gu, Y., Yen, J., Vogel, J.H., Eyre, T., Redmond, S., Banerjee, R., Chi, J., Fu, B., Langley, E., Maguire, S.F., Laird, G.K., Lloyd, D., Kenyon, E., Donaldson, S., Sehra, H., Almeida-King, J., Loveland J., Trevanion, S., Jones, M., Quail, M., Willey, D., Hunt, A., Burton, J., Sims, S., McLay, K., Plumb, B., Davis, J., Clee, C., Oliver, K., Clark, R., Riddle, C., Elliot, D., Threadgold, G., Harden, G., Ware, D., Begum, S., Mortimore, B., Kerry, G., Heath, P., Phillimore, B., Tracey, A., Corby, N., Dunn, M., Johnson, C., Wood, J., Clark, S., Pelan, S., Griffiths, G., Smith, M., Glithero, R., Howden, P.,

Barker, N., Lloyd, C., Stevens, C., Harley, J., Holt, K., Panagiotidis, G., Lovell, J., Beasley, H., Henderson, C., Gordon, D., Auger, K., Wright, D., Collins, J., Raisen, C., Dyer, L., Leung, K., Robertson, L., Ambridge, K., Leongamornlert, D., McGuire, S., Gilderthorp, R., Griffiths, C., Manthravadi, D., Nichol, S., Barker, G., Whitehead, S., Kay, M., Brown, J., Murnane, C., Gray, E., Humphries, M., Sycamore, N., Barker, D., Saunders, D., Wallis, J., Babbage, A., Hammond, S., Mashreghi-Mohammadi, M., Barr, L., Martin, S., Wray, P., Ellington, A., Matthews, N., Ellwood, M., Woodmansey, R., Clark, G., Cooper, J., Tromans, A., Grafham, D., Skuce, C., Pandian, R., Andrews, R., Harrison, E., Kimberley, A., Garnett, J., Fosker, N., Hall, R., Garner, P., Kelly, D., Bird, C., Palmer, S., Gehring, I., Berger, A., Dooley, C.M., Ersan-Ürün, Z., Eser, C., Geiger, H., Geisler, M., Karotki, L., Kirn, A., Konantz, J., Konantz, M., Oberländer, M., Rudolph-Geiger, S., Teucke, M., Lanz, C., Raddatz, G., Osoegawa, K., Zhu, B., Rapp, A., Widaa, S., Langford, C., Yang, F., Schuster, S.C., Carter, N.P., Harrow, J., Ning, Z., Herrero, J., Searle, S.M., Enright, A., Geisler, R., Plasterk, R.H., Lee, C., Westerfield, M., de Jong, P.J., Zon, L.I., Postlethwait, J.H., Nüsslein-Volhard, C., Hubbard, T.J., Roest Crollius, H., Rogers, J., Stemple, D.L., 2013. The zebrafish reference genome sequence and its relationship to the human genome. Nature, 496:498-503.

Huang, P., Xiong, F., Megason, S.G., Schier, A.F., 2012. Attenuation of Notch and Hedgehog signaling is required for fate specification in the spinal cord. PLoS Genetics, 8: e1002762

Huang, P., Zhu, Z., Lin, S., Zhang, B., 2012. Reverse genetic approaches in zebrafish. Journal of Genetics and Genomics, 39: 421-433.

Ingham, P.W., 2009. The power of the zebrafish for disease analysis. Human Molecular Genetics, 18: R107-R112.

Jääskeläinen, T., Makkonen, H., Palvimo, J.J., 2011. Steroid up-regulation of FKBP51 and its role in hormone signaling. Current Opinion in Pharmacology, 11: 326-331.

Jantzen, H.M., Strähle, U., Gloss, B., Stewart, F., Schmid, W., Boshart, M., Miksicek, R., Schütz, G., 1987, Cooperativity of glucocorticoid response elements located far upstream of the tyrosine aminotransferase gene. Cell, 49: 29-38.

Kassel, O., Herrlich, P., 2007. Crosstalk between the glucocorticoid receptor and other transcription factors: molecular aspects. Molecular and Cellular Endocrinology, 275: 13-29.

Kawakami, K., 2007. Tol2: a versatile gene transfer vector in vertebrates. Genome Biology, 1: S7.

Kellendonk, C., Tronche, F., Reichardt, H.M., Schütz, G., 1999. Mutagenesis of the glucocorticoid receptor in mice. The Journal of Steroid Biochemistry and Molecular Biology, 69: 253-259.

Kimmel, C.B., Ballard, W.W., Kimmel, S.R., Ullmann, B., Schilling, T.F., 1995. Stages of embryonic development in the zebrafish. Developmental Dynamics, 203: 253–310.

Koubovec, D., Ronacher, K., Stubsrud, E., Louw, A., Hapgood, J.P., 2005. Synthetic progestins used in HRT have different glucocorticoid agonist properties. Molecular and Cellular Endocrinology: 242: 23-32.

Kumar, R., Thompson, E.B., 2005. Gene regulation by the glucocorticoid receptor: structure:function relationship. The Journal of Steroid Biochemistry and Molecular Biology, 94: 383-394.

Kwan, K.M., Fujimoto, E., Grabher, C., Mangum, B.D., Hardy, M.E., Campbell, D.S., Parant, J.M., Yost, H.J., Kanki, J.P., Chien, C.B., 2007. The Tol2kit: a multisite gateway-based construction kit for Tol2 transposon transgenesis constructs. Developmental Dynamics 236: 3088-3099.

Lawrence, C., 2007. The husbandry of zebrafish (*Danio rerio*): a review. Aquaculture, 269: 1-20.

Leatherland, J.F., Li, M., Barkataki, S., 2010. Stressors, glucocorticoids and ovarian function in teleosts. Journal of Fish Biology, 76: 86-111.

Levavi-Sivan, B., Bogerd, J., Mañanós, E.L., Gómez, A., Lareyre, J.J., 2010. Perspectives on fish gonadotropins and their receptors. General and Comparative Endocrinology, 165: 412-437.

Mangelsdorf, D.J., Thummel, C., Beato, M., Herrlich, P., Schütz, G., Umesono, K., Blumberg, B., Kastner, P., Mark, M., Chambon, P., Evans, R.M., 1995. The nuclear receptor superfamily: the second decade. Cell, 83: 835-839.

McKenna, N.J., O'Malley, B.W., 2002. Combinatorial control of gene expression by nuclear receptors and coregulators. Cell, 108: 465-474.

Merkulov, V.M., Merkulova, T.I., 2009. Structural variants of glucocorticoid receptor binding sites and different versions of positive glucocorticoid responsive elements: analysis of GR-TRRD database. The Journal of Steroid Biochemistry and Molecular Biology, 115: 1-8.

Morishima, Y., Kanelakis, K.C., Murphy, P.J., Shewach, D.S., Pratt, W.B., 2001. Evidence for iterative ratcheting of receptor-bound

hsp70 between its ATP and ADP conformations during assembly of glucocorticoid receptor.hsp90 heterocomplexes. Biochemistry, 40: 1109-1116.

Moro, E., Vettori, A., Porazzi, P., Schiavone, M., Rampazzo, E., Casari, A., Ek, O., Facchinello, N., Astone, M., Zancan, I., Milanetto, M., Tiso, N., Argenton, F., 2013. Generation and application of signaling pathway reporter lines in zebrafish. Molecular Genetics and Genomics, 288: 231-242.

Mueller, M., Atanasov, A., Cima, I., Corazza, N., Schoonjans, K., Brunner, T., 2007. Differential regulation of glucocorticoid synthesis in murine intestinal epithelial versus adrenocortical cell lines. Endocrinology, 148: 1445-1453.

Muto, A., Orger, M.B., Wehman, A.M., Smear, M.C., Kay, J.N., Page-McCaw, P.S., Gahtan, E., Xiao, T., Nevin, L.M., Gosse, N.J., Staub, W., Finger-Baier, K., Baier, H., 2005. Forward genetic analysis of visual behavior in zebrafish. PLoS Genetics, 1: e66.

Muto, A., Taylor, M.R., Suzawa, M., Korenbrot, J.I., Baier, H., 2013. Glucocorticoid receptor activity regulates light adaptation in the zebrafish retina. Frontiers in Neural Circuits, 7: 145.

Nasiadka, A., Clark, M.D., 2012. Zebrafish breeding in the laboratory environment. ILAR Journal, 53: 161-168.

Nesan, D., Kamkar, M., Burrows, J., Scott, I.C., Marsden, M., Vijayan, M.M., 2012. Glucocorticoid receptor signaling is essential for mesoderm formation and muscle development in zebrafish. Endocrinology, 153: 1288-1300.

Nesan, D., Vijayan, M.M., 2013. Role of glucocorticoid in developmental programming: evidence from zebrafish. General and Comparative Endocrinology, 181: 35-44.

Nesan, D., Vijayan, M.M., 2013. The transcriptomics of glucocorticoid receptor signaling in developing zebrafish. PLoS One, 8: e80726.

Nicolaides, N.C., Kyratzi, E., Lamprokostopoulou, A., Chrousos, G.P., Charmandari, E., 2015. Stress, the stress system and the role of glucocorticoids. Neuroimmunomodulation, 22: 6-19.

Oakley, R.H., Cidlowski, J.A., 2011. Cellular processing of the glucocorticoid receptor gene and protein: new mechanisms for generating tissue-specific actions of glucocorticoids. The Journal of Biological Chemistry, 286: 3177-3184.

Oakley, R.H., Cidlowski, J.A., 2013. The biology of the glucocorticoid receptor: new signaling mechanisms in health and disease. Journal of Allergy and Clinical Immunology, 132: 1033-1044.

Otto, C., Reichardt, H.M., Schütz, G., 1997. Absence of glucocorticoid receptor-β in mice. The Journal of Biological Chemistry, 272: 26665-266658.

Parajes, S., Griffin, A., Taylor, A.E., Rose, I.T., Miguel-Escalada, I., Hadzhiev, Y., Arlt, W., Shackleton, C., Müller, F., Krone, N., 2013. Redefining the initiation and maintenance of zebrafish interrenal steroidogenesis by characterizing the key enzyme Cyp11a2. Endocrinology, 154: 2702-2711.

Pfaffl, M.W., 2009. Rest 2009 Software user guide. Hilden, Germany: Qiagen.

Pfaffl, M.W., Horgan, G.W., Dempfle, L., 2002. Relative expression software tool (REST) for group-wise comparison and statistical analysis of relative expression results in real-time PCR. Nucleic Acids Research, 30: e36.

Pikulkaew, S., Benato, F., Celeghin, A., Zucal, C., Skobo, T., Colombo, L., Dalla Valle, L., 2011. The knockdown of maternal glucocorticoid receptor mRNA alters embryo development in zebrafish. Developmental Dynamics, 240: 874-889.

Pikulkaew, S., De Nadai, A., Belvedere, P., Colombo, L., Dalla Valle, L., 2010. Expression analysis of steroid hormone receptor mRNAs during zebrafish embryogenesis. General and Comparative Endocrinology, 165: 215–220.

Pujols, L., Mullol, J., Roca-Ferrer, J., Torrego, A., Xaubet, A., Cidlowski, J.A., Picado, C., 2002. Expression of glucocorticoid receptor α- and β-isoforms in human cells and tissues. The American Journal of Physiology - Cell Physiology, 283: C1324-C1331.

Quaroni, A., Tian, J.Q., Göke, M., Podolsky, D.K., 1999. Glucocorticoids have pleiotropic effects on small intestinal crypt cells. The American Journal of Physiology: 277, G1027-G1040.

Rae, M.T., Niven, D., Critchley, H.O., Harlow, C.R., Hillier, S.G., 2004. Anti-inflammatory steroid action in human ovarian surface epithelial cells. Journal of Clinical Endocrinology and Metabolism, 89: 4538–4544.

Reddy, A.B., Maywood, E.S., Karp, N.A., King, V.M., Inoue, Y., Gonzalez, F.J., Lilley, K.S., Kyriacou, C.P., Hastings, M.H., 2007. Glucocorticoid signaling synchronizes the liver circadian transcriptome. Hepatology, 45: 1478-1488.

Reichardt, H.M., Kaestner, K.H., Tuckermann, J., Kretz, O., Wessely, O., Bock, R., Gass, P., Schmid, W., Herrlich, P., Angel, P., Schütz,

G., 1998. DNA binding of the glucocorticoid receptor is not essential for survival. Cell, 93: 531-541.

Ren, R., Oakley, R.H., Cruz-Topete, D., Cidlowski, J.A., 2012. Dual role for glucocorticoids in cardiomyocyte hypertrophy and apoptosis. Endocrinology, 153: 5346-5360.

Revollo, J.R., Cidlowski, J.A., 2009. Mechanisms generating diversity in glucocorticoid receptor signaling. Annals of the New York Academy of Sciences, 1179: 167-178.

Rog-Zielinska, E.A., Thomson, A., Kenyon, C.J., Brownstein, D.G., Moran, C.M., Szumska, D., Michailidou, Z., Richardson, J., Owen, E., Watt, A., Morrison, H., Forrester, L.M., Bhattacharya, S., Holmes, M.C., Chapman, K.E., 2013. Glucocorticoid receptor is required for foetal heart maturation. Human Molecular Genetics, 22: 3269-3282.

Ruiz, M., Hedman, E., Gåfvels, M., Eggertsen, G., Werner, S., Wahrenberg, H., Wikström, A.C., 2013. Further characterization of human glucocorticoid receptor mutants, R477H and G679S, associated with primary generalized glucocorticoid resistance. Scandinavian journal of clinical and laboratory investigation, 73: 203-207.

Sainte-Marie, Y., Nguyen Dinh Cat, A., Perrier, R., Mangin, L., Soukaseum, C., Peuchmaur, M., Tronche, F., Farman, N., Escoubet, B., Benitah, J.P., Jaisser, F., 2007. Conditional glucocorticoid receptor expression in the heart induces atrio-ventricular block. FASEB Journal, 21: 3133-3141.

Schaaf, M.J., Chatzopoulou, A., Spaink, H.P., 2009. The zebrafish as a model system for glucocorticoid receptor research. Comparative Biochemistry and Physiology - Part A: Molecular and Integrative Physiology, 153: 75-82.

Schoneveld, O.J., Gaemers, I.C., Lamers, W.H., 2004. Mechanisms of glucocorticoid signaling. Biochimica et Biophysica Acta, 1680: 114-128.

Selman, P.J., Wolfswinkel, J., Mol, J.A., 1996. Binding specificity of medroxyprogesterone acetate and proligestone for the progesterone and glucocorticoid receptor in the dog. Steroids, 6: 133-137.

Smoak, K.A., Cidlowski, J.A., 2004. Mechanisms of glucocorticoid receptor signaling during inflammation. Mechanisms of Ageing and Development, 125 : 697-706.

Song, C.Z., Tian, X., Gelehrter, T.D., 1999. Glucocorticoid receptor inhibits transforming growth factor-β signaling by directly targeting the transcriptional activation function of Smad3. Proceedings of the National Academy of Sciences of the United States of America, 96: 11776-11781.

Sorrells, S.F., Sapolsky, R.M., 2007. An inflammatory review of glucocorticoid actions in the CNS. Brain, Behavior, and Immunity, 21: 259-272.

Stolte, E.H., de Mazon, A.F., Leon-Koosterziel, K.M., Jesiak, M., Bury, N.R., Sturm, A., Savelkoul, H.F., van Kemenade, B.M., Flik, G., 2008. Corticosteroid receptors involved in stress regulation in common carp, *Cyprinus carpio*. Journal of Endocrinology, 198: 403-417.

Tadros, W., Lipshitz, H.D., 2009. The maternal-to-zygotic transition: a play in two acts. Development, 136: 3033-3042.

Takagi, C., Takahashi, H., Kudose, H., Kato, K., Sakamoto, T., 2011. Dual in vitro effects of cortisol on cell turnover in the medaka esophagus via the glucocorticoid receptor. Life Sciences, 88: 239-245.

Tavares, B., Santos Lopes, S., 2013. The importance of zebrafish in biomedical research. Acta Medica Portuguesa, 26: 583-592.

Tetsuka, M., Milne, M., Simpson, G.E., Hillier, S.G., 1999. Expression of 11β-hydroxysteroid dehydrogenase, glucocorticoid receptor and mineralocorticoid receptor genes in rat ovary. Biology of Reproduction, 60: 330–335.

Thisse, C., Thisse, B., 2008. High-resolution in situ hybridization to whole-mount zebrafish embryos. Nature Protocols, 3: 59-69.

Vacaru, A,M., Unlu, G., Spitzner, M., Mione, M., Knapik, E.W., Sadler, K.C., 2014. *In vivo* cell biology in zebrafish - providing insights into vertebrate development and disease. Journal of Cell Science, 127: 485-495.

Varshney, G.K., Burgess, S.M., 2014. Mutagenesis and phenotyping resources in zebrafish for studying development and human disease. Briefings in Functional Genomics, 13: 82-94.

Volff, J.N., 2005. Genome evolution and biodiversity in teleost fish. Heredity (Edinb), 94: 280-294.

Wang, J.M., Préfontaine, G.G., Lemieux, M.E., Pope, L., Akimenko, M.A., Haché, R.J., 1999. Developmental effects of ectopic expression of the glucocorticoid receptor DNA binding domain are alleviated by an amino acid substitution that interferes with

homeodomain binding. Molecular and Cellular Biology, 19: 7106-7122.

Weger, B.D., Weger, M., Jung, N., Lederer, C., Bräse, S., Dickmeis, T., 2013. A chemical screening procedure for glucocorticoid signaling with a zebrafish larva luciferase reporter system. Journal of Visualized Experiments, 79.

Weger, B.D., Weger, M., Nusser, M., Brenner-Weiss, G. Dickmeis, T., 2012. A chemical screening system for glucocorticoid stress hormone signaling in an intact vertebrate. ACS Chemical Biology, 7: 1178-1183.

Weigel, N.L., Moore, N.L., 2007. Kinases and protein phosphorylation as regulators of steroid hormone action. Nuclear Receptor Signaling, 5: e005.

Westerfield, M., 1995. The Zebrafish Book. A guide for the laboratory use of Zebrafish (*Danio rerio*), 3rd ed. University of Oregon Press, Eugene, OR.

Zhang, Z., Jones, S., Hagood, J.S., Fuentes, N.L., Fuller, G.M., 1997. STAT3 acts as a co-activator of glucocorticoid receptor signaling. The Journal of Biological Chemistry, 272: 30607-30610.

Zhou, H., Mak, W., Kalak, R., Street, J., Fong-Yee, C., Zheng, Y., Dunstan, C.R., Seibel, M.J., 2009. Glucocorticoid-dependent Wnt signaling by mature osteoblasts is a key regulator of cranial skeletal development in mice. Development, 136: 427-436.

Ziv, L., Muto, A., Schoonheim, P.J., Meijsing, S.H., Strasser, D., Ingraham, H.A., Schaaf, M.J.M., Yamamoto, K.R., Baier, H., 2013. An affective disorder in zebrafish with mutation of the glucocorticoid receptor. Molecular Psychiatry, 18: 681-689.